A tripartite relationship between floodplain, fish biodiversity, and flood control in the middle stream of the Chao Phraya River

田中, 亘

https://doi.org/10.15017/1654858

出版情報：九州大学, 2015, 博士（工学）, 課程博士
バージョン：

A tripartite relationship between floodplain, fish biodiversity, and flood control in the middle stream of the Chao Phraya River

By

WATARU TANAKA

A dissertation submitted in partially fulfillment of the requirements for the degree of Doctor of Engineering

Department of Urban and Environmental Engineering
Graduate School of Engineering
Kyushu University
Fukuoka, Japan
August, 2011

DEPARTMENT OF URBAN AND ENVIRONMENATL ENGINEERING
KYUSHU UNIVERSITY
FUKUOKA, JAPAN

CERTIFICATION

The undersigned hereby certify that they have read and recommended to the Graduate School of Engineering for the acceptance of this dissertation entitled "**A tripartite relationship between floodplain, fish biodiversity, and flood control in the middle stream of the Chao Phraya River**" by **Wataru Tanaka** in partial fulfillment of the requirements for the degree of **Doctor of Engineering**.

Dated: January, 2016

Thesis Supervisor:

Prof. Yukihiro SHIMATANI, Dr. Eng.

Examination Committees:

Prof. Haruyuki HASHIMOTO, Dr. Eng.

Prof. Kenichi TSUKAHARA, Dr. Eng.

Prof. Yasuhiro MITANI, Dr. Eng.

Acknowledgment

I have received generous supports from many people for the completion of this study. I would like to show my greatest appreciation to all the people who have made a contribution to this dissertation. Without their guidance and persistent help this dissertation would not have been possible.

First of all, I would like to express my sincere gratitude to my supervisor Prof. Yukihiro SHIMATANI for continuous support and excellent guidance for the completion of this study. His insightful comments and suggestions have significantly improved this dissertation.

I owe a very important debt to Dr. Apinun Suvarnaraksha, who supported the research of freshwater fishes in Thailand. The overseas research in Thailand was the bold challenge for me, because I had no academic connections with the country. He has supported me planning research and conducting a field survey. His kindness and vast knowledge has made my study and life in Thailand more meaningful and productive. My special thanks goes to the members of Apinun's laboratory. Especcially, my friends, Rottapon Wattanasiriserekul, Wikit Phinrub, and Tosapol Chamnivikaipong provided great help for field survey and identification of fishes. Their excellent warmth and hospitality has really given me moral support.

My sincere thanks also go to Dr. Tomomi Ymashita and Yuta Tomiyama, Dr. Yuichi Kano. They have always given their best suggestions and full cooperation.

I would like to thank to my doctoral examination committees; prof. Haruyuki HASHIMOTO, prof. Kenichi TSUKAHARA, and prof. Yasuhiro MITANI. Their invaluable comments and suggestions have considerably improved my dissertation quality.

I would like to express my sincere gratitude to the Program for Leading Graduate Schools (Graduate Education and Research Training Program in Decision Science for a Sustainable Society (DS3)), as my main sponsor for providing my financial incentive within two years. DS3 members and lecturers also have provided helpful advices and suggestion for my study.

I would also like to thank my parents and elder brother. They were always supporting me and encouraging me with their best wishes.

Fukuoka, Japan
January 18, 2016

Table of Contents

List of Figures

List of Tables

Chapter 1

Importance of floodplains on aquatic ecosystem and present status in the world

1.1 Introduction

1.1.1 What is floodplain?

A floodplain is the flat or nearly flat land which undergoes occasional flooding, and is the landform created and maintained by flood dynamics. Floodplains contain inundation area of midstream valley plain, alluvial fan, downstream alluvial plain, and delta (Fig. 1.1). There are many kinds of wetlands in floodplain such as an oxbow lake, side arm, side pool, backswamp and so on. The Wetlands in floodplains are formed in two major ways: one is meanders grow, and the other is natural levee formation.

Meanders are windings and bends occur in the middle and lower stream. Meanders eventually grow through sediment deposits and erosion of stream. When meanders grow large and increase sinuosity meanders will be cut off from mainstream. The cut off waterbody called an oxbow lake (Fig. 1.2). Also a secondary flow caused by a small scale cut off inside river bank in the same way called a side arm.

A natural levee is a slightly elevated land formed along the area adjacent to stream. Natural levees get gradually higher whenever floods overflow it, through repeated sediment deposits of mud and silt transported by floods (Fig. 1.3). A backswamp formed behind a natural levee where landside water is poorly drained. The physical characteristics of backswamps are variety of scale, depth, velocity, and frequency of flooding, and connectivity from streams, according to positions in floodplains and detailed land features which created by sediment deposits by floods (Brinson 1993).

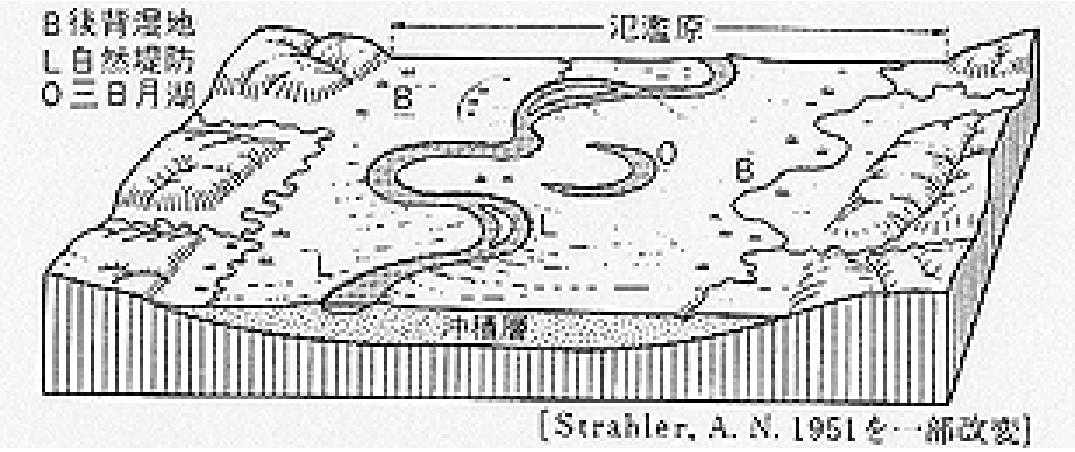

Fig. 1.1 Floodplain landforms. the figure is adapted from

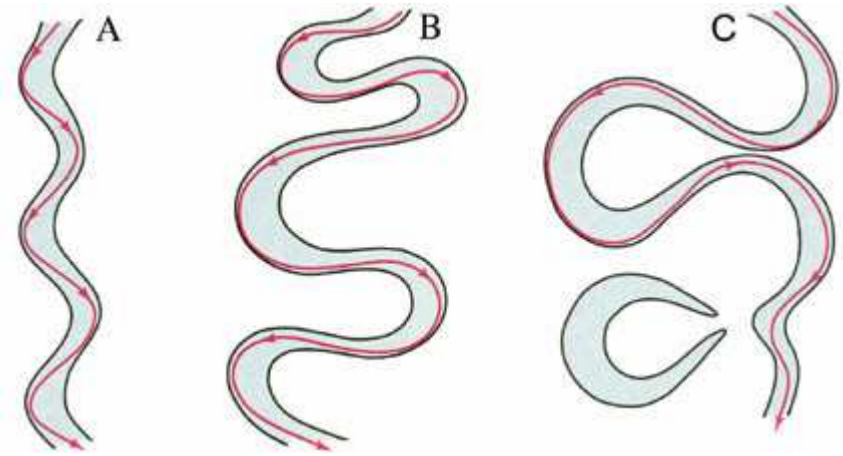

Fig. 1.2 Oxbow lake formation. (the figure is adapted from Indiana University Bloomington, http://www.indiana.edu/~g105lab/images/gaia_chapter_12/meander_formation.htm)

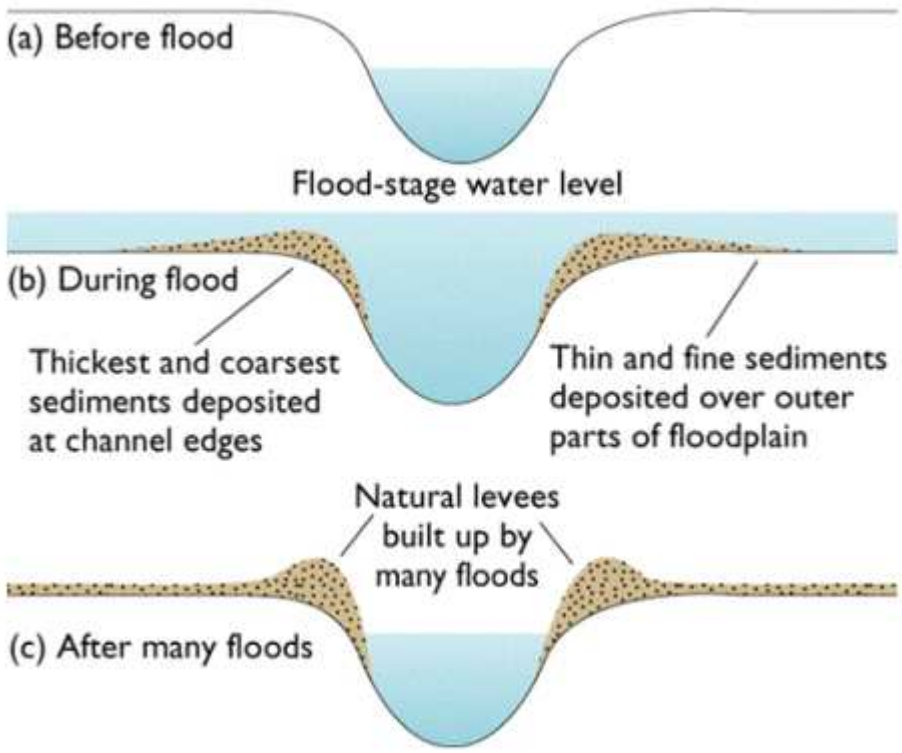

Fig. 1.3 Natural levee formation. (the figure is adapted from Indiana University Bloomington, http://www.indiana.edu/~g105lab/images/gaia_chapter_12/meander_formation.htm)

1.1.2 Importance of floodplains and floods on aquatic ecosystem

The importance of floodplains and floods on aquatic ecosystem is well known. Some of the effects of floodplains and floods on aquatic ecosystem include the following:

1. Occasional floods inundate the vast extent of terrestrial habitats and consequently overflows provide huge input of nutrients. The exchange of organic matter and inorganic nutrients drive floodplain ecosystem

(Amoros and Bornette 2002).

2. Heterogeneity of wetland habitats in floodplain results primarily from: (1) the distance from the floodplain wetlands to main streams; (2) the existence of permanent or temporary connections to main streams; and (3) the size and shape of waterbodies (length, width, depth and sinuosity) (Fig. 1.4). Large floods are important events for forming and maintaining the geographical features of floodplains. The heterogeneity of floodplain wetlands contributes to high biodiversity (Amoros and Bornette 2002).
3. The waterbodies of floodplain with lower current velocity and higher temperature may serve as suitable nursery habitats for some fish species (Agostinho et al. 2001, Pease et al. 2006). Floods provide reef litters and terrestrial plants to aquatic ecosystem, and invertebrate or vertebrate grazers may increase (Matthews 1998), result in enhance the growth of larval fishes (Gehrke 1992). Moreover, the waterbodies of floodplain with low Dissolved oxygen and shallow water prevent the intrusion of predators. (Anjos et al. 2008, Yamamoto et al. 2014).
4. Larval and nursery fishes may avoid displacement by floods by taking migratory behaviors into some waterbodies of floodplains. The same applies to relatively large aquatic orgasms, particularly in not complex habitats or in vulnerable habitat to flood disturbance (e.g. floating vegetation, sand sediment, water surface) (Heggenes 1988, Matthews et al. 1994, Inaguma et al. 2012). Namely, waterbodies of floodplains contribute to recovery of the floodplain ecosystem.
5. Ecological community in flood plain undergoes flood disturbances, and this annual changes prevent competitive species from dominance and allow the community to keep high biodiversity (Imanishi 2010).

Fig. 1.4 Wetlands in the floodplain around Nakhon Sawan, Thailand (Aerial photos are adapted from Google Earth)

1.2 Biodiversity and present status of floodplains in the world

1.2.1 Biodiversity of floodplains in the world

There are many species utilize unique function of floodplain previously mentioned in their life cycles. Fig. 1.5 shows the number of floodplain-dependent freshwater fish species among continents. The figure was created basing

on The IUCN Red List of Threatened Species (Version 2015-3, http://www.iucnredlist.org). The species type "floodplain-dependent" for each fish species was distinguished by the IUCN Red List in which described as utilize following habitats: seasonal/intermittent/irregular rivers/streams/creeks, and seasonal/intermittent freshwater lakes, seasonal/intermittent freshwater marshes pools. Of all described 5214 freshwater fish species in the world, 1662 species (24%) were floodplain-dependent species. 251 species of 1662 floodplain dependent species were endangered species (critical endangered (CR) + endangered (EN) + Vulnerable (VU)). It should be noted that 1279 species of all 2854 freshwater fish species (45%) in Sub-saharan Africa were floodplain dependent species. The region which estimated second largest species number of floodplain-dependent species was South and Southeast Asia, 258 freshwater fish species were floodplain-dependent. The total number of freshwater fish species in Sub-saharan Africa and Southeast Asia occupied 91.6% (1524 species) of all floodplain-dependent species in the world.

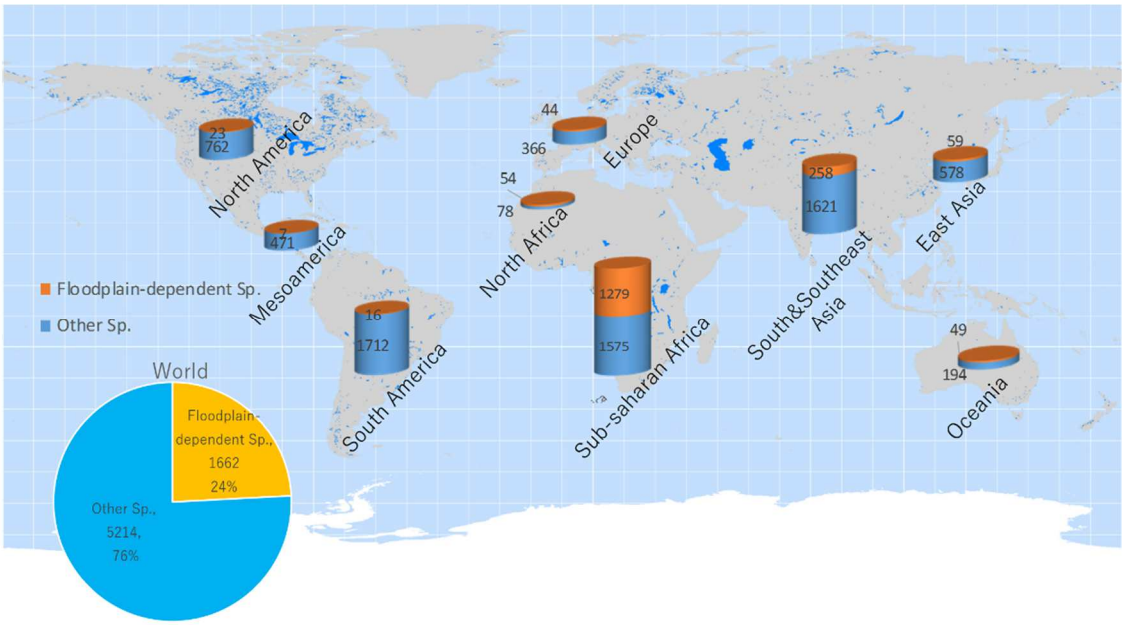

Fig. 1.5 Comparison of freshwater fish species number among continents. Species number and floodplain-dependent for each fish species is based on The IUCN Red List of Threatened Species (2015). The background map is adapted from the major waterbodies map made by Lehner and Döll (2004).

1.2.2 Present status and threats to floodplain in the world

The global area of wetlands was estimated 12.8 $\times 10^6$ km^2 (Finlayson and Davidson 1999) and the estimated global area of floodplains vary from 0.8 $\times 10^6$ km^2 (Aselmann and Crutzen 1989) to 1.65 $\times 10^6$ km^2 (Constanza et al. 1997) to 2.2 $\times 10^6$ km^2 (Ramsar and IUCN 1999), due to the difficulty of determining the extent of permanent and seasonal waterbodies. Despite the likelihood that floodplains cover less than 1.5 % of the earth's land surface and occupy less than 17% of the wetlands, quarter of freshwater fish diversity depends on floodplains.

Many of the large Asian, African and South American floodplains are disappearing or are being transformed at an accelerating rate as a result of water cycle change (Tockner and Stanford 2002). Although South and Southeast Asian and Sub-Saharan African floodplains boasts the highest biological biodiverse ecosystem in the world, the greatest decline in biodiversity is expected to occur in the freshwaters of the region in tandem with the reduction of

floodplains (Dudgeon 2002).

Since 1900, more than half the world's wetlands have disappeared (Moser et al. 1996) In North America, up to 90% of floodplains are already cultivated and therefore functionally extinct (Erwin 2009). Floodplain is one of the most altered landscape worldwide and it continue to disappear at an accelerating rate, since development pressure for reclamation of floodplains is much higher than other landscapes due to the facility to irrigation (Vitousek et al. 1997, Olson and Dinerstein 1998, Ravenga et al. 2000).

A large scale dam drastically changes water cycle in floodplain. Fig. 1.6 shows the discharge patterns of Nile river at Aswan. Aswan Dam is the largest storage capacity dam in Nile River. Aswan High Dam was opened in 1970. After Aswan High Dam was opened flood peak decreased drastically and low water discharge increased (Tockner and Stanford 2002). And the timing of the flood peak shifted in a several months. These changes may reduce the area of floodplains and disturb the life cycle of floodplain-dependent species, because floods drive and maintain floodplain landforms and floodplain ecosystem.

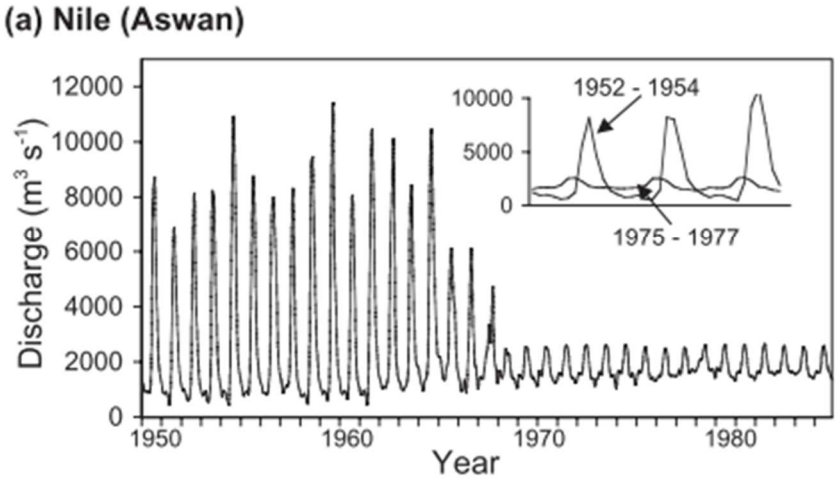

Fig. 1.6 Discharge patterns of Nile River below the Aswan dam. The figure is adapted from Tockner and Stanford (2002).

1.3 Biodiversity and present status of floodplains in Southeast Asia, and Thailand

1.3.1 Biodiversity of floodplains in Thailand

The fauna of the freshwater ecosystem of Southeast Asia is extremely diverse. Zakaria-Ismail (1994) pointed a recent estimate of about 1000 species is probably an understatement. The Chao Praya River is one of major rivers in Southeast Asia, and the basin of the river have vast floodplain system. The floodplains are maintained by a regular and long period floods, and many fish species of the basin utilize these predictable and prolonged floods in their life cycle (Rainboth 1996). More than 690 freshwater fish species have been recorded and it is estimated 10% of all freshwater fish species are still undescribed (Rainboth 1996, Kottelat and Whitten 1996). In the region, around 30 endemic species were described (Vidthayanon 2005). For example, some *Schistura* species such as *S. maejotigrina, S. sirindhornae, S. deansmarti, S. dubia, S. menanensis, S. pridii*, and *S. spilota*

are endemic to the Chao Phraya basin (Suvarnaraksha 2012, Suvarnaraksha 2015).

Inland fisheries have long been a part of Thai culture and are an important source of protein, especially for rural populations. The Thailand inland fishery ranked 13th in the world based on catch expect for fish cultivations (222500 tons), and the Thailand inland fishery ranked 6th based on catch per population (3.3kg/person/year) in the world in 2012 (Moffitt and Cajas-Cano 2014, UN Population Division 2015).

The Chao Phraya freshwater fish biodiversity and endemism is among the highest in the world. Regarding the high biodiversity of floodplain and the threats to development the floodplains (described later section), Chao Phraya River is one of Major global hotspots for freshwater fish biodiversity ("Indo-Burma hot spot", Myers et al. 2000). However, it is pointed that freshwater hotspots receive less attention than their terrestrial counterparts (Myers et al. 2000).

1.3.2 Problems and present status of floodplains in Thailand

Land-use transformation

Fig. 1.7 shows the relationship of developed area proportions on the plains between riparian area and whole catchment in the major basin in Southeast Asia and East Asia. Developed area was defined as intensively impacted land-use by human activities, and the proportion was calculated as the total area of land cover type "Croplands" and "Urban and Built-Up" in 0.5 km MODIS-based Global Land Cover Climatology (Broxton et al. 2014). The riparian area was defined as the land within 5 km of major streams. Land cover "Water" was eliminated from "riparian area" and "whole catchment" area, in order to avoid the underestimation of the developed area proportion of the areas in which the large proportion of land cover occupied by waterbody areas (For example, Biwa Lake in Yodo River Basin). The lands within 5 degrees of the slope were classified as plains. The major basins were defined as the basins with the areas was larger than 1000km^2 and stream lengths was longer than 100km based on Global Drainage Basin Database (GDBD) (Masutomi et al. 2009). Digital elevation model was derived from SRTM 90m Digital Elevation Database v4.1 (Jarvis et al. 2008). Southeast Asian and East Asian riverine floodplains are severely threatened by land-use development than whole catchment areas (Fig. 1.7), particularly in East Asia. The results supported high development pressure on floodplains as previous studies have pointed (Vitousek et al. 1997, Olson and Dinerstein 1998, Ravenga et al. 2000).

The most impacted riparian areas in the respective of land-use development were found in China and Japan. Dagu River (China), where is known for water pollution from land-based sources such as urban, industrial sewage, and cultivation (Jin et al. 2014, Liang et al. 2014), showed the highest impact on riparian areas of all rivers investigated. In Thailand, the threats to riparian areas by land-use development are also strong than that of whole basins (Fig. 1.7). However, the development ratios of the all basins of the country were lower than 40 %. The development ratio of Chao Phraya basin was 32.4% for the riparian area, 21.9% for the whole catchment.

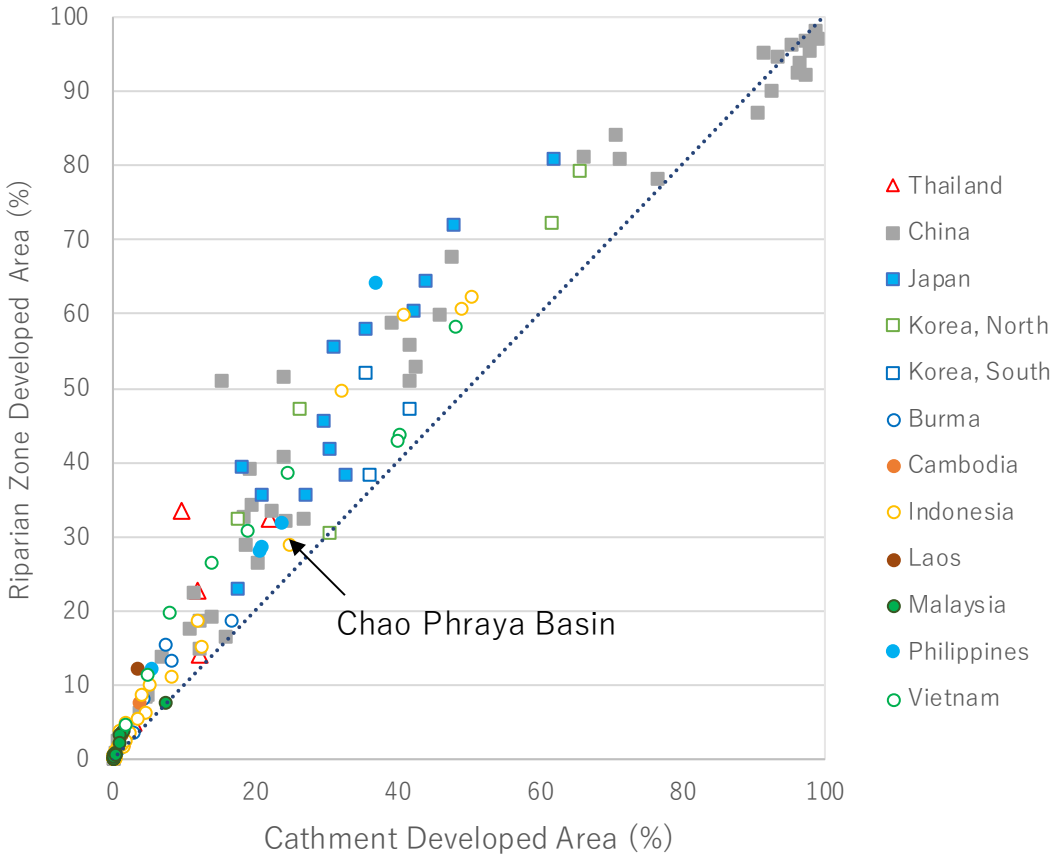

Fig. 1.7 The relationship of developed area proportions on the plains between riparian area and whole basin in the major basin in Southeast Asia and East Asia

Fig. 1.8 shows the relationship between developed area proportions and population densities in the riparian plain areas of major basins in Southeast Asia and East Asia.

Population density was derived from 2010 Gridded Population of the World, Version 3 (GPWv3) (CIESIN and CIAT 2005). Basin and major stream data was derived from Global Drainage Basin Database (GDBD) (Masutomi et al. 2009).

There are positive logarithmic relationships between human population density and land use of the riparian zone for East Asian and Southeast Asia ((East Asia: 12.015*ln(x)-15.301, R^2=0.39, p<0.001, Southeast Asia: 7.226*ln(x)-19.456, R^2=0.54, p<0.001; Fig. 1.8). East Asian riparian areas have the tendency to show higher land-use development ratios at a low level of population density than Southeast Asian riparian areas at the same level of population density. Present analyses excluded land cover type “Cropland/Natural Vegetation Mosaic” in developed area. For example, in Southeast Asia, the land cover type corresponds to rain-fed crop lands. Relatively low land-use development against population in Southeast Asia can be explained by the traditional and extensive farm land-use around riparian areas. In order to improve the production of crops, by taking measures against floods and constructing irrigation system, reclamation of floodplains for intensive agriculture has been occurring in Southeast Asia (Tockner and Stanford 2002).

The calculations of present analyses were conducted by ArcGIS ver. 10.2 (ESRI Japan, Tokyo, Japan).

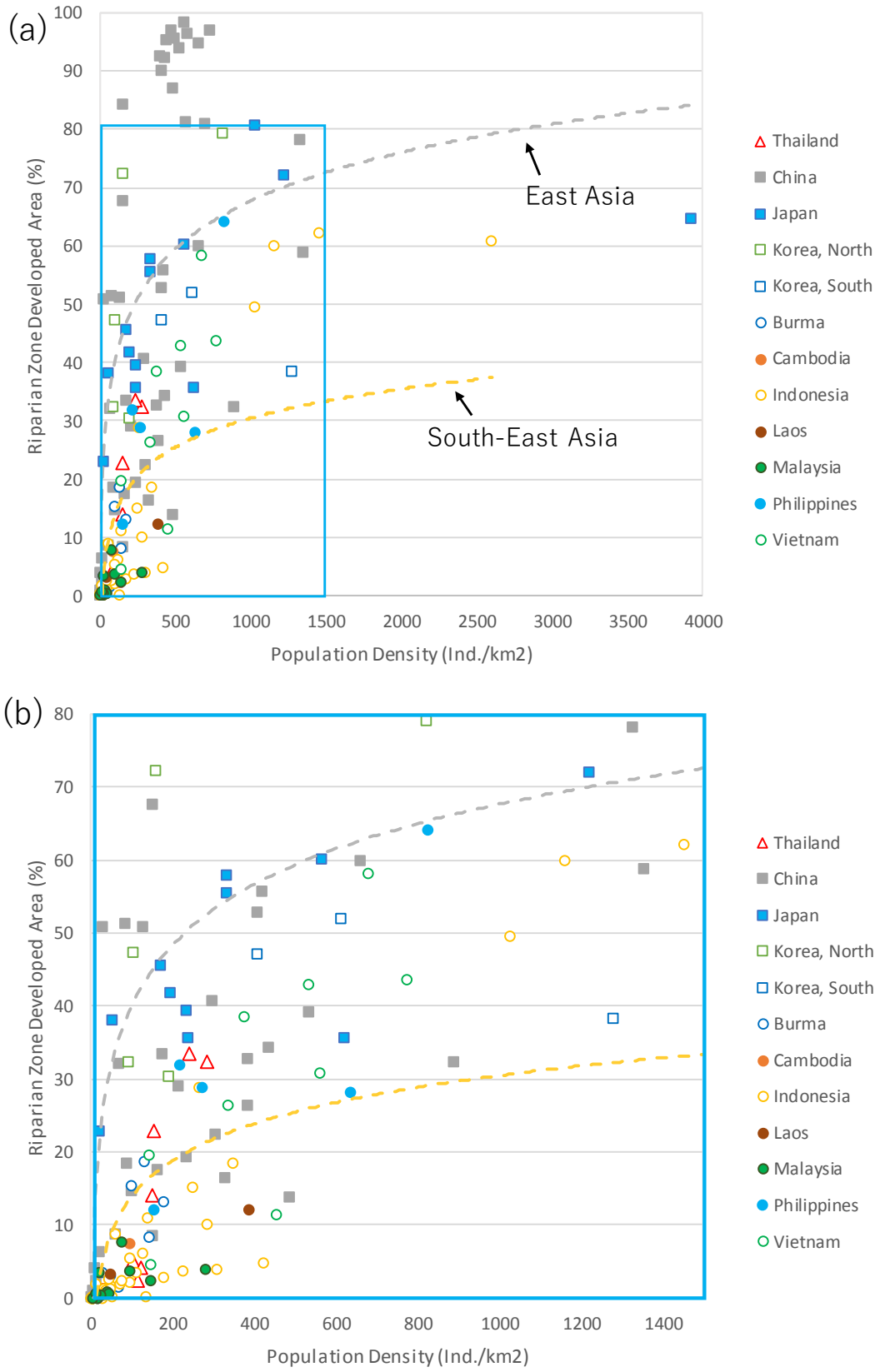

Fig. 1.8 the relationship between developed area proportions and population densities in the riparian plain areas of major basins in Southeast Asia and East Asia. (a) general view (b) enlarged view.

Large scale dams and water discharge change in the Chao Phraya Basin

There are two major large scale dams in the Chao Phraya Basin (Fig. 1.8). Bhumibol Dam was opened in 1963, Shirikit Dam was opened in 1974. Tebakari et al. (2005) mentioned that the reduction of flood peak is the result of coordinated operation between Bhumibol Dam and Shirikit Dam. Total capacities of the dams are 1350 MCM for Bhumibol Dam and 950 MCM for Shirikit Dam, and are respectively equivalent to the inflow discharges for 2 years and 1.5 years (Tamada et al. 2013). The catchments of two dams cover 15% of whole Chao Phraya basin. The river discharge pattern of The Chao Phraya River has been dramatically transformed by the dams. Fig. 1.9 shows Monthly runoff at Nakhon Sawan C.2 runoff station (Tebakari et al. 2005). From 1963 to the late 1970s, monthly low water discharge gradually increased in dry season. From 1980s, flood peaks notably decreased. Mateo et al. (2014) investigated the impact of the operation of the dams since the 2011 Thailand flood and found that the inundated area in the Chao Phraya River Basin was reduced by 40%.

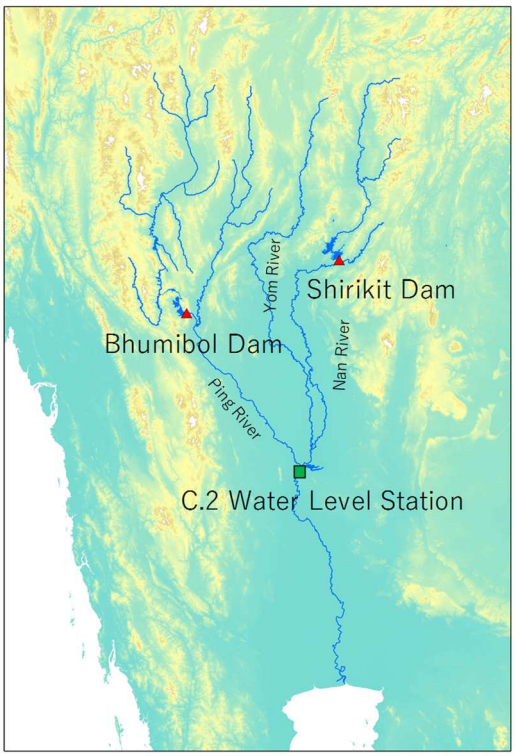

Fig. 1.9 Location of Bhumibol Dam and Shirikit Dam

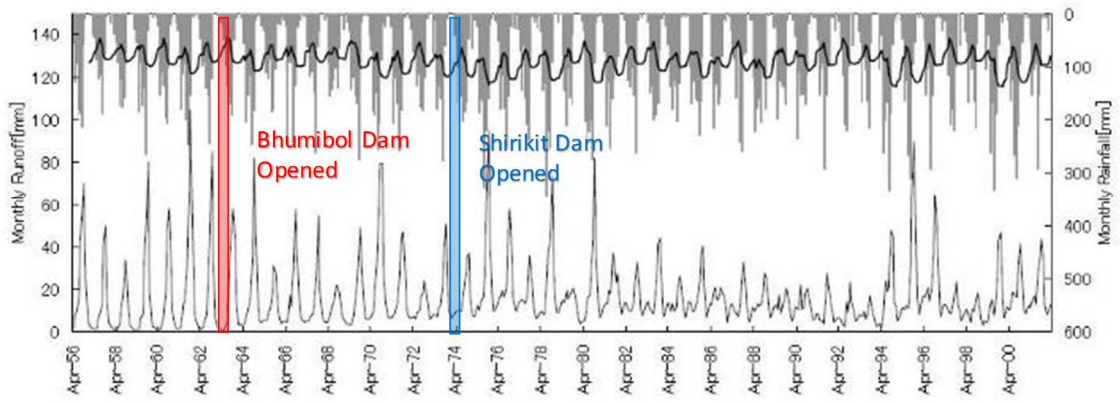

Fig. 1.10 Monthly runoff and rainfall at Nakhon Sawan C.2 runoff station (modified from Tebakari et al. 2005)

1.4 The state of flood control policies of Thailand Government

1.4.1 2011 Thailand floods

In Thailand, during the rainy season, floods generally occur from September to October. In 2011, heavy rains due to the rainy season caused severe disasters in Thailand, Cambodia, Bangladesh, the Philippines and India. A severe flood disaster, called 2011 Thailand floods, struck middle and downstream basin of the Chao Phraya River. The floods submerged approximately 17.3% of the Chao Phraya basin (Fig. 1.11), causing 813 deaths and 9.5 million victims (Centre for Research on the Epidemiology of Disasters (GREC) 2012).

The total economic damages and losses from the floods were estimated 1,425 billion baht, and reduced GDP growth in 2011 by 1.1 % (World Bank 2012). Compared to the 2011 Thailand government revenue, the damage account for 59% of the revenue. The flood directly impacted Thailand manufacturing, and the items for which Thailand manufacturing occupied large proportion of the world's supply of components such as computer hard disk drive (HDD), and automotive parts. The economic losses spread to other countries as global supply shortages.

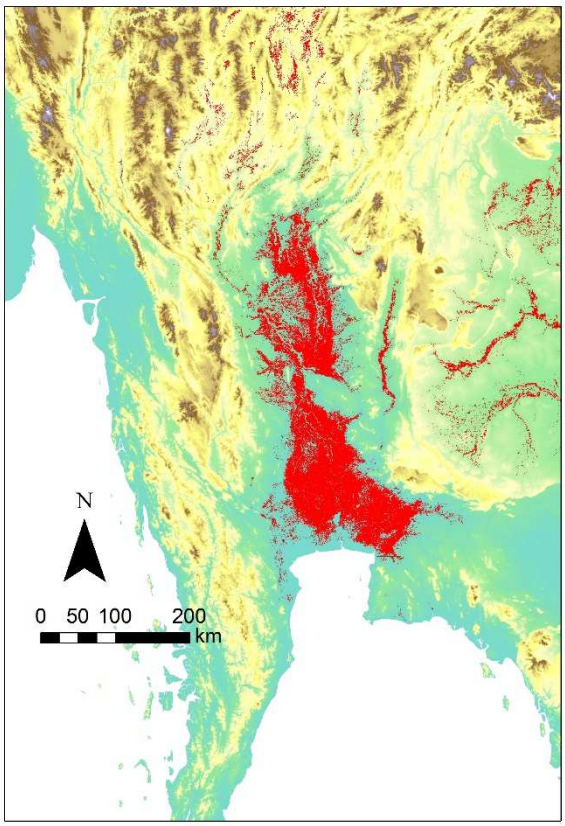

Fig. 1.11 Inundation area of 2011 Thailand flood. The inundation area is derived from GISTDA (http://flood.gistda.or.th/)

1.4.2 Flood control policies of Thailand Government

Considering the extensive damages and losses of 2011 Thailand floods, Strategic Committee for Water Resource Management (SCWRM) was set up by Yingluck cabinet in 2011. In 2012, SCWRM established "Master Plan on Water Resource Management" for long-term water resource management and against future drought and flood. The Master Plan consists of 8 major work plans and 2 action plans. The descriptions about principles of future flood control are summarized as follows:

The upper stream of the river basin: The upper stream of the river basin focused on slowing down the velocity of the flood current and on cutting the peak discharge of floods. The plan of upper stream included construction of suitable reservoirs in Ping, Yom, Nan, Skaekurng and Pasak rivers, and the improvement and conservation of soil in the upper river basin by reforestation and rehabilitation of water catchment forest area.

The middle stream of the river basin: The middle stream of the river basin focused on restoration of flood water. In order to mitigate flood impacts on Bangkok and its vicinity, the assigning of temporary flood retention areas and recovery of remaining retention areas in middle stream of the basin were proposed. The plan also included creating measures for compensation to those flood retention areas.

The downstream of the river basin: The downstream of the river basin focused on drainage of flood water. In order to efficiently deviate waters from the Chao Phraya River and Pa Sak River, the construction of flood

ways or drainage canals, and improvement of water drainage and remaining water gateway were claimed. The plan of downstream also included the improvement of remaining dikes and preventive dikes for key economic areas.

The master plan was developed based on His Majesty the King's initiatives after 1995 Thailand floods, that referred to flood control principles such as the restoration of riparian retention areas called Monkey cheek, the construction of King's Dike to protect central Bangkok against floodwater from upstream, and the improvement of flood way which flows on the east side of Bangkok. The master plan has described that the works for flood mitigation in the river basin begun in 2012 onwards with total amount of the budget at 300 billion baht. However, Yingluck cabinet was replaced by a Thailand's military in 2014 in the process of carrying out the master plan.

In January 2015, Thailand's military government claimed guiding principle for water management. According to the principle, the government intends to budget approximately 900 billion baht (more the twice the budget of Yingluck master plan) over the next decade, and in the first two years will mainly cover feasibility studies, designs and environmental impact assessments. (Bangkok Post 2015). In March 2015, Prime Minister Prayut Chan-o-cha stated at the Third United Nations World Conference that the government will push forward an integrated water management system including learning from His Majesty the King's initiatives (Permanent Mission of Thailand to the United Nations 2015).

The previous master plan of Yingluck cabinet and the new principle are same in terms of learning from His Majesty the King's initiatives. The flood control principle of Thailand's military government still remains unclear, therefore, will not greatly differ from the previous master plan.

1.5 Research objectives

Flood water management at the middle stream of the Chao Phraya River have a profound influence on the prevention of flooding at the downstream economic areas such as Bangkok and its vicinity (Cham et al. 2014). Although future flood control measures will bring a substantial change to floodplains and biodiversity at the region, the details of the impact are not clear.

Therefore, this study aimed to understand flood conditions and floodplain importance on biodiversity at region. Moreover, I tried to propose a practical protection plan for fish biodiversity in harmony with flood control. Objectives of this study were designed as follows:

1. To differentiate and describe fish species richness, composition, and environmental characteristics among the rivers and floodplain waterbodies based on statistical approaches.
2. To elucidate the relationship between fish species biodiversity and environmental factor. In particular, to elucidate the role of floodplain existence for the fish species diversity.
3. To develop the hydrological model to predict the floodplain area changes caused by future flood control measures.
4. To predict the impact of Kaeng Sua Ten Dam on the floodplain of the middle stream of the Chao Phraya River, and to elucidate its impact on fish species diversity.
5. To develop the assessment method to assess the integrity of floodplain quality among the three main tributaries in the middle stream of the Chao Phraya River.

6 To propose the conservation plan of floodplain ecosystem.

1.6 Study area

The study was conducted from the middle stream of the Chao Phraya River, where the three main tributary rivers of the Chao Phraya River meet (Fig. 1.12). The downstream end of Chao Phraya River of the study area is located at 100.11E, 15.67N, and 381km from the river mouth and 26 m above sea level with a flat slope of approximately 1/15,000. The river widths are roughly 200 m at Chao Phraya River, 120m at Ping River, 60 m at Yom River, and 90m at Nan River. The tributaries are the Ping River with a basin area 50,888 km^2 and an average discharge of 158 $m^3 s^{-1}$ and a maximum discharge of 403 $m^3 s^{-1}$ (P.7A water level station 2014), the Yom River with a basin 22,768 km^2 an average discharge of 101 $m^3 s^{-1}$ and a maximum discharge of 443 $m^3 s^{-1}$ (Y.17 water level station 2014), and the Nan River with a basin 35,355 km^2 and an average discharge of 201 $m^3 s^{-1}$ and a maximum discharge of 862 $m^3 s^{-1}$ (N.7A water level station 2014) (Hydro and Agro Informatics Institute (HAII) 2015). There are no barriers to the dispersal of fishes, such as large dams, on the rivers in the study area. The Bueng Boraphet Lake is located close to the downstream end of Chao Phraya River of the study area (100.23E, 15.71N). The Bueng Boraphet Lake (surface area 224 km^2) is an artificial freshwater lake constructed by damming a natural marsh in Thailand (Sriwongsitanon et al. 2007).

According to Thai Meteorological Department (2015), the region has three seasons: a rainy season, typically from mid-May to mid-October, a cool dry season, typically from mid-October to mid-February, and a hot dry season, typically from mid-February to mid-May. The annual mean precipitation of the region is 1275mm, the temperature ranges from 21.1(mean minimum) to 35.5(mean maximum). The region receives intensive rainfall from August to September. In the rainy seasons, floods due to the intensive rainfall generally occur from September to October.-Flood characteristics among the three sub-basins differ in terms of floodplain area. The floodplain area in the Ping River sub-basin is smaller than that in the Yom and Nan River sub-basins.

The land-use of the region is typically paddy fields in the riparian area, and sugar cane fields in the area far from rivers and not irrigated. Urban areas only distribute around Nakhon Sawan city (100.09E, 15.71N), Pichit city (100.42E, 16.22N), and Kamphaeng Phet city (99.53E, 16.48N).

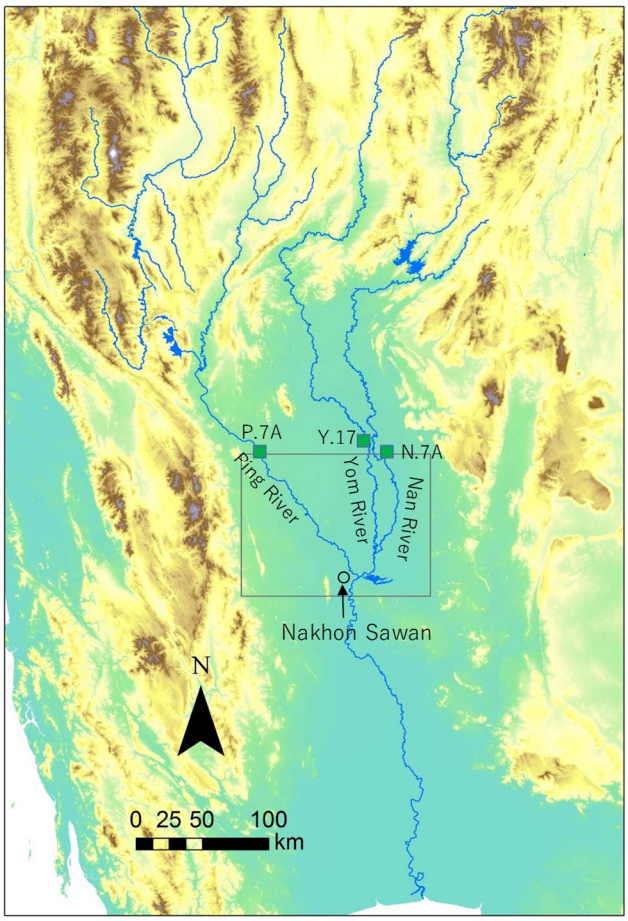

Fig. 1.12 Study area and Nakhon Sawan city location

1.7 Dissertation structure

Chapter 1: This chapter is introductory chapter which explain the importance of floodplains on aquatic ecosystem and present status in the world and highlighted the background of the research, research objectives, description of study area, and dissertation structure.

Chapter 2: This chapter will discuss about the fish composition and richness based on the fish sampling survey in the study area. Moreover, the important factors which determine the species richness in the region will be elucidated. This chapter will also provide the fundamental knowledge and estimation of the integrity of the rivers in terms of the species diverse.

Chapter 3: This chapter will discuss about the hydraulic model which predict the flood inundation in the region using iRIC model. The accuracy of the model will be validate comparing the observed inundation area by satellite image. This chapter will also discuss about the return periods of the annual rainfall of 2014 when is the

year the fish sampling conveyed.

Chapter 4: This chapter will provide the floodplain conditions in some scenarios using Storage Function Method. Scenario A will describe potential and original floodplain condition in which two largest dams don't exist. Scenario B will describe the future condition with a new dam construction in the Yom River which is the only major tributary that have no large scale dam on the mainstream.

Chapter 5: This chapter will discuss about the response of fish species richness to the scenarios. The potential species richness will be predicted in the region using Maxent. And gap analysis among original condition and scenarios will be conducted in order to elucidate the species loss and sensitivity due to environmental degradations.

Chapter 6: This chapter will discuss about what kinds of floodplains are an important environment for fish species and hat kinds of floodplain environments are lacking in the basin? These are essential knowledge for suggesting effective conservation plan. This chapter will also provide the conclusion of the dissertation.

Chapter 2

Fish species composition and influence of floodplain area on fish species richness in waterbodies of middle stream of the Chao Phraya River basin

2.1 Introduction

Floodplains are riparian ecotones in which there is a transition between terrestrial and aquatic communities (Kolding and Zwieten 2012). These areas feature high biodiversity and are a highly productive part of the aquatic ecosystem (Moss 1988, Junk 1996). Flood pulse concept (FPC; Junk et al. 1989) is the hypothesis that lateral interaction between main river and floodplain associated with flood disturbance is the major driving force for maintenance of aquatic biodiversity of floodplain ecosystem. FPC explain that aquatic biodiversity is resulted in great habitat diversity and the gradients of hydrological regime and hydrochemical environmental associated with the hydrological connectivity from main rivers to isolated floodplain waterbodies, and in prevention of competitive species domination allowing successional pioneer species associated with flood disturbance (Junk et al. 1989).

Previous studies on river–floodplain ecosystems have demonstrated the importance of flooding, which allows aquatic organisms to migrate into inundated floodplains and to use resources from the submerged terrestrial landscape for feeding and breeding. Therefore, the area of floodplains affects the recruitment of aquatic organisms (Moss 1988, Junk 1996, King and Lake 2003, Carolsfeld et al., 2004, Arthington et al., 2005). Flood disturbance creates habitat heterogeneity and gradients of hydrochemical environment in floodplain waterbody, which affects distribution and richness of aquatic orgasms (Junk et al. 1989, Ward et al. 1999).

Many studies have demonstrated species richness pattern of various biota was affected by floods and emphasized the significance of flood and floodplain in large-scale rivers around the world; for example, fishes and phytoplankton in Danube River (Ward et al. 1999, Mihaljević et al. 2015), hydrochorous plants in Twentekanaal Canal (Boedeltje et al. 2004), zooplankton and phytoplankton in La Plata River (Simões et al. 2013, Izaguirre et al. 2001), fishes and zooplankton in Amazon River (Petry and Markle 2003,Bozelli 2015). However, these information in South-East Asia are poorly understood, despite whose floodplains are one of world's most threatened floodplains due to human activities (Vitousek et al. 1997, Ravenga et al. 2000, Tockner and Stanford 2002).

The Chao Phraya River is one of major rivers in South-East Asia, and the basin of the river have vast floodplain system. The floodplains are maintained by a regular and long period flood, and many fish species of the basin utilize the predictable and prolonged flood in their life cycle (Rainboth 1996). In the basin, flood control measures have been carried out in accelerating progress, due to the damages of 2011 Thailand flood. Understanding of significance of floodplain and flood event on fishes in the basin would help the assessment and mitigation of the impact of flood control measures for river-floodplain ecosystem and inland fishery. However, previous studies about fishes in the basin have focused on taxonomy and fauna (e.g. Zakaria-Ismail 1994, Kottelat and Whitten 1996, Kottelat 2013, Suvarnaraksha 2015), ecological aspects have received

relatively less attention (Rainboth 1996, Vidthayanon 2002), and further study assessing the significance of floodplain and flood for fishes remain notably absent.

In this chapter, I investigated fish distributions and physical environments of main rivers and floodplain waterbodies in the middle of The Chao Praya Basin. I described fish assemblage and conducted nMDS and X-means analyses to elucidate the fish species composition, and GLMM analysis to elucidate the flood significance for the fishes in the region.

2.2 Materials and methods

2.2.1 Study Area

The study was conducted in the floodplains of the mid-Chao Phraya River Basin (Fig. 2.1 a) where the three main tributary rivers of the Chao Phraya River meet. There are no barriers to the dispersal of fishes, such as large dams, on the rivers in the study area. The floodplain area in the Ping River sub-basin is smaller than that in the Yom and Nan River sub-basins (Fig. 2.1b). Thus the study area is the suitable area for comparing the fish species composition among the environments which belongs to different size of floodplain.

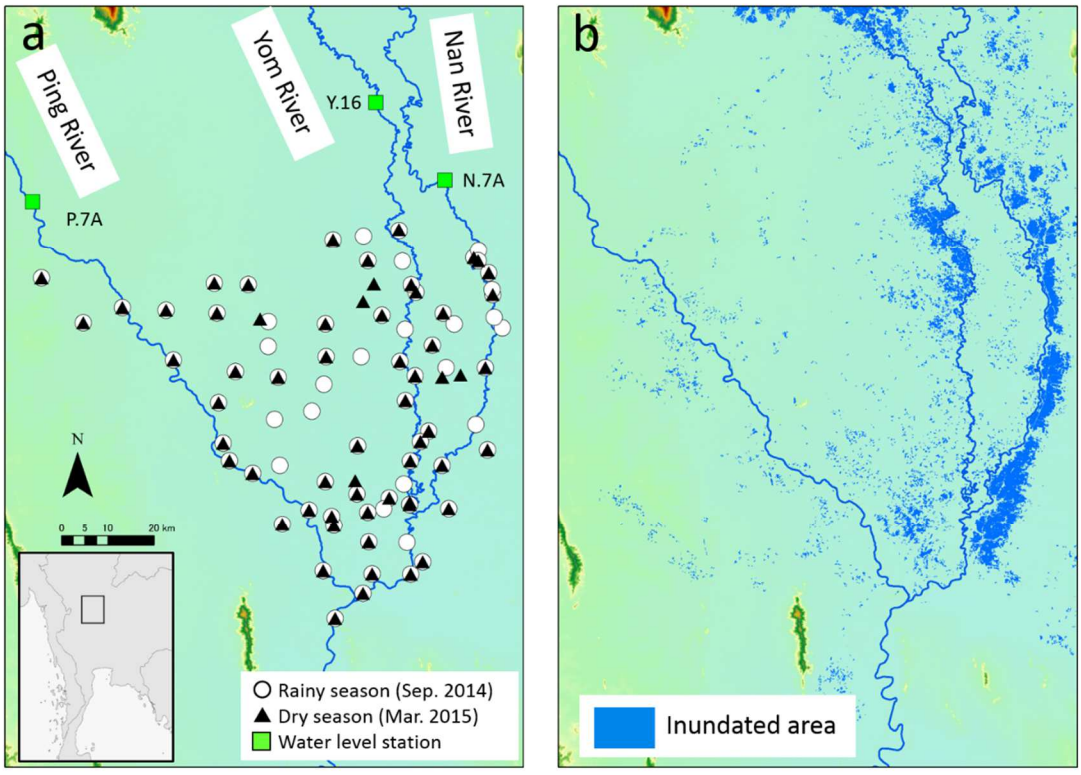

Fig. 2.1 Maps of the study area. (a) Open circles indicate the sites surveyed in the rainy season (September 2014). Black triangles indicate the sites surveyed in the dry season (March 2015). (b) Inundated areas in 2014 floods. The inundated area data was derived from GISTDA (2015)

2.2.2 Fish sampling and environmental parameter assessment

Fish sampling was conducted using cast nets with a 20-mm mesh size and scoop nets with a 2-mm mesh size. The fishing effort at all sampling sites was 20 man-minutes for cast nets and 10 man-minutes for scoop nets. In total, 135 waterbodies were sampled in the Ping River sub-basin, the Yom River sub-basin, and the Nan River sub-basin (Fig. 2.1a) in September 2014 (the rainy season: 15 rivers, 19 diversion canals, 12 ponds, 5 irrigation ditches, 18 paddies, and six wetlands) and March 2015 (the dry season: 15 rivers, 18 diversion canals, 12 ponds, 5 irrigation ditches, 11 paddies, and one wetland). The different waterbody types are shown in Fig. 2.2. For safety reasons, sampling from rivers and ponds with a water depth >2 m was carried out from the edge of the waterbody. Captured fishes were identified at species level and their total length was measured. Most individuals were released at the same site where they were caught, but some were preserved in formalin when further identification was required. The fishes were identified according to Rainboth (1996), Apinun (unpublished data), and the online database of Fishes of Mainland Southeast Asia (http://ffish.asia/; Kano et al. 2013).

Fig. 2.2 Photographs of the types of waterbodies surveyed. (a) River, (b) diversion canal, (c) pond, (d) irrigation ditch, (e) paddy field, and (f) wetland.

At each study site, the following environmental parameters were measured in the field: electric conductivity (EC, μS; PCS Tester 35, Oakton Instruments, IL, USA), turbidity (Turb, NTU; HI 93703; Hanna Instruments Japan, Tokyo, Japan), dissolved oxygen (DO, mg L^{-1}; DO-5509; Mother Tool Co., Ltd., Ueda, Japan), water depth (Dep, m), and current velocity (Vel, m s^{-1}; CR-11; Cosmo-riken Co., Ltd., Kashiwara, Japan). These environmental parameters were measured once at the surface in the center of each study site. In addition to the above environmental parameters, waterbodies were classified as temporarily connected to main rivers by an annual flood or as isolated at the time of survey (Con; 1 for temporary connection, 0 for no connection).

2.2.3 Landscape parameter assessment

At each sampling location, the following landscape parameters were measured by geographic information system (GIS) manipulation: route distance of each waterbody via the channel network from the nearest river (Dist, km), and the floodplain area around each survey site (FA, km2). The floodplain area was calculated within a buffered circle around each survey site according to Kano et al. (2010) and Tanaka et al. (2011) (Fig. 2.3). Because the spatial scale at which the floodplain area should be extracted was not clear, buffers of a given radius (500 m, 1000 m, 2000 m, 3000 m, and 4000 m) were generated around the center of each study site. The floodplain GIS data were obtained from the Thailand Flood Monitoring System (GISTDA 2015). Data for the 2014 inundation range were used and areas that experienced flooding in that year were classified as floodplains. The landscape parameters were calculated using ArcGIS ver. 10.2 (ESRI Japan, Tokyo, Japan).

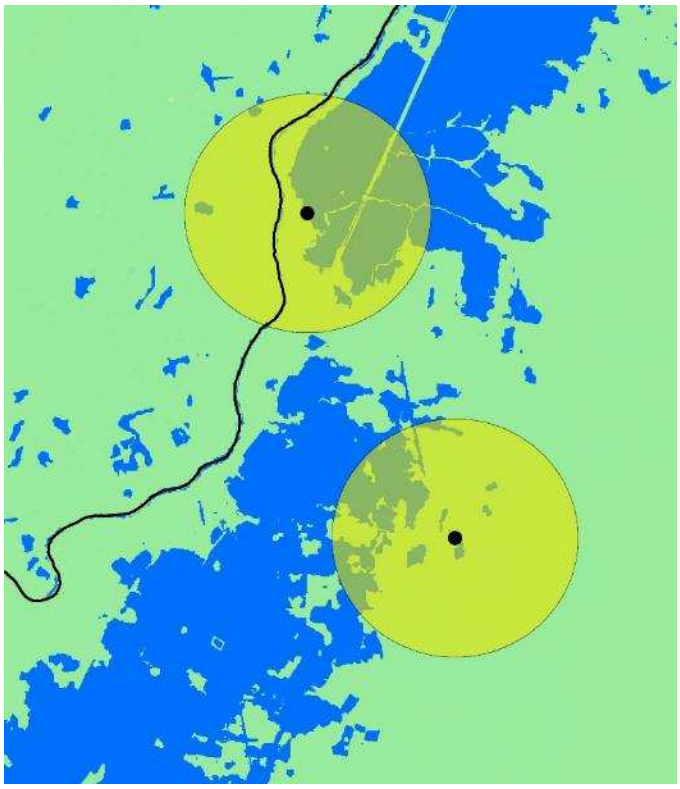

Fig. 2.3 The buffer shapes which extracted the flood plain area within. The blue areas are floodplains.

2.2.4 Data analysis

To determine the size composition of fishes in the waterbodies connected to main rivers by an annual flood and in isolated waterbodies, total length histograms were constructed for the species with more than 50 individuals captured from both connected and isolated waterbodies during the rainy season survey (Esomus metallicus, Trichopsis vittata, Trichopodus trichopterus, and Trichopodus microlepis).

Fish species composition in the middle stream of the Chao Phraya River

According to Miyazaki et al. (2013), a "Minchin-type" Nonmetric multidimensional scaling (NMDS: Kruskal 1964, Minchin 1987) and a X-means (Ishioka 2000) were conducted to elucidate the similarity of fish fauna among survey sites and to cluster the fish species composition patterns. NMDS based on a Bray-Curtis similarity index was used to depict two-dimensional ordination plots of the fish assemblage at each sampling site. X-means is a clustering method to partition n observations into X clusters. The cluster division is decided to minimize the sum of distance from each cluster center to each point belongs to the cluster. The number of clusters X decided by computing the Bayesian Information Criterion (BIC). The fish assemblage coordinate of each sampling site obtained from NMDS was used as the set of observations.

The identification of indicator species

To analyze the indicator species, which typically characterized the cluster split by the NMDS and X-means, a IndVal analysis (Dufrene and Legendre 1997) was conducted. IndVal is calculated based on a specificity A_{ij} and a fidelity B_{ij} of species for each cluster. The IndVal of species i in cluster j is calculated by flowing formula:

$$\mathrm{IndVal} = A_{ij} \times B_{ij}$$

Here

$$A_{ij} = \frac{\text{The number of sites where species } i \text{ occurred within cluster } j}{\text{The number of sites where species } i \text{ occurred}}$$

$$B_{ij} = \frac{\text{The number of sites where species } i \text{ occurred within cluster } j}{\text{The number of sites within cluster } j}$$

The species whose IndVal exceed 0.25 is considered as an indicator species. 0.25 fo IndVal indicates the equivalent level that the occurrence proportion of the certain species that are in the certain cluster is 50%, and the proportion of sites in the cluster that contain the species is 50%.

The relationship between fish species richness and environmental factor

A generalized linear mixed model (GLMM; Pinheiro and Bates 2000) was used to identify the environmental and landscape parameters that influence fish species richness (Table 2.1). The analysis was performed for overall fish species richness and for each waterbody type surveyed at twenty or more locations (rivers, diversion canals, ponds, and paddy fields). A correlation matrix between environmental and landscape parameters was calculated to avoid multicollinearity. The Pearson's correlation coefficients (R) were <0.7, indicating that multicollinearity

did not distort the GLMMs using these variables as predictors (Table 2.2) (Dormann et al. 2013).

Table 2.1 Variables used during GLMM and model selection.

Variables	Description	Variable type	Unit
EC	Electric conductivity of survey site	Continuous	μS
Dep	Water depth of survey site	Continuous	m
Do	Dissolved oxygen of survey site	Continuous	$mg\ L^{-1}$
Turb	Turbidity of survey site	Continuous	NTU
Vel	Current velocity of survey site	Continuous	ms^{-1}
Con	Connected by an annual flood or not	Dummy	0,1
Dist	Route distance from the nearest river	Continuous	km
FA	Floodplain area around each survey site	Continuous	km^2

Table 2.2 Correlation matrix of variables used during GLMM and model selection

Total	1	2	3	4	5	6	7	8
1 EC	1							
2 Dep	-0.26	1						
3 Do	-0.02	-0.03	1					
4 Turb	0.03	-0.09	0.06	1				
5 Vel	-0.25	0.31	0.27	0.13	1			
6 Con	-0.15	0.00	-0.03	-0.11	-0.09	1		
7 Dist	0.14	-0.16	-0.05	0.20	-0.29	-0.14	1	
8 FA †	0.09	0.06	-0.16	-0.27	-0.06	0.33	-0.46	1
River	1	2	3	4	5	6	7	8
1 EC	1							
2 Dep	-0.32	1						
3 Do	0.21	-0.27	1					
4 Turb	0.06	0.69	0.15	1				
5 Vel	-0.11	0.46	0.46	0.53	1			
6 Con	-	-	-	-	-	-		
7 Dist	-	-	-	-	-	-	-	
8 FA †	-0.36	0.2	-0.38	-0.21	-0.01	-	-	1
Canal	1	2	3	4	5	6	7	8
1 EC	1							
2 Dep	-0.37	1						
3 Do	0.00	-0.15	1					
4 Turb	0.10	-0.22	0.07	1				
5 Vel	-0.12	0.48	-0.10	-0.07	1			
6 Con	-	-	-	-	-	-		
7 Dist	0.17	0.06	-0.15	0.16	0.26	-	1	
8 FA †	0.19	-0.08	0.10	-0.26	-0.1	-	-0.40	1
Paddy	1	2	3	4	5	6	7	8
1 EC	1							
2 Dep	-0.34	1						
3 Do	-0.07	-0.02	1					
4 Turb	0.04	-0.31	0.06	1				
5 Vel	-0.10	0.29	-0.26	-0.08	1			
6 Con	-0.32	0.59	-0.09	-0.31	0.32	1		
7 Dist	0.10	-0.42	0.16	0.33	-0.17	-0.36	1	
8 FA †	0.02	0.48	-0.27	-0.41	0.27	0.54	-0.59	1
Pond	1	2	3	4	5	6	7	8
1 EC	1							
2 Dep	-0.18	1						
3 Do	0.12	0.12	1					
4 Turb	0.07	-0.28	0.27	1				
5 Vel	-0.04	-0.16	-0.15	0.25	1			
6 Con	-0.32	-0.06	0.23	-0.07	-0.06	1		
7 Dist	-0.02	-0.16	0.52	0.23	-0.13	-0.16	1	
8 FA †	-0.03	0.13	-0.43	-0.13	0.12	0.21	-0.65	1

† Radius of buffer is 2000m, -: Unused

In the GLMMs, the dependent values were the species richness of native fish species, migratory native fish species, and non-migratory native fish species in each waterbody type. The floodplain migratory behavior for each fish species was defined according to FishBase (http://www.fishbase.org/). The independent variables were EC, Turb, DO, Dep, Vel, Con, Dist, and FA as fixed factors, and season (rainy season, dry season) and waterbody type (river, diversion canal, pond, irrigation ditch, paddy field, and wetland) as random effect intercepts. A Poisson distribution with log link function was applied to the GLMMs, which were performed for all possible sets of independent variables. Model selection was made using Akaike's information criterion (AIC; Akaike 1974). The model with the lowest AIC was defined as the best model.

It is possible that fish species richness showed spatial autocorrelation among the study sites (e.g., the fish

species richness was less in the Ping River sub-basin study sites compared with the Yom and Nan River sub-basins). Species–environment models that have spatial autocorrelation in the residuals may be not appropriate because they can overestimate or underestimate the importance of environmental variables (Ferrer-Castán and Vetaas 2005, Overmars et al. 2003, Keitt et al. 2002). To test for spatial autocorrelation, Moran's *I* (Moran 1950) was computed using the residuals from the best models. Moran's *I* is widely used to assess the existence and effect of spatial autocorrelation in species–environment regression models (e.g. Lichstein et al. 2002, Zhou et al. 2004). Moran's *I* ranges from −1 to +1; a positive and high value indicates a spatial dispersion distribution pattern (positive autocorrelation), a zero value indicates a random distribution pattern, and a negative and low value indicates a spatial correlation distribution pattern (negative autocorrelation). The significance of Moran's *I* was tested by computing the Z score. According to the two-tailed Z test with a significance threshold (P value) of 0.05, P values <0.05 were considered significantly spatially autocorrelated.

All statistical analyses were conducted using R statistical software (ver. 3.1.1; R Development Core Team) and its optional packages "vegan" for NMDS, "lme4" for GLMM, "MuMIn" for model selection, and "spdep" for Moran's *I* test, and its source program "X-means.prog"(Ishioka (2000): opened to http://www.rd.dnc.ac.jp/~tunenori/src/X-means.prog) for X-means.

2.3 Results

2.3.1 Fish species richness and environmental characteristics

In total, 103 species (6555 individuals) belonging to 27 families were recorded (see Appendix 2.1 for details). Of the 135 study sites, 11 were inundated by the annual flood when the survey was conducted during the rainy season. The general characteristics of environmental and landscape parameters for each waterbody type during the rainy and dry seasons are shown in Table 3.3. No major differences were observed between the seasons except for Turb, which tended to be higher during the rainy season. Figure 2.3 shows the total-length histograms for fishes captured in the study sites connected to main rivers by an annual flood and in isolated study sites during the rainy season survey. For all species, the proportion of small fish tended to be higher in connected study sites compared with isolated waterbodies.

Table 2.3 General characteristics of environmental and landscape parameters at each waterbody type

		River Mean (SD)		Diversion canal Mean (SD)		Irrigation ditch Mean (SD)	
	Unit	Rainy	Dry	Rainy	Dry	Rainy	Dry
EC	μS	214(39.4)	207(61.2)	239(45.7)	357(156)	345(143)	665(257)
Dep	m	1.05(0.367)	0.691(0.311)	1.10(0.505)	0.581(0.356)	0.680(0.232)	0.452(0.142)
Do	mg L^{-1}	5.61(1.41)	4.76(1.48)	3.40(1.28)	3.66(1.56)	3.35(1.51)	3.68(1.24)
Turb	NTU	130(85.3)	12.6(8.04)	70.9(79.6)	141(228)	108(70.8)	51.2(58.4)
Vel	ms^{-1}	0.824(0.419)	0.38(0.303)	0.183(0.184)	0.0189(0.0621)	0.0267(0.0533)	0(0)
Con	0,1	0(0)	0(0)	0(0)	0(0)	0(0)	0(0)
Dist	km	0.152(0.132)	0.152(0.132)	0.144(0.165)	0.166(0.185)	0.206(0.127)	0.239(0.0987)
FA	km^2	3.90(2.58)†	3.902(2.58)†	2.80(3.02)†	3.05(3.18)†	3.41(2.09)†	3.88(1.79)†
		Pond Mean (SD)		Paddy field Mean (SD)		Wetland Mean (SD)	
	Unit	Rainy	Dry	Rainy	Dry	Rainy	Dry
EC	μS	318(104)	533(328)	344(163)	586(549)	263(91.0)	199(0)
Dep	m	0.997(0.328)	1.10(0.498)	0.426(0.317)	0.218(0.126)	0.365(0.0946)	0.47(0)
Do	mg L^{-1}	3.68(3.05)	3.66(2.02)	3.96(2.31)	4.11(2.08)	4.19(2.29)	0.300(0)
Turb	NTU	47.8(36.4)	19.6(22.5)	156(167)	36.9(34.1)	21.9(7.44)	0.640(0)
Vel	ms^{-1}	0.0139(0.0461)	0(0)	0.0456(0.167)	0(0)	0(0)	0(0)
Con	0,1	0.167(0.373)	0(0)	0.4444(0.4969)	0(0)	0.167(0.373)	0(0)
Dist	km	0.428(0.206)	0.387(0.204)	0.397(0.250)	0.333(0.249)	0.325(0.173)	0.0662(0)
FA	km^2	6.05(2.92)†	5.44(2.82)†	5.17(3.25)†	4.99(3.47)†	5.23(2.71)†	1.11(0)†

† Radius of buffer is 2000m

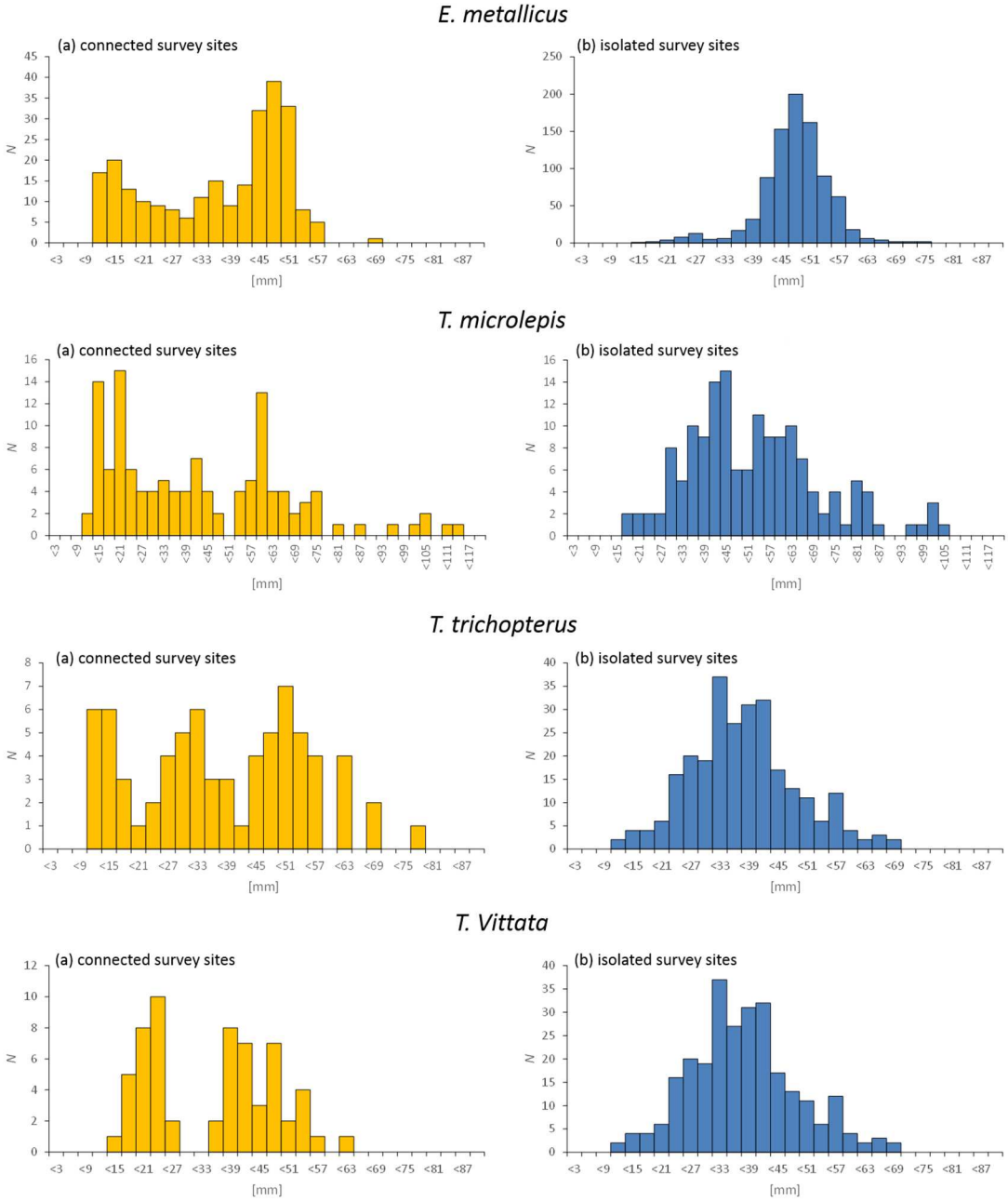

Fig. 2.4 Total-length histograms for four common fish species (more than 50 individuals captured from both temporarily connected and isolated waterbodies) recorded during the rainy season survey. (a) Temporarily connected study sites and (b) isolated study sites.

2.3.2 Fish species composition and its indicator species

Sampling sites were clustered into three partitions by NMDS and X-means. The fish composition was divided into three partitions based on the similarity of the fish assemblage among sites: Cluster 1 containing river and diversion canal sites, Cluster 2 containing all waterbody types, and Cluster 3 containing diversion river, diversion canal, pond, and wetland (Fig. 2.5, waterbody types see Fig. 2.2). Table 2.4 shows environmental and landscape characteristics of each cluster. Cluster 1-3 contained 38, 75, and 24 sites respectively. Each cluster

contained sampling sites both the rainy season and the dry season, indicating there was no seasonal bias for the clustering result. The Cluster 1 is generally lotic environment, while cluster2 and cluster 3 are generally lentic environment. Mean distance from mainstream increased in the following order: cluster 1, cluster 2, and cluster 3. The cluster 3 showed a relatively high electric conductivity, indicating worse water quality. In terms of fish species, the cluster 3 showed a relatively low fish biodiversity and fish species richness then other clusters (Fig. 2.6).

Fig. 2.5 Similarity pattern of the fish assemblage among sampling sites by NMDS and X-means method. The fish composition was divided into three partitions: Cluster 1 (green symbols) containing river and diversion canal sites, Cluster 2 (orange symbols) containing all waterbody types, and Cluster 3 (blue symbols) containing diversion river, diversion canal, pond, and wetland.

Table 2.4 General characteristics of environmental and landscape parameters at each cluster.

Cluster	1		2		3	
	Mean(±SD)		Mean(±SD)		Mean(±SD)	
EC	261.3(±213.4)		344.5(±179.3)		466.2(±416.1)	
Dep	0.90(±0.40)		0.72(±0.44)		0.55(±0.6)	
Do	4.92(±1.42)		3.56(±2.04)		4.03(±2.45)	
Turb	79.8(±118.7)		86.0(±136.3)		62.3(±100.4)	
Vel	0.48(±0.44)		0.04(±0.12)		0.08(±0.21)	
Con	0(±0)		0.13(±0.34)		0.04(±0.20)	
Dist	1.9(±4.0)		5.4(±5.3)		9.2(±6.7)	
FA	0.33(±0.23)		0.37(±0.25)		0.25(±0.23)	
	Rainy	Dry	Rainy	Dry	Rainy	Dry
Season(*N*)	21	17	44	31	10	14

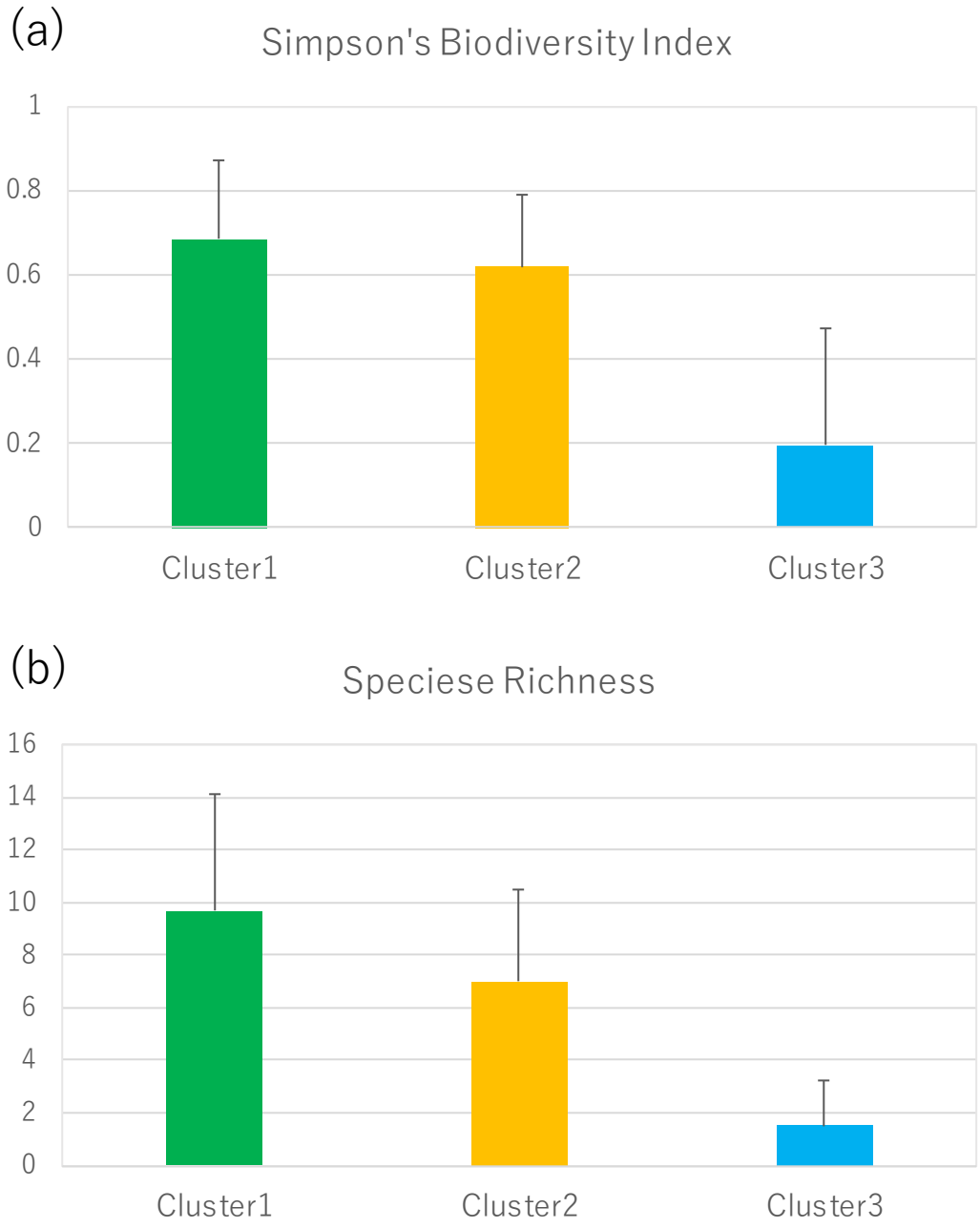

Fig. 2.6 Biodiversity and species richness among the clusters. Biodiversity was calculated by Simpson index (*D*). The equation is:

$$D = 1 - \sum_{i=1}^{s} {p_i}^2$$

Here, *s*: sampling species richness, p_i: the proportional abundances of species *i*

IndVal analysis elucidated that the indicator species for each cluster. As the result of the analysis, 8 species represented the cluster 1, and 5 species represented cluster 2. While no species represented cluster 3. Cluster 1 was characterized rheophilic species (e.g. *Mystercoleucus marginatus*, *Acantopsis spp.*, and *Henicorhynchus siamensis*). Cluster 2 was characterized limnophilic species (e.g. *Trichopodus trichophterus*, *Trichopodus*

microlepis, and *Trichopsis vittat*a).

Table 2.5 Indicator species of each cluster. The species with IndVal > 0.25 was listed. For cluster 3, there was no indicator species, thus top five IndVal species was listed.

Cluster1		Cluster2		Cluster3	
Mystacoleucus marginatus	0.62	Trichopodus trichopterus	0.73	Dermogenys siamensis	0.08
Acantopsis spp.	0.42	Trichopsis vittata	0.69	Anabas testudineus	0.06
Parambassis siamensis	0.41	Esomus metallicus	0.61	Parambassis wolffii	0.05
Henicorhynchus siamensis	0.35	Amblypharyngodon chulabhorn	0.29	Pristolepis fasciata	0.04
Puntioplites proctozysron	0.29	Trichopodus microlepis	0.26	Rasbora paviana	0.03
Barbonymus altus	0.28				
Barbonymus gonionotus	0.27				
Rasbora dusonensis	0.26				

2.3.3 GLMM analysis and model selection

Table 2.6 shows the results of GLMM analysis with AIC model selection for fish species richness. The differences between the AIC value for the best models and null models (ΔAIC) were >4 except for the model for non-migratory fish species richness in canals, indicating substantial support for the best models (Burnham & Anderson, 2002). No spatial autocorrelation was detected in the residuals of the best models, indicating spatial autocorrelation didn't distort the GLMM results.

Fig. 2.8 shows the relationship between floodplain area (2000 m buffer size; the best buffer size for GLMM analysis of the richness of all native fish in a waterbody) and richness of all native species in each waterbody type. The broken lines represent linear regression lines for significant correlations ($P < 0.05$). Significant positive correlations between native fish richness and floodplain area were found for rivers and ponds, but not for other waterbody types.

2.4 Discussion

The fish composition of study area was divided into major two clusters, namely cluster 1 consists of stream habitats and cluster 2 consists of floodplain habitats. Despite cluster 2 contained variety of waterbody types, these waterbodies consolidated in the same fish composition. While cluster 3 could be estimated to be the group of deteriorated floodplains with less fish species, poor connectivity from streams, and bad water quality, rather than to be a certain classification of fish composition. It was suggested that fish composition pattern was not corresponded with waterbody types and physical environmental factors except for water quality, fish composition was essentially determined by the given landscape and geographical factors such as connectivity from mainstream and surrounding floodplain area, rather than local environment such as depth, current velocity, and DO in the region.

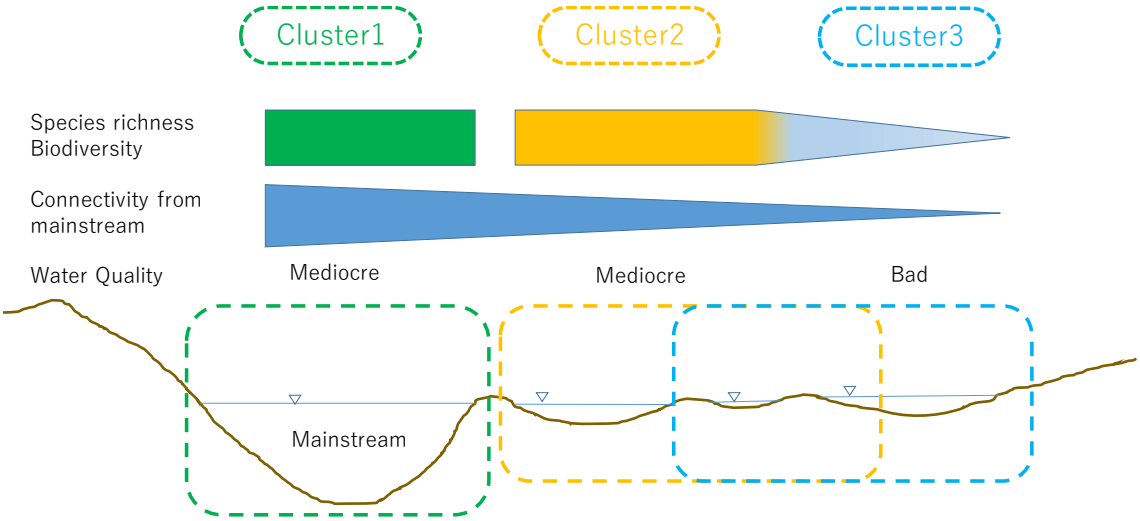

Fig. 2.7 The summary of relationship between fish composition clusters and environmental characteristics

The most important finding of the present study is that the area of floodplains around each study site is a primary factor that determines fish species richness in rivers, diversion canals, and ponds in the study area. The contribution of floodplain area to fish species richness was equivalent to hydrology (Con, Vel, and Dep) and water quality (DO, Turb) parameters. This was supported by the fact that the best models for richness of all native fish species, floodplain migratory native fish species, and floodplain non-migratory native fish species showed a positive effect of floodplain area, and most were significant (Table 2.6; Fig. 2.8), and by the fact that floodplain area was one of the top three parameters in all model selections in the terms of the selection frequency of the variables (Table 2.6).

In paddy fields, the parameters EC and Con were the major determinants of fish species richness (Table 2.6). The variable selection of EC may reflect the usage of fertilizers and pesticides, which increase electric conductivity, and the difficult access into isolated paddy field waterbodies because of migration barriers between paddy fields and ditches. In the GLMM selection of paddy fields, Con was selected one of major factor to determine fish species richness. Submerged paddy fields connected to other waterbodies by flooding play biological functions for the aquatic orgasm as submerged floodplains. The biological importance of submerged floodplains in fish ecology is well known. Shallow standing water and water with low dissolved oxygen provide refuge habitats from predators and flood disturbance (e.g. Petry et al. 2003); high nutrient inputs from rivers and high concentrations of feed organisms, such as phytoplankton (Keruzoré et al 2013), zooplankton (Simões et al. 2013), and fish (e.g. Gordon 1989, Pander et al. 2015), provide foraging and nursery habitats (e.g. Gordon 1989, Pander et al. 2015), and new connections between waterbodies and water level fluctuations caused by floods, trigger lateral spawning migration and egg deposition in some species (e.g. Merron and Mann 1995, Agostinho et al. 2004, Bonvechio and Allen 2005).

Table 2.6 Results of the general linear mixed model analysis of richness of all native species, floodplain migratory native species, and floodplain non-migratory native species in each waterbody type.

Waterbody type	Species richness	AIC	ΔAIC (from Null)	Wi	Morn's *I*	Intercept	Random intercept: Season		Random intercept: Waterbody Type					
							Rainy	Dry	River	Canal	Pond	Ditch	Paddy	Wetland
Total	All native fish	765.8	96.6	0.296	0.0346^{NS}	1.35***	-0.0486	0.0486	0.600	0.178	-0.0743	0.0969	-0.651	-0.125
	Floodplain migratory	650.4	48.4	0.145	0.0596^{NS}	0.698**	-0.00203	0.00203	0.579	0.143	-0.135	0.171	-0.648	-0.0756
	Floodplain non-migratory	509	46.6	0.128	0.0390^{NS}	-0.0291	0	0	1.13	0.240	-0.350	-0.270	-0.609	-0.0659
River	All native fish	143.8	54.1	0.159	-0.0844^{NS}	3.14***	1.25e-17	-1.25e-17	-	-	-	-	-	-
	Floodplain migratory	133.5	40.3	0.177	-0.0136^{NS}	2.01***	0	0	-	-	-	-	-	-
	Floodplain non-migratory	119.4	14.7	0.117	0.0107^{NS}	2.72***	1.13e-18	-1.13e-18	-	-	-	-	-	-
Canal	All native fish	214.5	14.7	0.178	0.0707^{NS}	1.37***	0	0	-	-	-	-	-	-
	Floodplain migratory	182.3	12.2	0.161	0.0646^{NS}	0.904***	0	0	-	-	-	-	-	-
	Floodplain non-migratory	140.0	1.39	0.0479	-0.0106^{NS}	0.380$^{.}$	0	0	-	-	-	-	-	-
Paddy	All native fish	147.6	49.0	0.0730	0.105^{NS}	1.17**	0	0	-	-	-	-	-	-
	Floodplain migratory	120.0	19.6	0.0757	-0.107^{NS}	0.978*	0	0	-	-	-	-	-	-
	Floodplain non-migratory	85.4	33.8	0.0816	0.0137^{NS}	1.65*	0	0	-	-	-	-	-	-
Pond	All native fish	107.8	8.89	0.0765	-0.216^{NS}	1.02***	0	0	-	-	-	-	-	-
	Floodplain migratory	97.2	4.55	0.0651	-0.205^{NS}	0.835**	0	0	-	-	-	-	-	-
	Floodplain non-migratory	85.4	4.92	0.0519	-0.0878^{NS}	-0.475^{NS}	0	0	-	-	-	-	-	-

† Appearance rate of containing model in the models with ΔAIC<4 from the best model [%]

Waterbody type	Species richness	Coefficient of independent variables EC (appearance) †	Dep (appearance) †	Do (appearance) †	Turb (appearance) †	Vel (appearance) †	Con (appearance) †	Dist (appearance) †	FA [Buffer Size] (appearance) †	
Total	All native fish	-0.000399$^{\cdot}$ (50%)	(100%)	(33.3%)	0.000955*** (100%)	-0.347* (100%)	0.867*** (100%)	0.00709* (66.7%)	0.106*** (100%)	[2000]
	Floodplain migratory	-0.000454$^{\cdot}$ (50%)	0.698^{NS} (50%)	(50%)	0.00119*** (100%)	-0.288^{NS} (50%)	0.764*** (100%)	0.00877* (100%)	0.118*** (100%)	[2000]
	Floodplain non-migratory	(37.5%)	0.504** (100%)	(37.5%)	0.000689^{NS} (43.8%)	-0.576** (93.8%)	1.04*** (100%)	(37.5%)	0.0758* (93.8%)	[1000]
River	All native fish	(50%)	-0.412* (42.9%)	-0.245*** (100%)	0.00180* (57.1%)	(42.9%)	ND	-	0.166*** (100%)	[2000]
	Floodplain migratory	(42.9%)	(50%)	-0.202** (100%)	(50%)	(42.9%)	ND	-	0.202*** (100%)	[2000]
	Floodplain non-migratory	(28.6%)	(38.1%)	-0.252*** (95.2%)	(38.1%)	(38.1%)	ND	-	(47.6%)	
Canal	All native fish	(36.4%)	(36.4%)	(36.4%)	0.00116*** (100%)	(36.4%)	ND	0.0102*** (100%)	0.0957** (100%)	[500]
	Floodplain migratory	(35.7%)	(28.6%)	(28.6%)	0.0031*** (100%)	(28.6%)	ND	0.0121** (92.9%)	0.0872* (78.6%)	[500]
	Floodplain non-migratory	(28.8%)	(40.4%)	(21.2%)	0.00997$^{\cdot}$ (50%)	1.17$^{\cdot}$ (51.9%)	ND	(25%)	0.102* (65.4%)	[1000]
Paddy	All native fish	-0.00198** (100%)	(38.9%)	0.0684^{NS} (63.9%)	0.00133* (58.3%)	(36.1%)	1.27*** (100%)	(27.8%)	(47.2%)	
	Floodplain migratory	-0.00160* (100%)	(44.8%)	(37.9%)	0.00162* (65.5%)	(31%)	1.12*** (100%)	(24.1%)	(27.6%)	
	Floodplain non-migratory	-0.00432** (100%)	(28.6%)	(42.9%)	(28.6%)	(32.1%)	1.83*** (100%)	(25%)	-0.171$^{\cdot}$ (57.1%)	[1000]
Pond	All native fish	(23.3%)	(26.7%)	0.0793* (86.7%)	-0.00468^{NS} (56.7%)	(36.7%)	(23.3%)	(23.3%)	0.144** (100%)	[2000]
	Floodplain migratory	(23.3%)	(23.3%)	(23.3%)	(23.3%)	(23.3%)	(23.3%)	(26.7%)	0.130* (96.7%)	[2000]
	Floodplain non-migratory	(24.4%)	(31.1%)	0.171** (100%)	-0.00739^{NS} (51.1%)	(26.7%)	(26.7%)	(42.2%)	0.148* (68.9%)	[1000]

† Appearance rate of containing model in the models with ΔAIC<4 from the best model [%]

Level of significance: *** P < 0.001, ** P < 0.01, * P< 0.05, $^{\cdot}$ P< 0.1, ^{NS} P> 0.1

.24 ND: No data, -: Unused

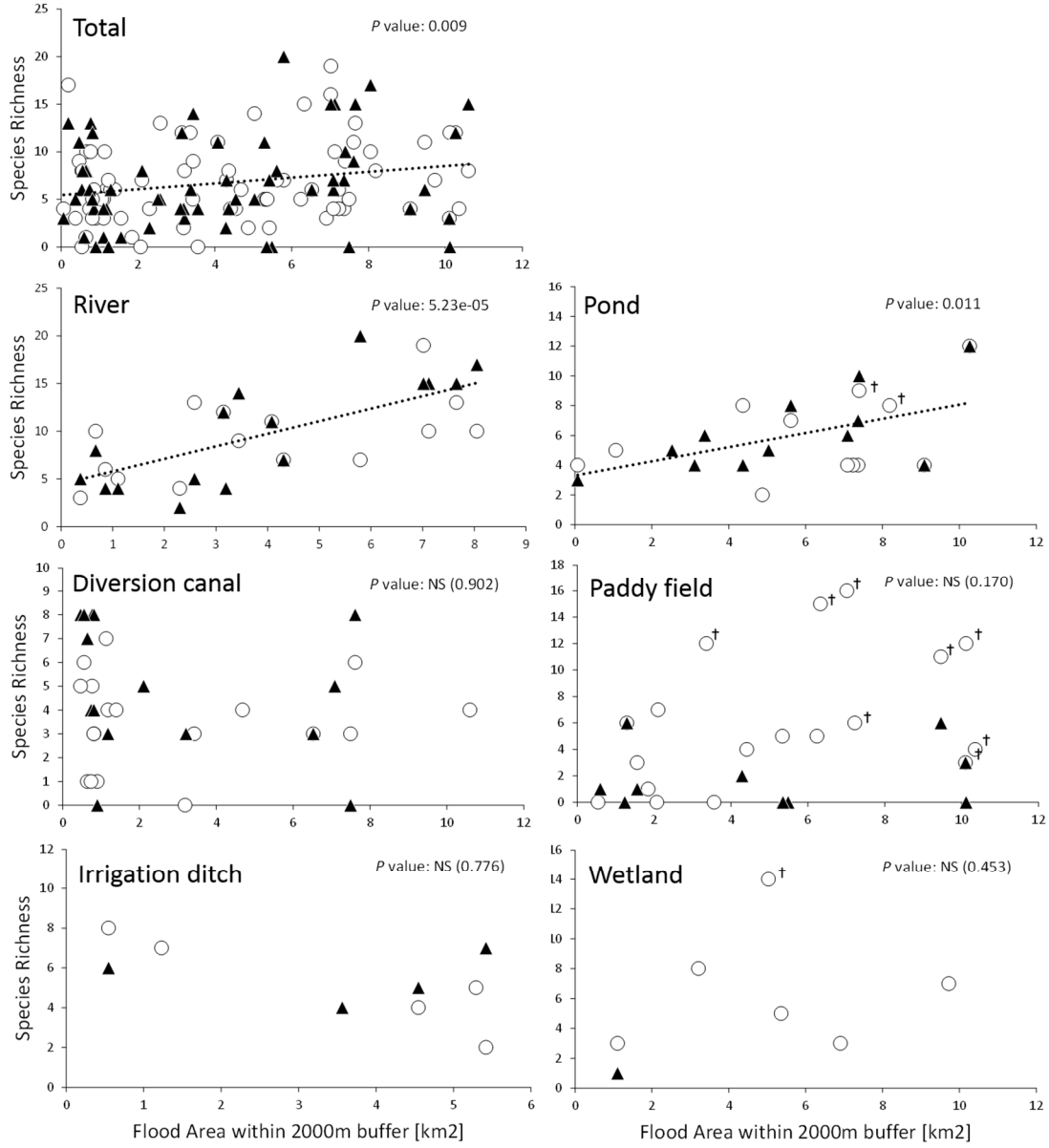

Fig. 2.8 The relationship between floodplain area (2000-m buffer size) and richness of all native fish species for each waterbody type. The broken lines represent significant linear regressions ($P < 0.01$). P values are shown in the top right of each plot. Open circles indicate sites surveyed in the rainy season. Black triangles indicate sites surveyed in the dry season. Crosses to the upper right open circles represent the study sites temporarily connected to main rivers by floodwaters in the rainy season survey.

In the present study, increasing fish richness with increasing floodplain area probably reflected a direct association with floodplain utilization by migratory fish species. The parameter FA was retained with relatively higher frequency in model selections for floodplain migratory species compared with those for non-migratory species in every waterbody type except paddy fields (Table 2.6). In addition, the proportion of small size fishes (<20 mm total length) of four common species (*Esomus metallicus*, *Trichopsis vittata*, *Trichopodus trichopterus*, and *Trichopodus microlepis*), classified as 0+ juveniles, was increased in temporarily connected survey sites

compared with isolated survey sites (Fig. 2.4). Furthermore, although numbers were less than for the four common species mentioned above, some fluvial and lacustrine fish species, such as *Xenentodon cancila*, *Barbonymus gonionotus*, *Cyclocheilichthys apogon*, *Cyclocheilichthys lagleri*, *Puntius brevis*, and *Amblypharyngodon chulabhornae* (Appendix 2.1), were captured in temporarily inundated study sites. This finding indicates that individuals of these species moved into floodplains from permanent waterbodies in the early part of the rainy season, even before maximum flood levels occurred.

Previous studies have demonstrated that lateral connectivity between rivers and floodplain waterbodies influences fish distribution and richness in floodplain. Most of these studies reported that fish richness decreases with the reduction of lateral connectivity from rivers to isolated waterbodies (e.g. Ward et al. 1999, Petry et al. 2003, Tockner et al. 2000, Pander et al. 2015). My observation corresponded to these studies. In this study, Con, Dist and FA were the variables that represent lateral connectivity from main rivers. Contrary to my expectation, I found no evidence that Dist affect fish richness in the waterbodies except for canal. While FA showed significant positive correlation with fish richness in the result of GLMM and AIC model selection. Dist was defined as the route distance from the nearest river via channel network, it means that Dist doesn't always reflect the accurate connectivity considering migration barriers such as dams. The result is, however, seems to me that temporary connection between rivers and floodplain waterbodies caused by "flood event" is more dominant factor determine fish species richness rather than ordinary connection via channel network for these kind of waterbodies in the region.

This study revealed the importance of floodplain existence and flood event for fishes in the mid-region of the Chao Phraya River basin. However, this chapter couldn't answer the question that what kind of characteristics of flood event in each floodplain (i.e. flood regime of each floodplain) are important for fish species in the region. Poff et al. (1997) and Richter (1996) characterized the composition element of flood regime by the four factors (: magnitude, frequency, timing, duration). The description and biological role of each factor are follows:

Magnitude of flood regime: The magnitude of flood can refer either to absolute or to relative discharge (e.g., the water depth of inundated floodplain). Maximum and minimum magnitudes of flood vary with climate and watershed scale. The magnitude of flood defines habitat attributions as inundated are or volume, or position and shape of the waterbodies in floodplain.

Frequency of flood regime: The frequency of occurrence refers to how often a flow above a given magnitude. Frequency of occurrence is inversely related to flow magnitude. The frequency of flood events may be associated with reproduction and mortality (e.g. disturbance stress or wash-out for individuals, provide reproduction opportunities) events for many species, thereby impact population dynamics.

Duration of flood event: The duration is the period of time associated with a specific flow condition. Duration can be defined relative to a particular flow event (e.g., a flood- plain may be inundated for a specific number of days by a flood). The duration of flood event can determine whether a species with certain lifecycle phase (for example, egg hatching, nursery phase for larval fishes in a inundated floodplain).

Timing of flood regime: The timing of flood of defined magnitude refers to the regularity with which they occur. This regularity can be defined formally or informally and with reference to different time scales (Poff 1996). For example, annual peak floods may occur with low seasonal predictability or with high seasonal predictability. The timing of occurrence of particular flood event can determine whether a species with certain lifecycle requirements are met, it result in the mortality and productivity of species associated with floods.

In order to examine the impacts of these four flood regime factors for the fish species in the region, I established the hydraulic model which simulate the flooding of the middle stream of the Chao Phraya River in the next chapter. Than the flood regime characteristics of each sampling sites were obtained from the simulation result (Chapter 5).

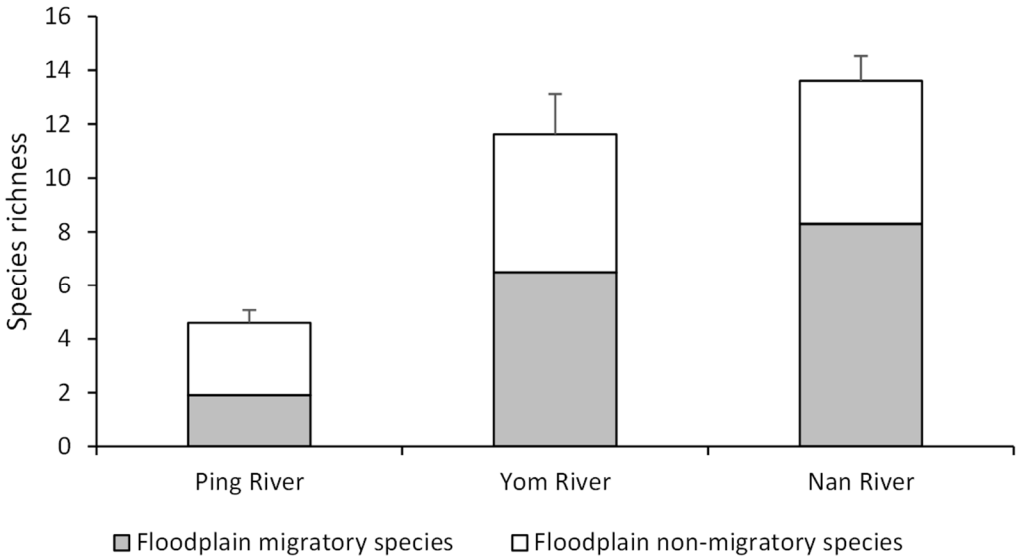

Figure. 2.9 Native fish species richness and composition for each of the three rivers surveyed. Bars indicate the standard error.

Table 2.7 The appearance probability of native fish species for each of the three rivers surveyed.

Species	Lateral migration	Basin: Ping	Yom	Nan
Oryzias sp.				10
Xenentodon cancila	○		25	20
Xenentodon sp.	○			20
Dermogenys siamensis		10	12.5	10
Corica laciniata			12.5	
Clupeoides borneensis				10
Clupeichthys aesarnensis		10		40
Clupeichthys sp.			25	
Acantopsis spp.		40	62.5	60
Lepidocephalichthys (c.f. berdmorei)				10
Pangio anguillaris	○			20
Yasuhikotakia eos			12.5	
Barbichthys laevis	○			10
Barbonymus altus	○	20	50	30
Barbonymus gonionotus	○		50	40
Barbonymus schwanenfeldii	○	20	12.5	40
Barbonymus sp.	○	10		10
Crossocheilus reticulatus	○	10		10
Cyclocheilichthys armatus	○		25	40
Cyclocheilichthys apogon	○	20	12.5	
Cyclocheilichthys enoplos	○	10	25	30
Cyclocheilichthys lagleri	△			10
Esomus metallicus	○		37.5	30
Henicorhynchus siamensis	○		37.5	70
Henicorhynchus sp.	○	10		
Hypsibarbus malcolmi		30	12.5	10
Hypsibarbus vernayi		20	25	10
Hypsibarbus wetmorei		10	12.5	
Labiobarbus siamensis			25	20
Labiobarbus leptocheila			12.5	40
Labiobarbus sp.				10
Mystacoleucus greenwayi				
Mystacoleucus marginatus		100	87.5	50
Osteochilus vittatus	○		12.5	60
Osteochilus waandersii	○			10
Osteochilus sp.				10

Species	Lateral migration	Basin: Ping	Yom	Nan
Paralaubuca typus	○		25	60
Paralaubuca sp.				
Parachela oxygastroides	○		25	10
Parachela siamensis	○			10
Parachela williaminae				
Parachela sp.	○			10
Puntioplites proctozysron	○	10	87.5	20
Puntius brevis	○			30
Raiamas guttatus	○	40		
Systomus rubripinnis	○			10
Thynnichthys thynnoides	○			10
Rasbora aurotaenia				10
Rasbora borapetensis	○			20
Rasbora dusonensis		10	12.5	60
Rasbora paviana		10		30
Doryichthys martensii				10
Chitala ornata				10
Notopterus notopterus	○		12.5	
Oxyeleotris marmorata	○			10
Parambassis siamensis	○	20	87.5	70
Parambassis wolffii	○		12.5	10
Anabas testudineus	○			20
Channa striata	○		12.5	
Oreochromis niloticus		10		10
Gobiopterus chuno			12.5	
Mugilogobius rambaiae			25	

Species	Lateral migration	Basin: Ping	Yom	Nan
Pristolepis fasciata			25	10
Osphronemus goramy				20
Trichopsis pumila				
Trichopsis vittata	○		12.5	
Trichopodus microlepis		10		10
Trichopodus trichopterus	○	10	25	
Brachirus harmandi		10	37.5	40
Cynoglossus feldmanni		10		
Hemibagrus filamentus	○		25	20
Hemibagrus spilopterus	○			
Mystus albolineatus			25	10
Mystus multiradiatus	○			10
Mystus mysticetus	○			10
Pseudomystus siamensis			12.5	
Pangasius sanitwongsei			12.5	10
Pangasius macronema	○		12.5	20
Pangasius sp.			12.5	
Kryptopterus cryptopterus		12.5		
Phalacronotus bleekeri		12.5	10	
Bagarius yarrelli		12.5		
Mastacembelus armatus		12.5	30	
Tetraodon cambodgiensis			10	

Appendix 2.1 Summary of fish sampling data

Order	Family	Scientific name	Lateral migration †	Alien	Sites	*N*	Prevalence at each wtaerbody type					
							River	Diversion canal	Pond	Irrigation ditch	Paddy field	Wetland
Beloniformes												
	Adrianichthyidae	*Oryzias sp.*			22	108	○	○	○	○	○	○
	Belonidae	*Xenentodon cancila* (Hamilton 1822)	○		6	10	○		○		○	
		Xenentodon sp.			2	2	○					
	Hemiramphidae	*Dermogenys siamensis* (Fowler 1934)			27	103	○	○	○	○	○	○
Clupeiformes												
	Clupeidae	*Corica laciniata* (Fowler 1935)			1	1	○					
		Clupeoides borneensis (Bleeker 1851)			1	4	○					
		Clupeichthys aesarnensis (Wongratana 1983)			6	15	○					
		Clupeichthys sp.			2	4	○					
Cypriniformes												
	Cobitidae	*Acantopsis spp.*			16	42	○	○				
		Lepidocephalichthys hasselti (Cuvier & Valenciennes 1846)	○		4	7		○	○		○	
		Lepidocephalichthys (c.f. hasselti) (Cuvier & Valenciennes 1846)			2	10		○				
		Lepidocephalichthys (c.f. berdmorei) (Blyth, 1860)			1	1	○					
		Pangio anguillaris (Vaillant 1902)	○		3	3	○	○				
		Yasuhikotakia eos (Taki 1972)			1	11	○					

† According to FishBase (http://www.fishbase.org).

Order	Family	Scientific name	Lateral migration †	Alien	Sites	*N*	Prevalence at each wtaerbody type					
							River	Diversion canal	Pond	Irrigation ditch	Paddy field	Wetland
Cypriniformes												
	Cyprinidae	*Amblypharyngodon chulabhornae* (Vidthayanon & Kottelat 1990)	○		22	75		○	○	○	○	○
		Barbichthys laevis (Cuvier & Valenci– ennes 1842)	○		1	1	○					
		Barbonymus altus (Günther, 1868)	○		15	98	○	○	○	○		
		Barbonymus gonionotus (Bleeker, 1849)	○		22	109	○	○	○	○	○	○
		Barbonymus schwanefeldii (Bleeker 1854)	○		10	78	○	○				
		Barbonymus sp.	○		2	6	○					
		Crossocheilus reticulatus (Fowler 1934)	○		2	3	○					
		Cyclocheilichthys armatus (Cuvier & Valenciennes 1842)	○		13	82	○	○	○			
		Cyclocheilichthys apogon (Cuvier & Valenciennes 1842)	○		13	211	○	○	○	○		
		Cyclocheilichthys lagleri (Sontirat 1985)	○		7	15	○	○	○			
		Cyclocheilichthys repasson (Bleeker 1853)	○		1	2	○	○	○		○	○
		Cyclocheilichthys sp.			4	10		○				
		Cyclocheilos enoplos (Bleeker 1849)	○		9	11		○			○	
		Esomus metallicus (Ahl 1924)	○		72	1572	○	○	○	○	○	○
		Gymnostomus siamensis (Sauvage 1881)	○		19	54	○	○	○		○	○
		Henicorhynchus sp.	○		1	37	○					
		Hypsibarbus malcolmi (Smith 1945)			6	73	○					
		Hypsibarbus vernayi (Norman 1925)			5	14	○					
		Hypsibarbus wetmorei (Smith 1931)			2	64	○					
		Labeo chrysophekadion (Bleeker 1849)	○		1	1		○				
		Labeo rohita (Hamilton 1822)	○		2	5		○	○			
		Labeo sp.	○		1	3		○				
		Labiobarbus siamensis (Sauvage 1881)			22	73	○	○	○		○	
		Labiobarbus leptocheilus (Cuvier & Valenciennes 1842)			8	24	○	○	○			○
		Labiobarbus sp.			4	13	○	○			○	
		Mystacoleucus obtusirostris (Cuvier & Valenciennes 1842)			26	298	○	○				
		Osteochilus vittatus (Cuvier & Valenciennes 1842)	○		13	19	○	○				
		Osteochilus waandersii (Bleeker 1853)	○		1	1	○					
		Osteochilus sp.			6	11	○	○				○
		Paralaubuca typus (Bleeker 1864)	○		13	83	○	○		○	○	
		Paralaubuca sp.			3	5		○			○	
		Parachela oxygastroides (Bleeker 1852)	○		6	43	○	○				
		Parachela siamensis (Günther 1868)	○		1	1	○					
		Parachela williaminae (Fowler 1934)			1	1			○			
		Parachela sp.	○		4	4	○	○			○	
		Puntioplites proctozysron (Bleeker 1864)	○		18	45	○	○			○	
		Puntius brevis (Bleeker 1849)	○		17	125	○	○	○	○	○	○
		Puntius (cf. masyai) (Smith 1945)			3	4			○		○	
		Puntius sp.			1	2					○	
		Raiamas guttatus (Day 1870)	○		4	20	○					
		Systomus rubripinnis (Cuvier & Valenciennes 1842)	○		1	3	○					
		Thynnichthys thynnoides (Bleeker 1852)	○		1	10	○					
		Rasbora aurotaenia (Tirant 1885)			5	15	○	○	○		○	
		Rasbora borapetensis (Smith 1934)	○		10	20	○		○	○	○	○
		Rasbora dusonensis (Bleeker 1850)			10	52	○		○			
		Rasbora paviana (Tirant 1885)			11	51	○	○	○		○	
		Rasbora sp.			4	14		○			○	
		Systomus rubripinnis (Cuvier & Valenciennes 1842)	○		2	6		○	○			

† According to FishBase (http://www.fishbase.org).

Order	Family	Scientific name	Lateral migration †	Alien	Sites	*N*	Prevalence at each wtaerbody type					
							River	Diversion canal	Pond	Irrigation ditch	Paddy field	Wetland
Gasterosteiformes												
	Syngnathidae	*Doryichthys martensii* (Peters 1868)			1	1	○					
Osteoglossiformes												
	Notopteridae	*Chitala ornata* (Gray 1831)			1	1	○					
		Notopterus notopterus (Pallas 1769)	○		6	8	○	○		○	○	
Perciformes												
	Ambassidae	*Parambassis siamensis* (Fowler 1937)	○		40	418	○	○	○	○	○	○
		Parambassis wolffii (Bleeker 1850)	○		4	14	○	○			○	
	Anabantidae	*Anabas testudineus* (Bloch 1792)	○		24	78	○	○	○	○	○	○
	Channidae	*Channa striata* (Bloch 1793)	○		13	110	○	○	○		○	
	Cichlidae	*Oreochromis niloticus* (Linnaeus 1758)		○	13	66	○	○	○	○	○	○
	Eleotrididae	*Oxyeleotris marmorata* (Bleeker 1852)	○		5	8	○	○	○		○	
	Gobiidae	*Gobiopterus chuno* (Hamilton 1822)			9	23	○	○	○		○	○
		Mugilogobius rambaiae (Smith 1945)			3	11	○	○				
		Mugilogobius sp.			1	1		○				
		Rhinogobius sp.			2	4		○			○	
		Brachygobius sp.			3	4		○	○		○	
	Nandidae	*Pristolepis fasciata* (Bleeker 1851)			14	38	○	○	○		○	○
	Osphronemidae	*Osphronemus goramy* (La Cepède 1801)			2	2	○					
		Trichopsis pumila (Arnold 1936)			24	99	○	○	○	○	○	○
		Trichopsis vittata (Cuvier & Valenciennes 1831)	○		70	576	○	○	○	○	○	○
		Trichopodus microlepis (Günther 1861)			39	409	○	○	○	○	○	○
		Trichopodus pectoralis (Regan 1910)	○		8	23		○	○			○
		Trichopodus trichopterus (Pallas 1770)	○		67	682	○	○	○	○	○	○
Pleuronectiformes												
	Soleidae	*Brachirus harmandi* (Sauvage 1878)			8	14	○					
	Cynoglossidae	*Cynoglossus feldmanni* (Bleeker 1854)			1	1	○					
Siluriformes												
	Bagridae	*Hemibagrus filamentus* (Chaux & Fang 1949)	○		4	6	○					
		Hemibagrus spilopterus (Ng & Rainboth 1999)	○		2	8			○		○	
		Mystus albolineatus (Roberts 1994)			11	22	○	○		○	○	
		Mystus multiradiatus (Roberts 1992)	○		11	40	○	○	○	○	○	○
		Mystus mysticetus (Roberts 1992)	○		9	43	○	○	○		○	
		Pseudomystus siamensis (Regan 1913)			3	11	○	○				
	Clariidae	*Clarias macrocephalus* (Günther 1864)			1	1		○				
		Clarias batrachus (Linnaeus, 1758)			1	1			○			
	Loricariidae	*Pterygoplichthys sp.*		○	3	5		○		○		
	Pangasiidae	*Pangasius sanitwongsei* (Smith 1931)			2	5	○					
		Pangasius macronema (Bleeker 1850)	○		3	4	○					
		Pangasius sp.			1	2	○					
	Silurida	*Kryptopterus cryptopterus* (Bleeker 1851)			1	14	○					
		Phalacronotus bleekeri (Günther 1864)	○		2	3	○					
	Sisoridae	*Bagarius yarrelli* (Sykes 1839)			1	1	○					
Synbranchiformes												
	Mastacembelidae	*Mastacembelus armatus* (La Cepède 1800)	○		6	8	○					
	Synbranchidae	*Monopterus javanensis* (La Cepède, 1800)			1	1			○			
Tetraodontiformes												
	Tetraodontidae	*Pao cambodgiensis* (Chabanaud 1923)			1	1	○					

† According to FishBase (http://www.fishbase.org).

Chapter3

Flood simulation of 2011 and 2014 Thailand flood using iRIC

3.1 Introduction

There are many previous studies which simulate the 2011 Thailand floods or past large floods (e.g. 1995 and 2006) in The Chao Phraya River in terms of flood risk management. For example, Mateo et al. (2014) simulated the dam operation impact on the mitigation of 2011 floods, and concluded the dams reduced 40 % of inundated area. Oki (2012) and Prajamwong (2009) clarified flood condition in the downstream of The Chao Phraya River basin and proposed some flood control measures. Cham et al. (2015) estimated the impact of improving existing reservoirs in middle stream of the Chao Phraya in order to mitigate downstream floods based on the 2011 floods. Sayama et al. (2015) simulated the relationship between long-term rain-runoff and inundation volume in the whole The Chao Phraya River basin, and elucidated the flood sensitivity of the basin that 1% increase in rainfall causes 4.2% increase in flood inundation volume.

However, flood conditions at the usual-scale floods years, which primarily dominates the long-term fish community dynamics and structure, were paid less attention and poorly understood.

In this chapter, I simulated the flood conditions in the middle stream of The Chao Phraya River using river flow analysis software package International River Interface Cooperative (iRIC) in 2011 and 2014. Then the accuracy of the model was validated.

3.2 Materials and methods

3.2.1 Estimation of return period of rainfall in 2011 and 2014

To estimate the magnitude of the floods in the middle stream of The Chao Phraya River for year 2014 when I conducted the fish survey, the return period of precipitation in 2014 in Northern part of Thailand was calculated (Fig. 3.1).

Prior estimating the return period of 2014 precipitation in Northern part of Thailand, the precipitation statistic which can properly explain the magnitude of the floods (for example, annual maximum daily precipitation, annual maximum monthly precipitation, and maximum annual precipitation) is need to elucidate. An appropriate precipitation statistic to describe flood magnitude is known to differ from location to location by the factors such as basin characteristics (slope, area, degree of roughness), and rainfall characteristics. The appropriate period to estimate the precipitation in this region is determined by examining the relationship between annual maximum inundated area and four annual precipitation statistics (: annual maximum monthly precipitation, annual maximum three-month precipitation, annual maximum six-month precipitation, and annual precipitation; monthly precipitation characteristics see Fig. 3.2). The annual maximum areas that experienced flood inundation in the region from 2005 to 2014 were obtained from GISTDA (2015), and the rainfall data of rainfall stations in Thailand was obtained from NNDC Climate data online

(http://www7.ncdc.noaa.gov/CDO/cdo). 17 rainfall stations in Northern part of Thailand were used for the analysis based on the Thiessen polygon (Fig. 3.1). The annual maximum six-month precipitation showed highest correlation with the flood magnitude (R^2=0.902, Fig. 3.3) and was considered the most adequate precipitation statistics which describe the flood magnitude of the region among the four statistics used in this analysis.

The analysis of the return period of 2014 precipitation was conducted by adapting annual maximum six-month precipitations into possible 13 frequency models (Table 3.1) in the period from 1976 to 2014 (39 years). To assess the fitness of each frequency model, Standard Least Squares Criterion (SLSC) was examined (Takasao et al. 1986). The model with SLSC $\leqq$ 0.04 was considered as a good fit model. The analyses were computed by Hydrological Statistics Utility (JICE, ver. 1.5). 17 rainfall stations in Northern part of Thailand with no missing value in the period from 1976 to 2014 and its Thiessen polygon were used for calculating the maximum annual 6-month precipitation (Fig. 3.1).

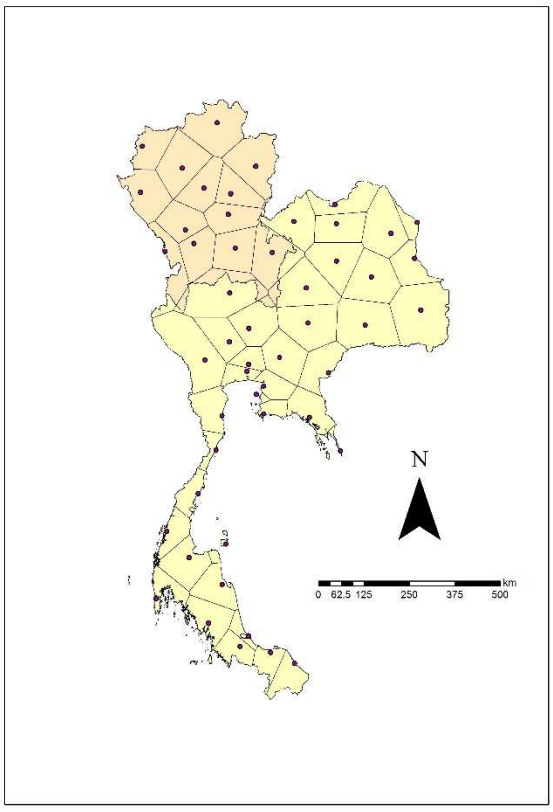

Fig. 3.1. Rainfall station locations from NNDC Climate data online and the its Thiessen polygons. The orange area is the northern part of Thailand.

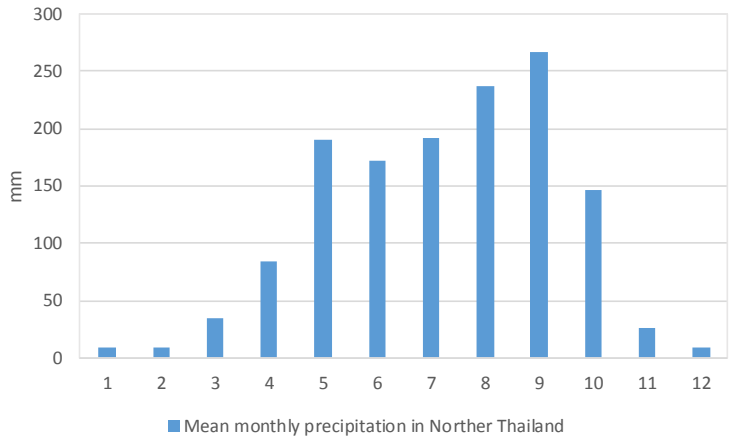

Fig. 3.2. Mean monthly precipitation in the northern part of Thailand from 1976 to 2014.

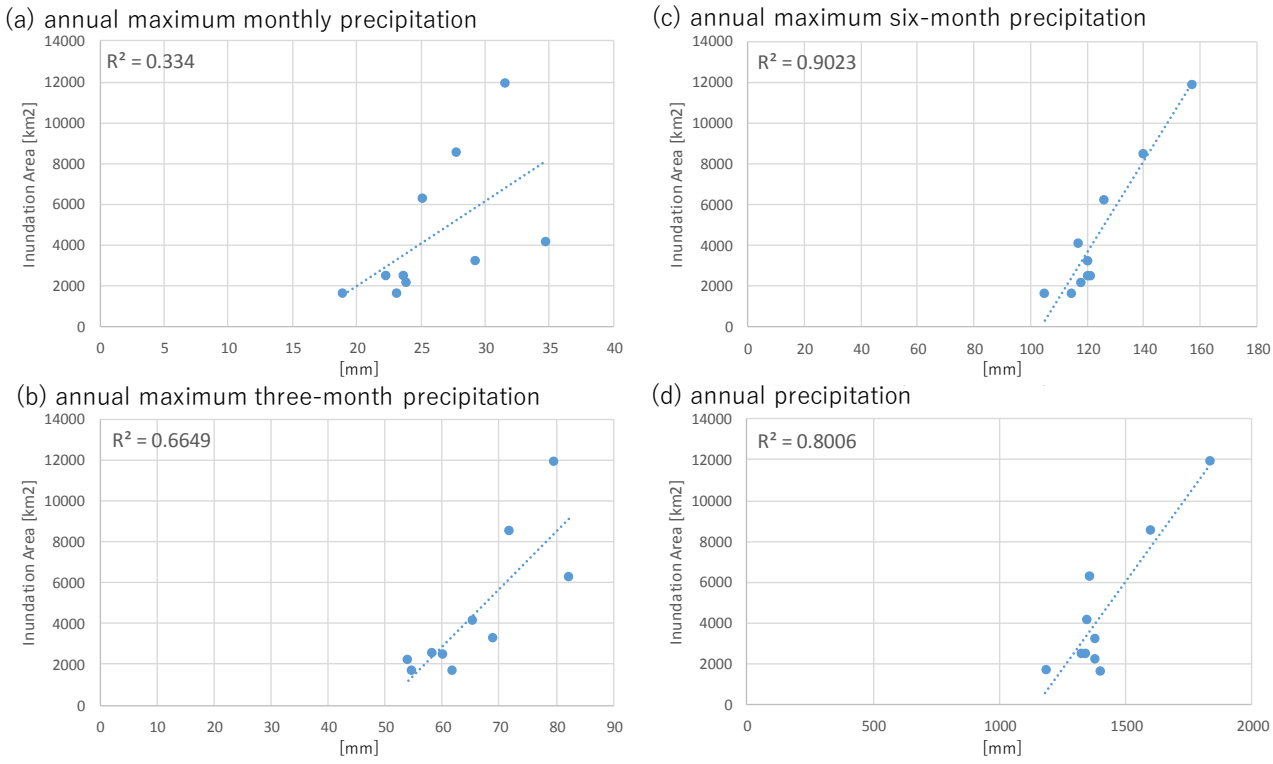

Fig. 3.3. Relationship between the annual maximum inundated area and (a) annual maximum monthly precipitation, (b) annual maximum three-month precipitation, (c) annual maximum six-month precipitation, (d) annual precipitation from 2005 to 2014.

Table. 3.1. Frequency models used for calculating return period

Name of Model	Abbreviation
Exponential Distribution	Exp
Gumbel Distribution	Gumbel
Generalized Extreme Value Distribution	GEV
Square-Root Exponential Type Distribution	Sqrt-Et
Log Pearson type III Distribution (Real Number Calculations)	LP3Rs
Log Pearson type III Distribution (Logarithmic Calculations)	LogP3
Iwai Method	Iwai
Ishihara-Takase Method	IshiTaka
Log normal Distribution 3 Population Quantile Method	LN3Q
Log normal Distribution 3 Population (Slade II)	LN3PM
Log normal Distribution 2 Population (Slade I, L Moment)	LN2LM
Log normal Distribution 2 Population (Slade I, Product Moment)	LN2PM
Log normal Distribution 4 Population (Slade IV, Product Moment)	LN4PM

3.2.2 Objected area and simulation period for iRIC

An iRIC model was established in the area with in the black rectangle shown in Fig. 3.4 The nearest upstream runoff stations are P.7A for Ping River, Y.17 for Yom River, and N.7A for Nan River. The simulation was computed from July 1 to November 30, 2011 and from July 1 to November 30, 2014.

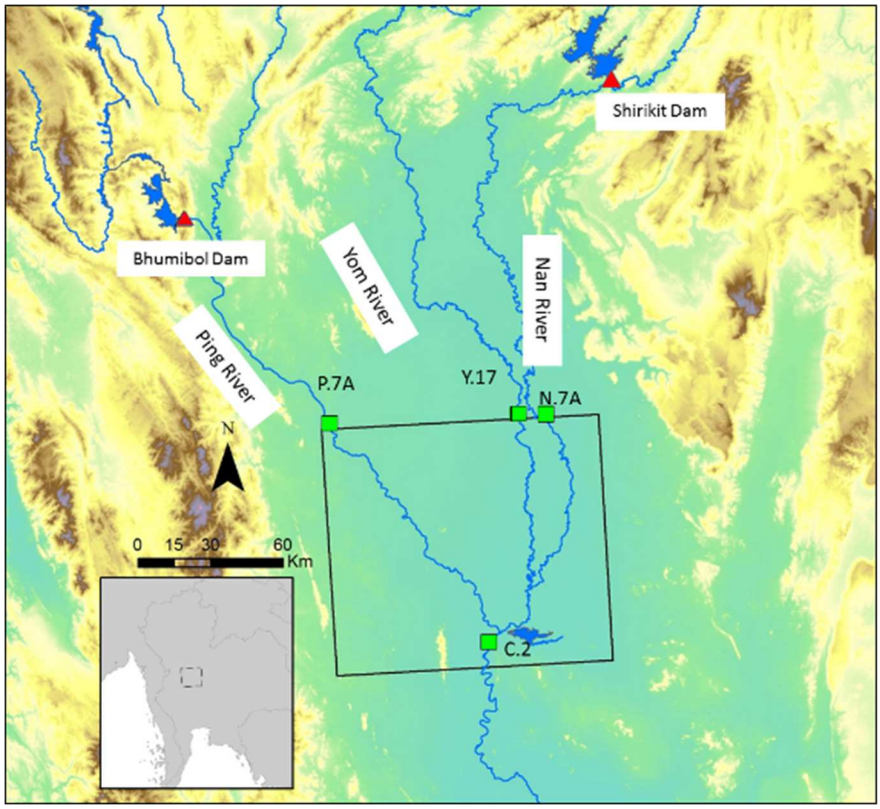

Fig. 3.4. Objected Area.

3.2.3 Modeling and basic equation

The floods were simulated using Nays 2D Flood solver in iRIC software (iRIC project, ver. 2.3). Nays 2D Flood is a flood flow analysis solver, which is applied to unsteady two dimensional plane flow simulation. It has been applied to the flood flow analysis of small/mid-scale rivers, primitive rivers, and rivers in developing countries (Akashi et al. 2012). The equations used in Nays 2D Flood as follows:

[Equation of continuity]

$$\frac{\partial h}{\partial t}+\frac{\partial(\gamma_x hu)}{\partial x}+\frac{\partial(\gamma_y hu)}{\partial y}=q$$

[Equation of motion]

$$\frac{\partial(uh)}{\partial t}+\frac{\partial(hu^2)}{\partial x}+\frac{\partial(huv)}{\partial y}=-\gamma_v gh\frac{\partial H}{\partial x}-\frac{\tau_x}{\rho}+D^x+hR_x$$

$$\frac{\partial(vh)}{\partial t}+\frac{\partial(huv)}{\partial x}+\frac{\partial(hv^2)}{\partial y}=-\gamma_v gh\frac{\partial H}{\partial y}-\frac{\tau_y}{\rho}+D^y+hR_y$$

Where,

$$\frac{\tau_x}{\rho}=C_f u\sqrt{u^2+v^2} \qquad \frac{\tau_y}{\rho}=C_f v\sqrt{u^2+v^2}$$

$$hR_x=\frac{h}{2}C_d{}'(1-\gamma_x)u\sqrt{u^2+v^2} \qquad hR_y=\frac{h}{2}C_d{}'(1-\gamma_y)v\sqrt{u^2+v^2}$$

$$D^x=\frac{\partial}{\partial x}\left[v_t\frac{\partial(uh)}{\partial x}\right]+\frac{\partial}{\partial y}\left[v_t\frac{\partial(uh)}{\partial y}\right]$$

$$D^y=\frac{\partial}{\partial x}\left[v_t\frac{\partial(vh)}{\partial x}\right]+\frac{\partial}{\partial y}\left[v_t\frac{\partial(vh)}{\partial y}\right]$$

$$C_f=\frac{g\gamma_v {n_m}^2}{h^{1/3}}$$

h: water depth

t: time

u: flow velocity in the x direction

v: flow velocity in the y direction

g: gravitational acceleration

H: water surface elevation

τ_x: riverbed shear stress in the x direction

τ_y: riverbed shear stress in the y direction

C_f: riverbed friction coefficient

n_m: Manning's roughness coefficient of a grid cell

ν_t: eddy velocity coefficient

ρ: the density of water

C_d': drag coefficient per representative length of a building (=0.392)

γ_v: the porosity of a grid cell (1- urban density(%)/100)

γ_x: the porosity of a grid cell in the x direction

γ_y: the porosity of a grid cell in the y direction

Here, put the hypothesis for simplification: $\gamma_v=\gamma_x=\gamma_y$

q: inflow through a box culvert, a sluice pipe or a pump per unit area

3.2.4 Simulation setup and input data

A grid cell size was defined as 300m×300m, and upper end of the objective area was defined inflow boundary, downstream end of the area was defined as free outflow boundary, right and left edges of the area were defined wall boundary (Fig. 3.5). The grid cell size was examined by comparing the calculation times among various grid sizes, and decided as finer resolution within an acceptable calculation time (approximately 35 hours).

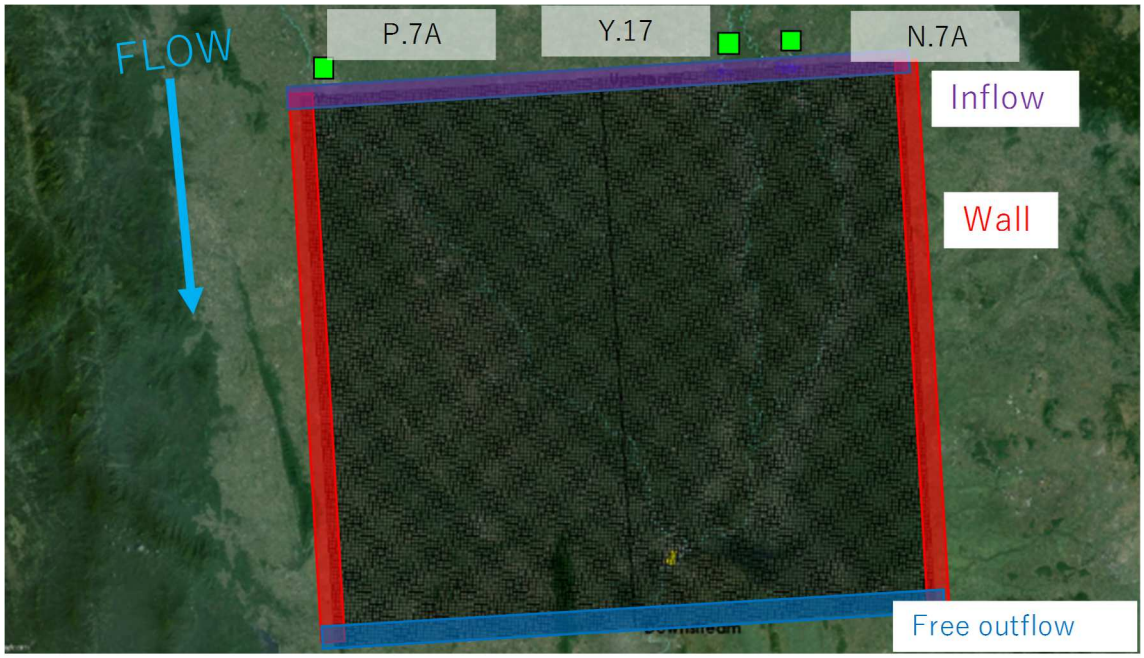

Fig. 3.5 Grid cells and boundary conditions of each side. Sattelite image is adapted from Landsat OLI image on March 29, 2014.

Stream discharges for runoff station Y.17, N.7A and P.7A are used as inflows located at the upper end of the objective area across the three rivers (Fig. 3.6, Fig. 3.7). Stream discharge data in 2011 and 2014 were obtained from RID (http://hydro-2.com/). Digital Elevation Model (DEM) data was derived from Shuttle Radar Topography Mission (SRTM, resolution: 1 arc-second) in 2010. The SRTM data was resampled into 300m. Manning's roughness coefficient of each mesh was assigned 0.03. The initial water surface of each mesh was a water depth of zero. Time step was 12 seconds. Projection of the iRIC model was defined as Universal

Transverse Mercator (UTM) zone North 47.

Urban density (urban density(%)/100=1- γ_v, see Equation of motion adobe) was assigned at each grid cell. Urban density was estimated by a remote sensing using Landsat OLI image (See chapter Appendix).

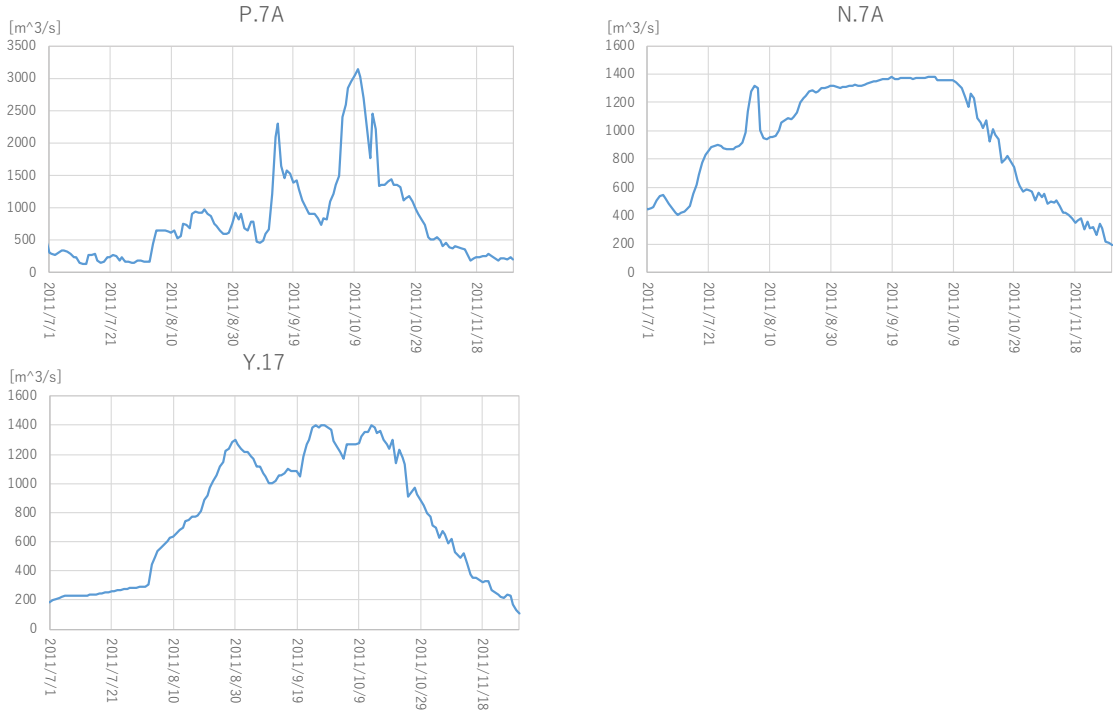

Fig. 3.6 Stream discharges at P.7A, Y.17, and N.7A from July 1 to November 1, 2011

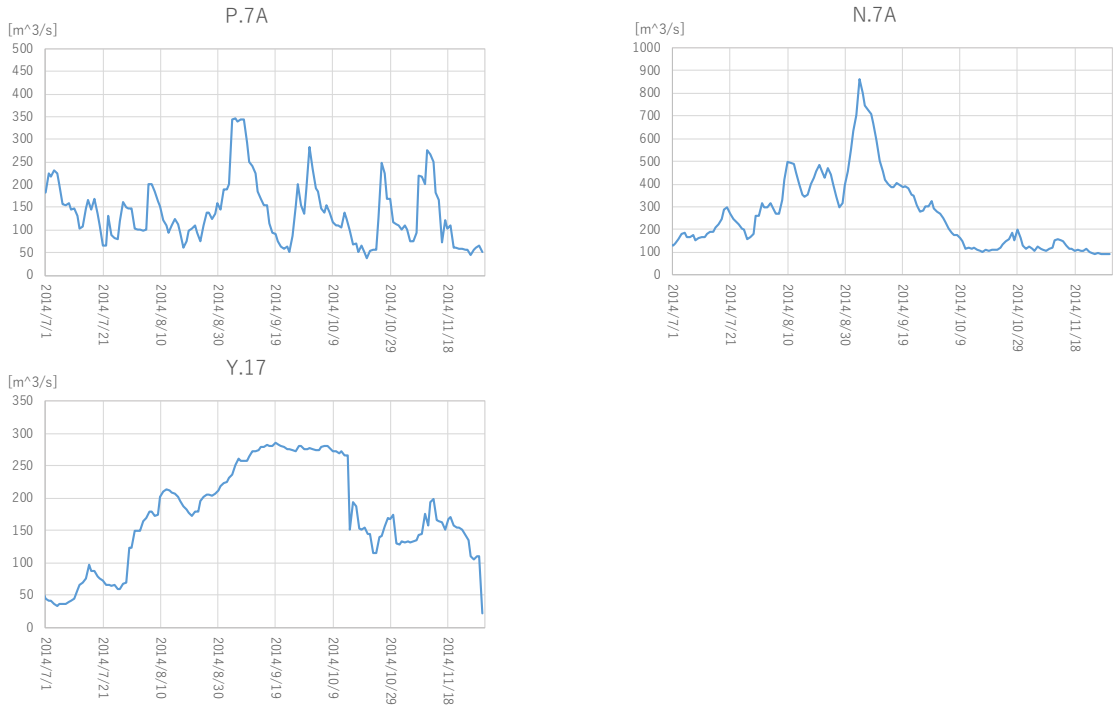

Fig. 3.7 Stream discharges at P.7A, Y.17, and N.7A from July 1 to November 1, 2014

3.2.5 Validation

The validation of the result of iRIC was estimated by comparing with the daily observed inundated area data from GISTDA (2015). The grid cells with the water depth more than 20 cm in the iRIC model were defined as the inundated areas for the iRIC result. While the grid cells, which GISTDA observed inundated area occupied more than 50 % within, was defined as the inundated areas of GISTDA observation.

The simple percent agreement between the iRIC result and GISTDA data may overestimate the predictive power of the model, because it doesn't take into account the agreement occurring by chance.

To avoid this, present study used Cohen's kappa. Given the account of agreements and disagreements between iRIC model and GISTDA data as Table 3.2, the equations of κ value are follows:

$$\kappa = \frac{p_0 - p_e}{1 - p_e}$$

p_0 : relative observed agreement between iRIC model and GISTDA observed data.

$$p_0 = \frac{n_{11} + n_{22}}{N}$$

p_e : hypothetical probability of chance agreement.

$$p_e = \frac{n_{.1}}{N} \times \frac{n_{1.}}{N} + \frac{n_{.2}}{N} \times \frac{n_{2.}}{N}$$

The model with κ value >0.4 indicates moderate accuracy (Fig. 3.6, Fleiss (1981)). The chance agreement generally increases in the circumstances that the ratio of classify objects into categories shows extreme low or high value (i.e. $n_{1.}/N$ or $n_{.1}/N$ is nearly 0 or 1 in Table 3.2), just as the proportion of the inundated areas to the objected area in present study.

Table. 3.2 Example of the count for agreements and disagreements between iRIC result and GISTDA observed data.

		GISTDA data		
		0	1	計
iRIC result	0	n_{11}	n_{12}	$n_{1.}$
	1	n_{21}	n_{22}	$n_{2.}$
	計	$n_{.1}$	$n_{.1}$	$N_{(Total)}$

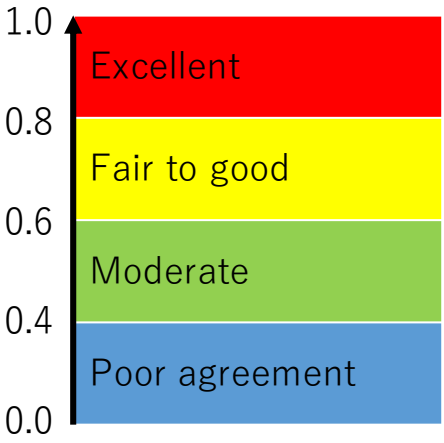

Fig. 3.8 Cohen's kappa value and accuracy estimation.

The agreement validation of inundated area between iRIC result and GISTDA observed data was conducted in the basin of . Because it is possible to overestimate the agreement of inundated area between iRIC result and GISTDA observed data, the grid cells across the permanent waterbodies namely rivers and the Bueng Boraphet Lake, were eliminated from the account of agreements and disagreements (Fig. 3.9).

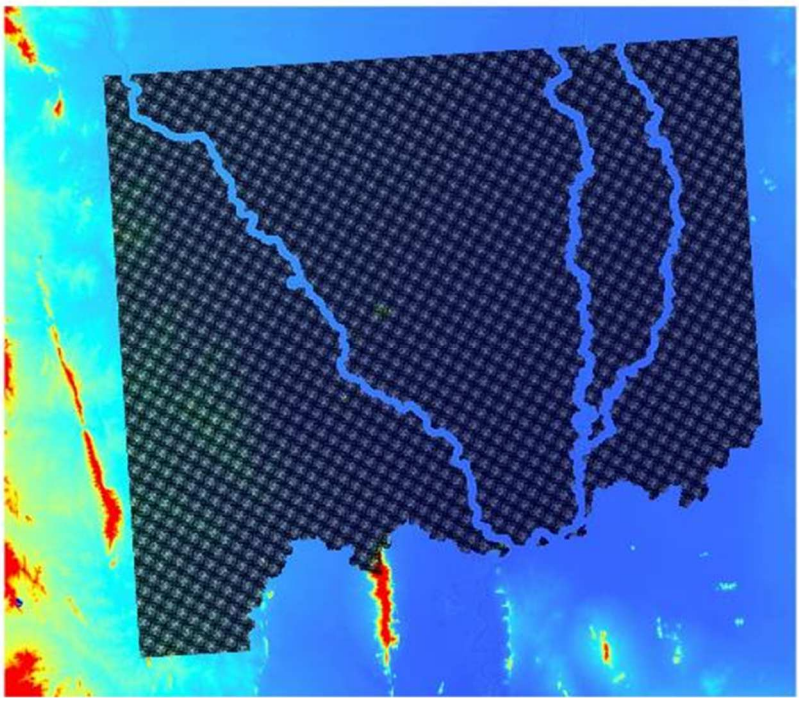

Fig. 3.9 The gird cells estimated the coincidence of iRIC model using Cohen's kappa between iRIC result and GISTDA observed data.

3.3 Result and discussion

Annual maximum six-month precipitations in Northern part of Thailand were calculated as 1569mm for 2011, 1051mm for 2014, and 1052mm as the average maximum six-month precipitation from 1976 to 2014. Fig. 3.10

shows the lognormal probability plots for annual precipitations in the northern part of Thailand from 1976 to 2014. LP3Rs, LogP3, IshiTaka, LN3Q, and LN3PM were the probability distribution model with SLSC ≦ 0.04 (see Table 3.1 for the abbreviations). The return periods were estimated that 100-200 years for 2011, approximately 2 years for 2014 (Table 3.3). The return period for 2011 generally agree with those reported earlier (e.g. 50 years for the whole basin (Sayama et al. 2015), 53-345 years for the northern part of the basin (CTI 2013)). Thus the 2011 and 2014 rainfall could be respectively assumed to be a devastating and usual flood year.

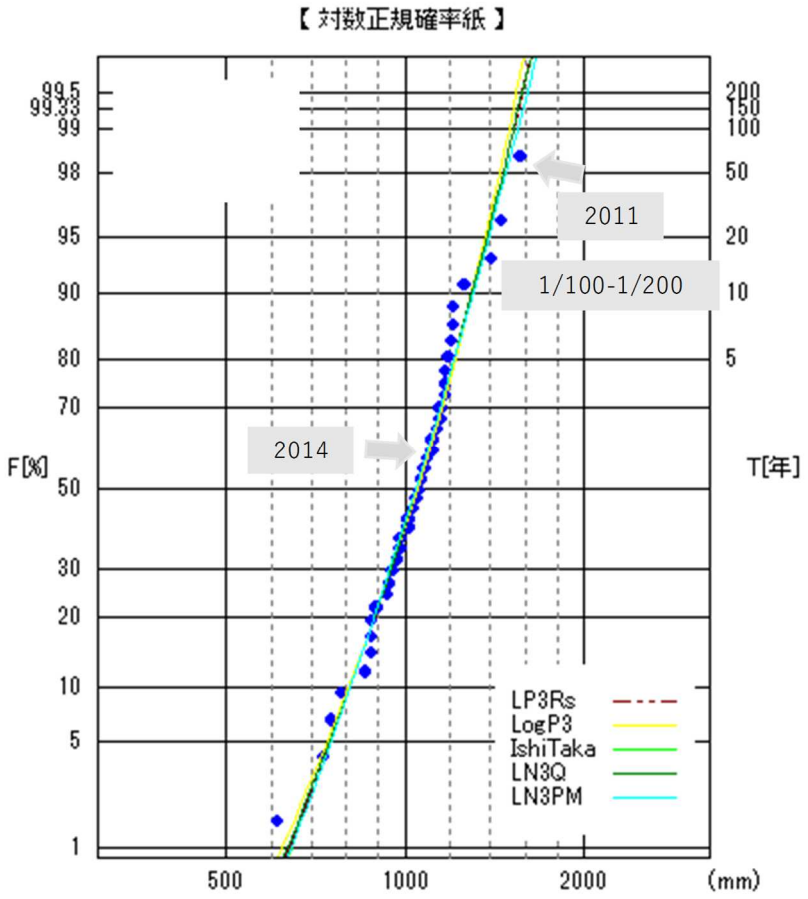

Fig. 3.10 Lognormal probability plot for annual precipitation in the northern part of Thailand

Table 3.3 Return periods for the probability distribution model with SLSC ≦ 0.04.

		LP3Rs	LogP3	IshiTaka	LN3Q	LN3PM
SLSC(99%)		0.031	0.03	0.031	0.031	0.031
Return Period	2	1045.8	1050.7	1042.5	1046.2	1042.6
	3	1131	1135.2	1127.1	1129.3	1127.2
	5	1214.3	1215.9	1211.3	1210.8	1211.4
	10	1305.3	1301.8	1305.6	1300.5	1305.5
	20	1381.6	1371.7	1386.7	1376.5	1386.5
	30	1421.6	1407.6	1430.1	1416.8	1429.8
	50	1468.3	1448.8	1481.7	1464.3	1481.3
	80	1508.3	1483.5	1526.6	1505.4	1526.1
	100	1526.4	1499	1547.3	1524.1	1546.7
	150	1558	1525.9	1583.7	1557.1	1583
	200	1579.6	1544	1608.9	1579.8	1608.1
	400	1628.9	1584.8	1667.5	1632.2	1666.5

Percent agreement between iRIC model and GISTDA observed data ranged more than 85% in both 2011 and 2014 (Table 3.4, Table 3.5). κ values ranged more than 0.4 expect for start and end periods of flooding in both 2011 and 2014 (Table 3.4, Fig. 3.11) However, the model seemed to increase the goodness of fit with observed data within a week in tandem with the increasing flood magnitude (Fig. 3.11).

According to GISTDA data in 2011, inundations started at surrounding areas of the upper reach of Yom and Nan River on August 6, then inundated areas spread at surrounding areas of all reach of the Yom and Nan River on September 11. Subsequently, inundations started at surrounding areas of the lower reach of Ping River on September 21. The maximum inundated area was recorded on October 6 in this region. Inundations came near the end in late November (Table 3.4). While in the iRIC model in 2011, flood inundations behaved in a similar manner, the start and end timing of the inundations was about 1-2 weeks earlier than GISTDA observed data (Table 3.4). This also supported by the fact that κ values ranged less than 0.4 at the start and end periods of flooding (Table 3.4, Fig. 3.11). This might due to the limitation of accuracy of the 300m grid DEM. Namely, the300m grid size was low resolution to consider the micro-topography which primely dominates the flood behavior, in particular at the start and end periods of flooding.

According to GISTDA data in 2014, inundations started at surrounding areas of the upper reach of Yom and Nan River on September 1, then inundated areas spread at surrounding areas of all reach of the Nan River on September 7. Inundations came near the end on October 2 (Table 3.5). While in the iRIC model in 2014, flood inundations behaved in a similar manner, the start and end timing of the inundations gave relatively close agreement with GISTDA observed data compared to year 2011.

Table 3.4 Inundated areas and κ values between iRIC model and GISTDA observed data in 2011. Magenta and aquamarine areas respectively represent the GISTDA observed inundated areas and iRIC predicted inundated areas.

TFMS observed data	iRIC result	
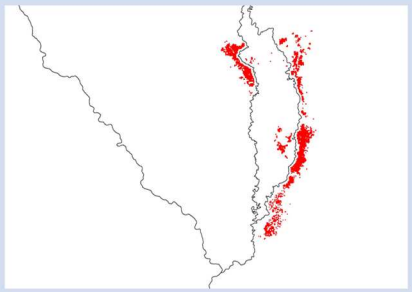	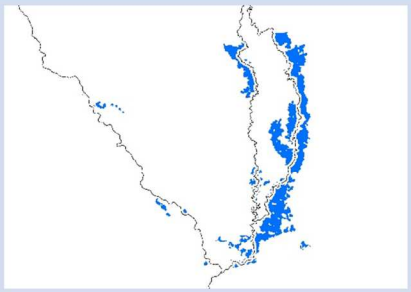	2011/8/6 Percent agreement： 95.3% κ value： 0.366
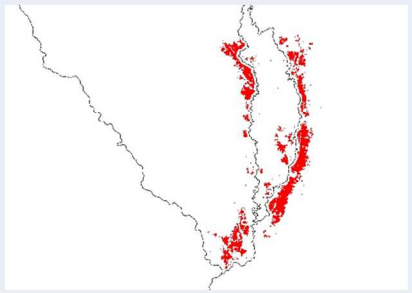	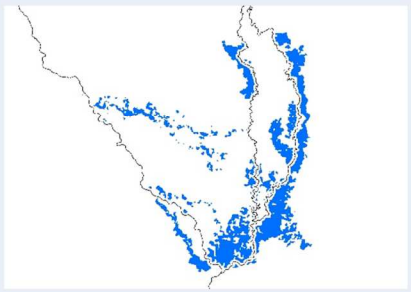	2011/8/16 Percent agreement： 92.3% κ value： 0.426
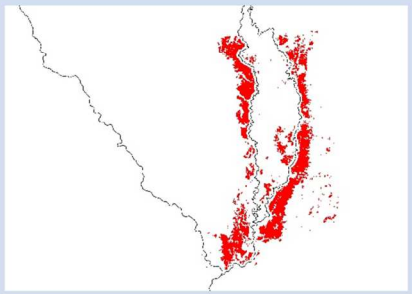	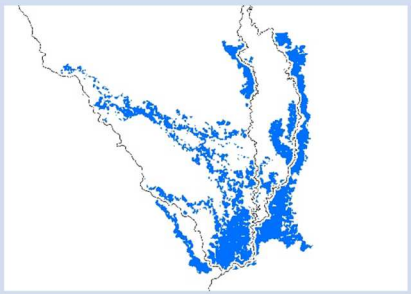	2011/8/23 Percent agreement： 89.1% κ value： 0.434

TFMS observed data	iRIC result	
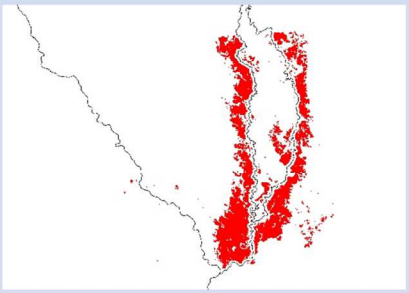	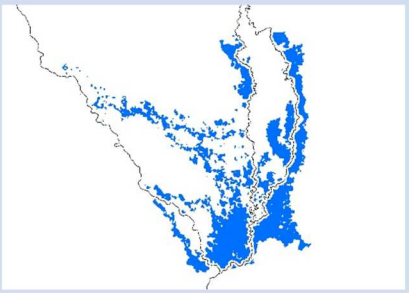	2011/9/4 Percent agreement： 89.9% κ value： 0.552
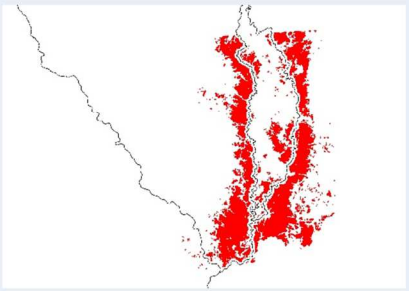	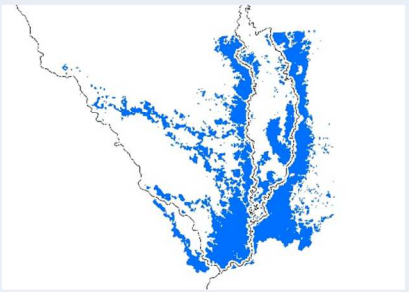	2011/9/11 Percent agreement： 90.8% κ value： 0.607
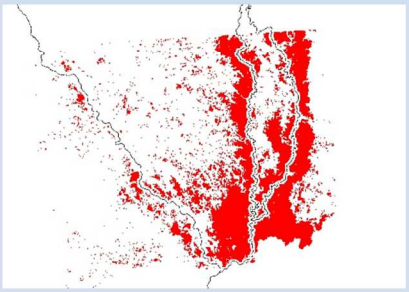	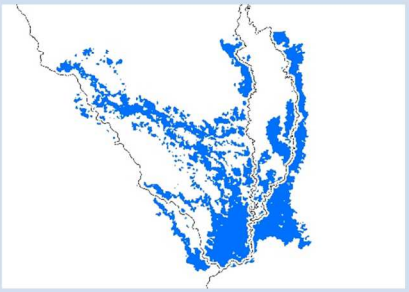	2011/9/21 Percent agreement： 83.8% κ value： 0.516

TFMS observed data	iRIC result	
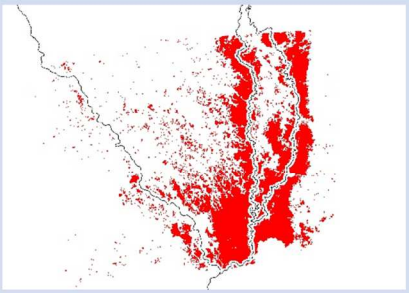	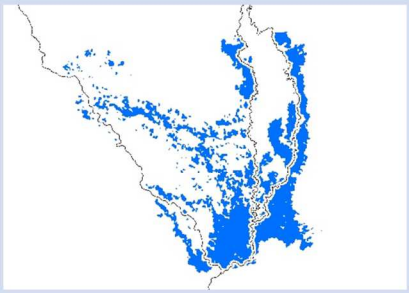	2011/9/28 Percent agreement： 87.4% κ value： 0.579
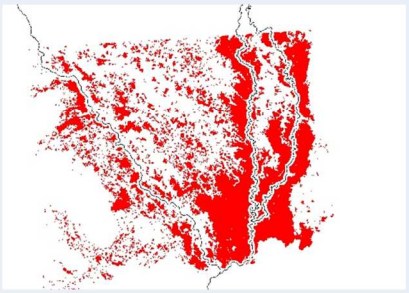	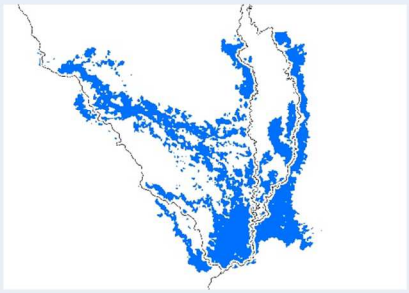	2011/10/6 Percent agreement： 78.3% κ value： 0.449
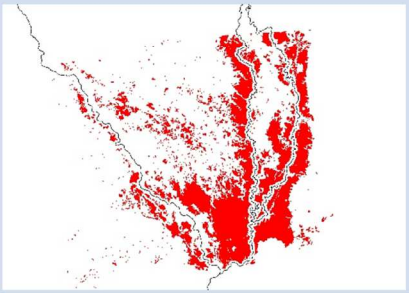	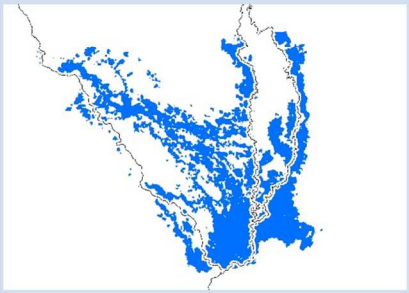	2011/10/15 Percent agreement： 84.8% κ value： 0.564

TFMS observed data	iRIC result	
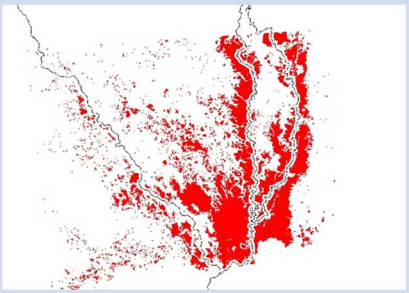	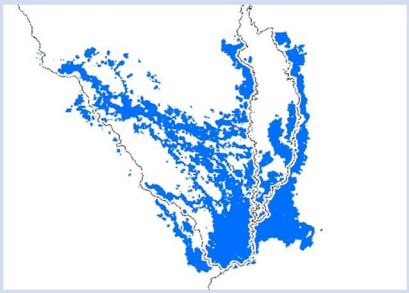	2011/10/21 Percent agreement： 85.3% κ value： 0.550
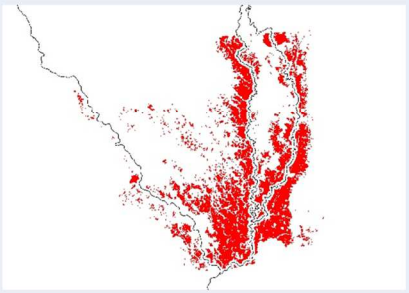	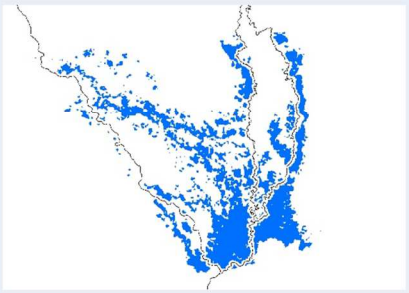	2011/10/29 Percent agreement： 87.8% κ value： 0.550
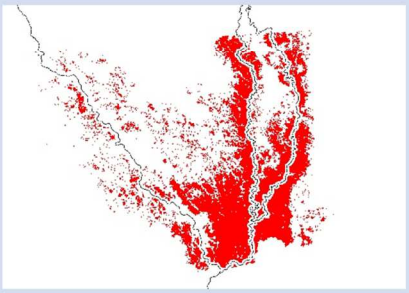	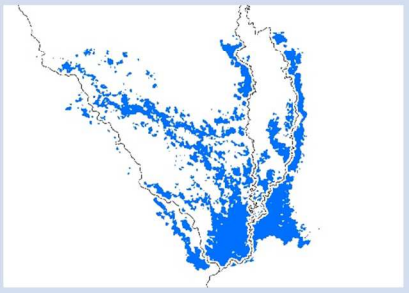	2011/11/8 Percent agreement： 85.3% κ value： 0.476

TFMS observed data	iRIC result	
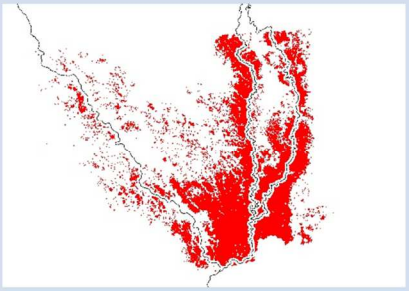	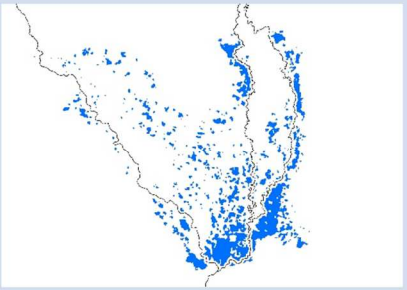	2011/11/15 Percent agreement： 87.9% κ value： 0.453
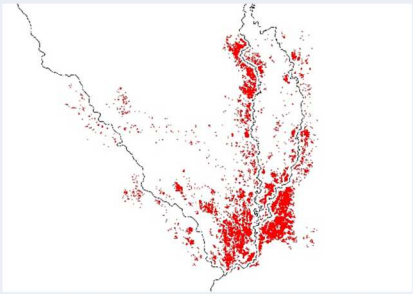	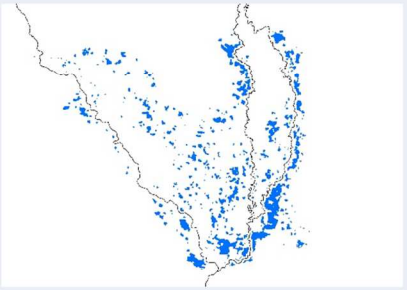	2011/11/23 Percent agreement： 90.8% κ value： 0.607

Table 3.5 Inundated areas and κ values between iRIC model and GISTDA observed data in 2014. Magenta and aquamarine areas respectively represent the GISTDA observed inundated areas and iRIC predicted inundated areas.

TFMS observed data	iRIC result	
	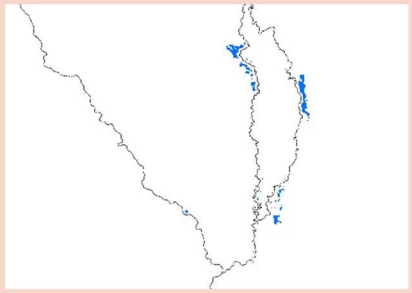	2014/9/1 Percent agreement： 99.1% κ value： 0.199
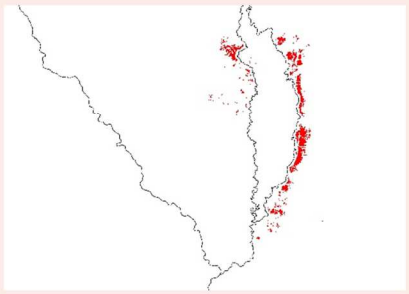	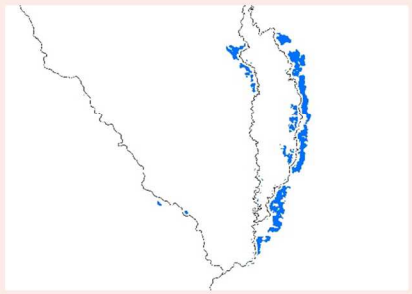	2014/9/7 Percent agreement： 97.7% κ value： 0.476
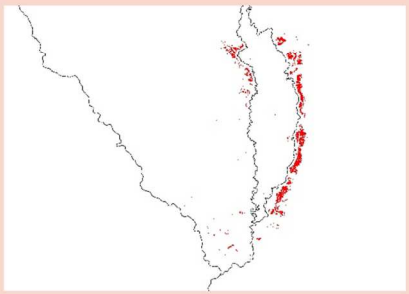	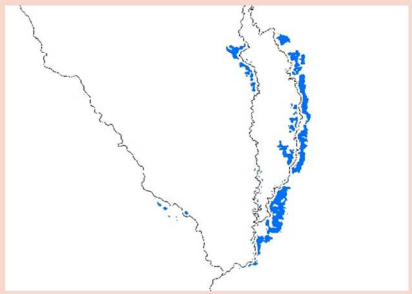	2014/9/11 Percent agreement： 97.6% κ value： 0.445

TFMS observed data	iRIC result	
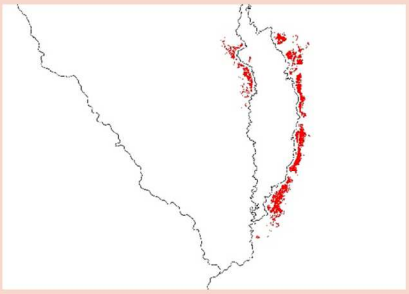	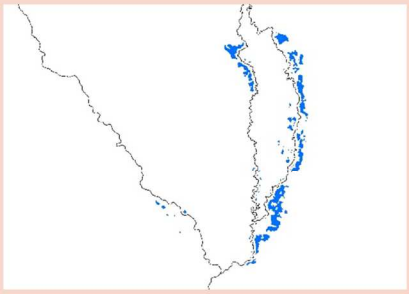	2014/9/17 Percent agreement： 98.2% κ value： 0.554
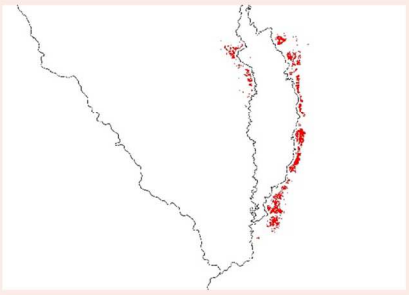	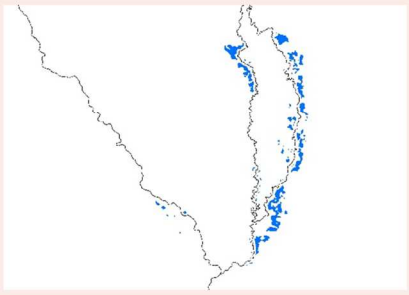	2014/9/24 Percent agreement： 98.3% κ value： 0.459
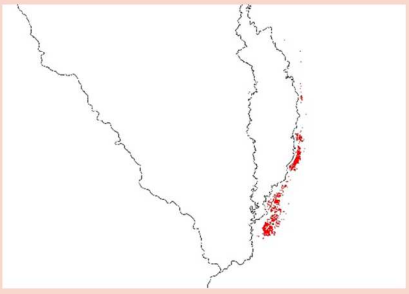	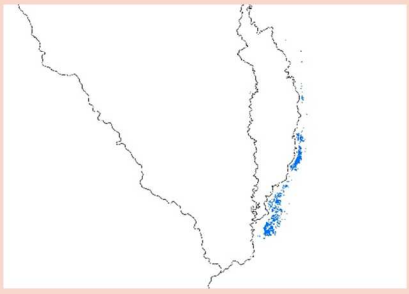	2014/10/2 Percent agreement： 98.3% κ value： 0.170

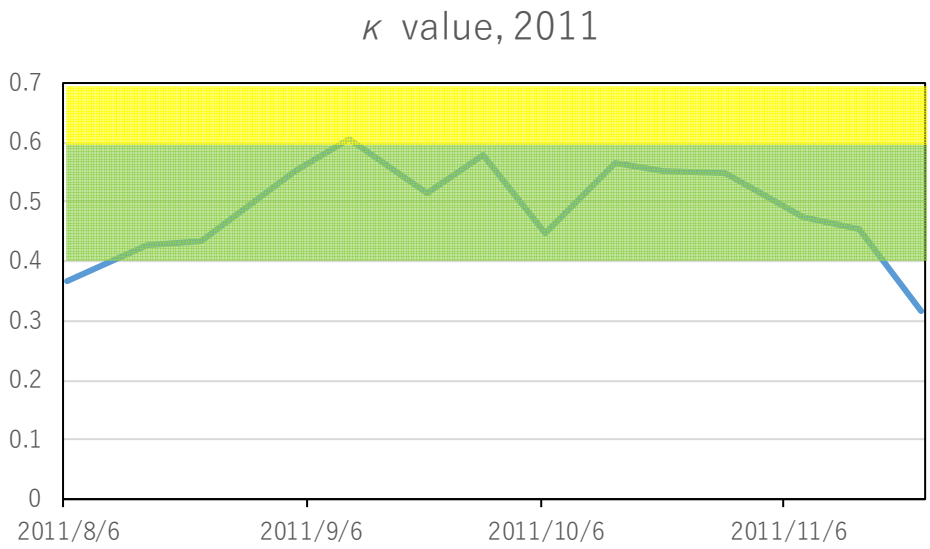

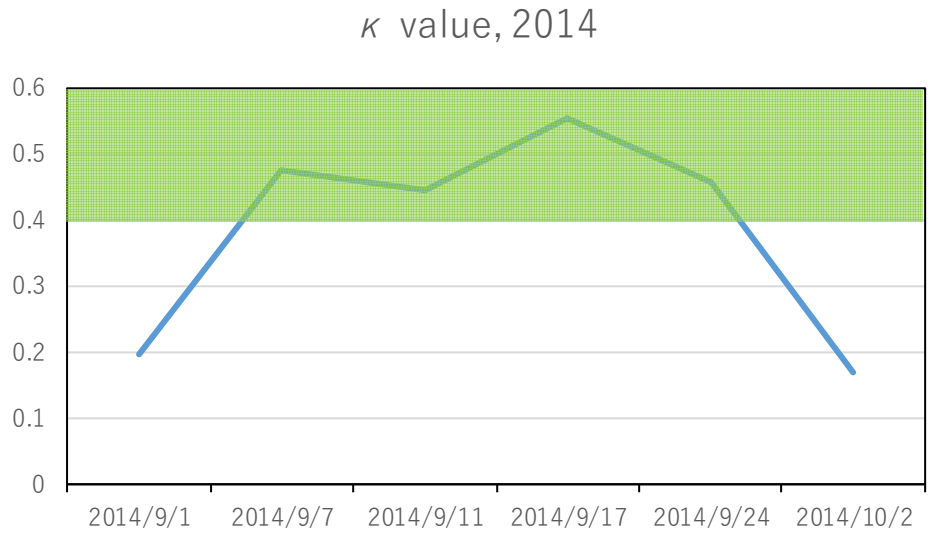

Fig. 3.11 κ values in 2011 and 2014

3.4 Conclusion

In this chapter, I computed (1) the estimation of the return periods of annual rainfall in northern part of Thailand, (2) the simulation of the 2011 and 2014 flood using iRIC model, in the middle stream of The Chao Phraya River basin.

The return period of 2011 and 2014 rainfall were respectively estimated 100-200 years and approximately 2 years. Thus the 2011 and 2014 rainfall could be respectively assumed to be a devastating and usual flood year. The result of the simulation of the 2011 and 2014 flood using iRIC model showed moderate accuracy. The validation of the model comparing with GISTDA observed data showed moderate agreement. In order to predict the impact on floodplains caused by future flood control measures, the model which describe the flood phenomena in the region was developed.

Possible several scenarios which might come true were developed and discussed in the next chapter.

Chapter4

The impact of a future flood control on floodplain area

4.1 Introduction

In the previous chapter, the model to simulate the floods in the middle stream of the Chao Phraya River basin was developed. The model has moderate accuracy for predicting the inundated area and timing of floods in the region.

At present status, flood control policy of the military government remains in feasibility studies and designs, and lacks concrete countermeasures. As chapter 2 showed, floodplain areas impact on fish species diverse, in particular on floodplain migratory species, in the region. Therefore, future flood control measures would impact river-floodplain ecosystem through a floodplain deterioration. Understanding of the impact on floodplain and floodplain ecosystem would help the accurate assessment of flood control measures and the development of flood control program.

In this chapter, I simulated the 2014 flood conditions in the middle stream of the Chao Phraya River using the model developed in previous chapter based on following scenarios:

- Scenario A: No dam scenario. Scenario A describes potential and original floodplain condition in which two largest dams, namely the Bhumibol Dam and the Shirikit Dam, don't exist.
- Scenario B: New dam scenario. Scenario B describes the future condition with a new dam construction in the Yom River which is the only major tributary that have no large scale dam on the mainstream.

After the impacts of a future flood control and of the existing dams on floodplain area were estimated using adobe scenarios, the gap analysis was conducted in order to elucidate the difference of floodplain area among original 2014 and scenarios.

4.2 Runoff estimation

4.2.1 Methodology of runoff estimation for the scenarios

A storage function model (SFM) was developed by Kimura (1967). SFM is widely used in Japan as a simple method which can explain non-linear relationship between runoff and rainfall. The method considers basin or river channel as storage reservoir and presumes a stream discharge expressed as a function of the storage volume of the hypothetical reservoir. The SFM equation is as follows:

[watershed model]

$$\begin{cases} S_l = K \times {Q_l}^P & (1) \\ \dfrac{dS_l}{dt} = \dfrac{1}{3.6} \times f \times r_{ave} \times A - Q_l & (2) \end{cases}$$

Here,

S_l: watershed storage volume (m^3)

Q_l: direct runoff (m^3/s)

K,*P*: storage coefficients

r_{ave}: areal effective rainfall depth per hour (mm/hr)

A: drainage area (km^2)

f: funoff factor

In the storage function method, it is assumed that runoff does not occur at the beginning of a rainfall and occurs only in a part of the riparian basin called the runoff area. The method also accounts for the initial loss of rainfall. Once the initial loss is satisfied, due to the rainfall which occurs over all of the basin, the entire basin contributes to runoff. Based on the assumption above, the total runoff *Q* is calculated as follows:

$$\begin{cases} Q = \frac{A}{3.6}\left(f_1 \times q_l + (f_{sa} - f_1) \times q_{sa,l}\right) + Q_b & (3) \\ Q_l(t) = Q(t + T_l) & (4) \end{cases}$$

Here,

f_1: primary runoff ratio

f_{sa}: saturation runoff ratio (f_{sa}=1)

q_l: runoff rate per km^2 before saturation (mm/hr)

$q_{sa,l}$: runoff rate per km^2 after saturation (mm/hr)

Q_b: baseflow (m^3/s)

T_l: a storage function time delay of the watershed

[river channel model]

$$\begin{cases} S = K \times Q_o(t)^P - T_l \times Q_0(t) & (5) \\ \frac{dS}{dt} = \mathrm{Q}_i(t) - Q_o(t + T_l) & (6) \end{cases}$$

Here,

S: river channel storage volume (m^3)

Q_i: inflow runoff (m^3/s)

Q_o: outflow runoff (m^3/s)

K,*P*: storage coefficients

T_l: a storage function time delay of the river channel

4.2.2 Input data and Scenario setup for Scenario A

In scenario A, the discharges at P.7A and N.7A runoff stations without Bumibol and Shirikit Dams were simulated, in order to use it in iRIC model (Fig. 4.1). The simulation was computed from July 1 to November 30, 2014.

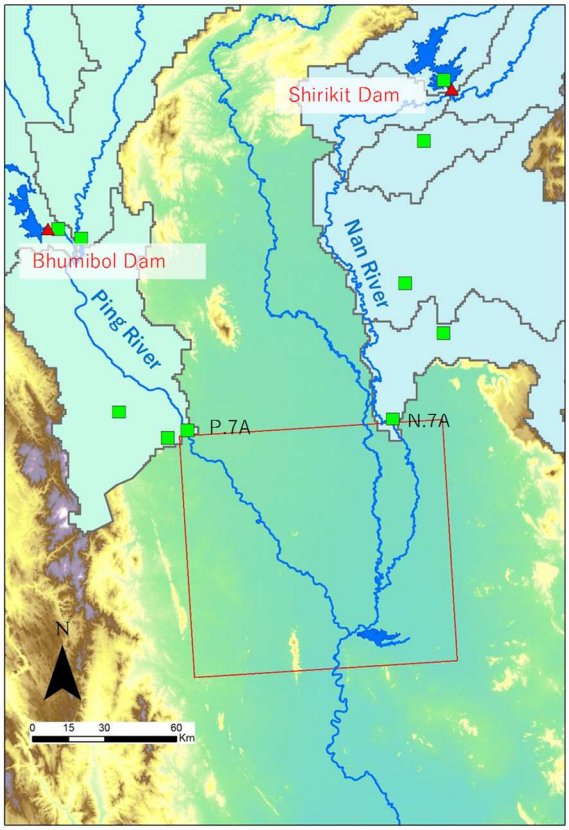

Fig. 4.1 Objected area of scenario A. A red rectangle represents the objected area of iRIC model. Red triangles indicate the large scale dams (the Bhumibol Dam and the Shirikit Dam).

Fig. 4.2 shows the divided watersheds for SFM in the upper Ping River basin. the upper Ping River basin was divided into 3 partitions. The discharge data from P. 12, P. 50A, P. 26A and W. 4A runoff stations were used as inflows (Fig. 4.2b). Fig. 4.3 shows the divided watersheds for SFM in the upper Nan River basin. The upper Nan River basin was divided into 4 partitions. The discharge data from N. 6A, N. 28, N. 22, N. 24, DR. 15.8, and DR.2.8 runoff stations were used as inflows (Fig. 4.3b).

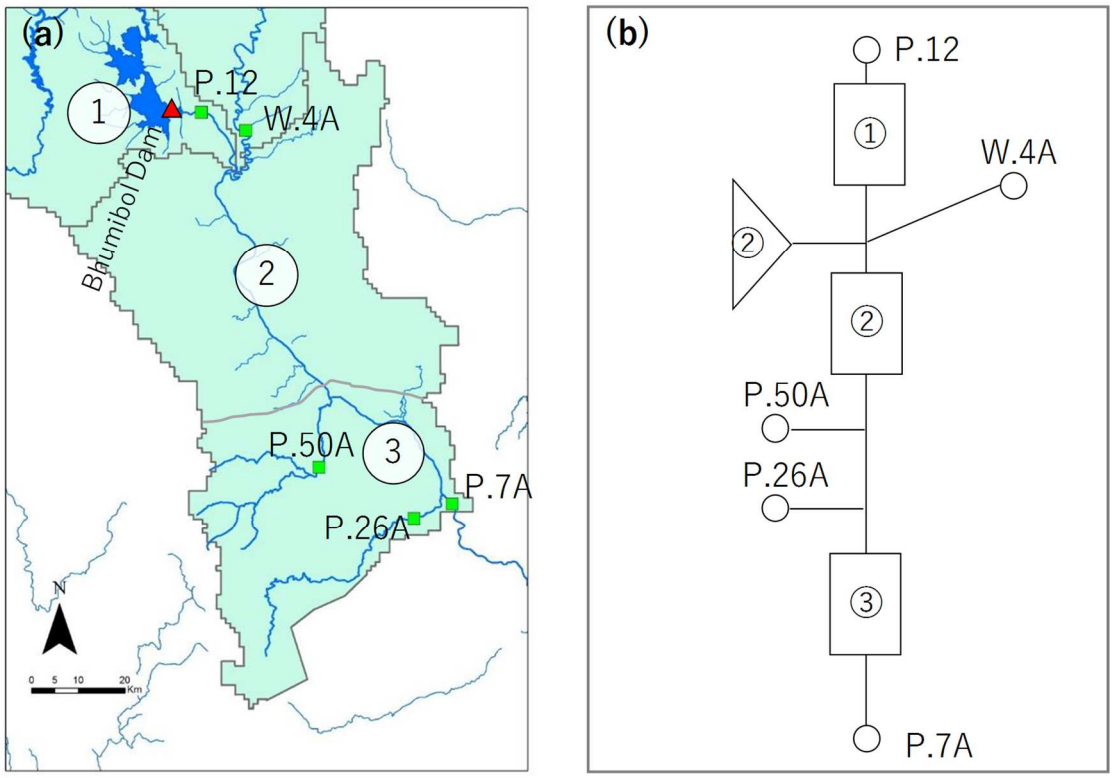

Fig. 4.2 The divided watersheds for SFM in the upper Ping River basin. (a) location map. Green rectangles indicate runoff stations. (b) pattern diagram. Rectangles indicate river channel sections, a triangle indicate watershed section. Open circles indicate runoff stations.

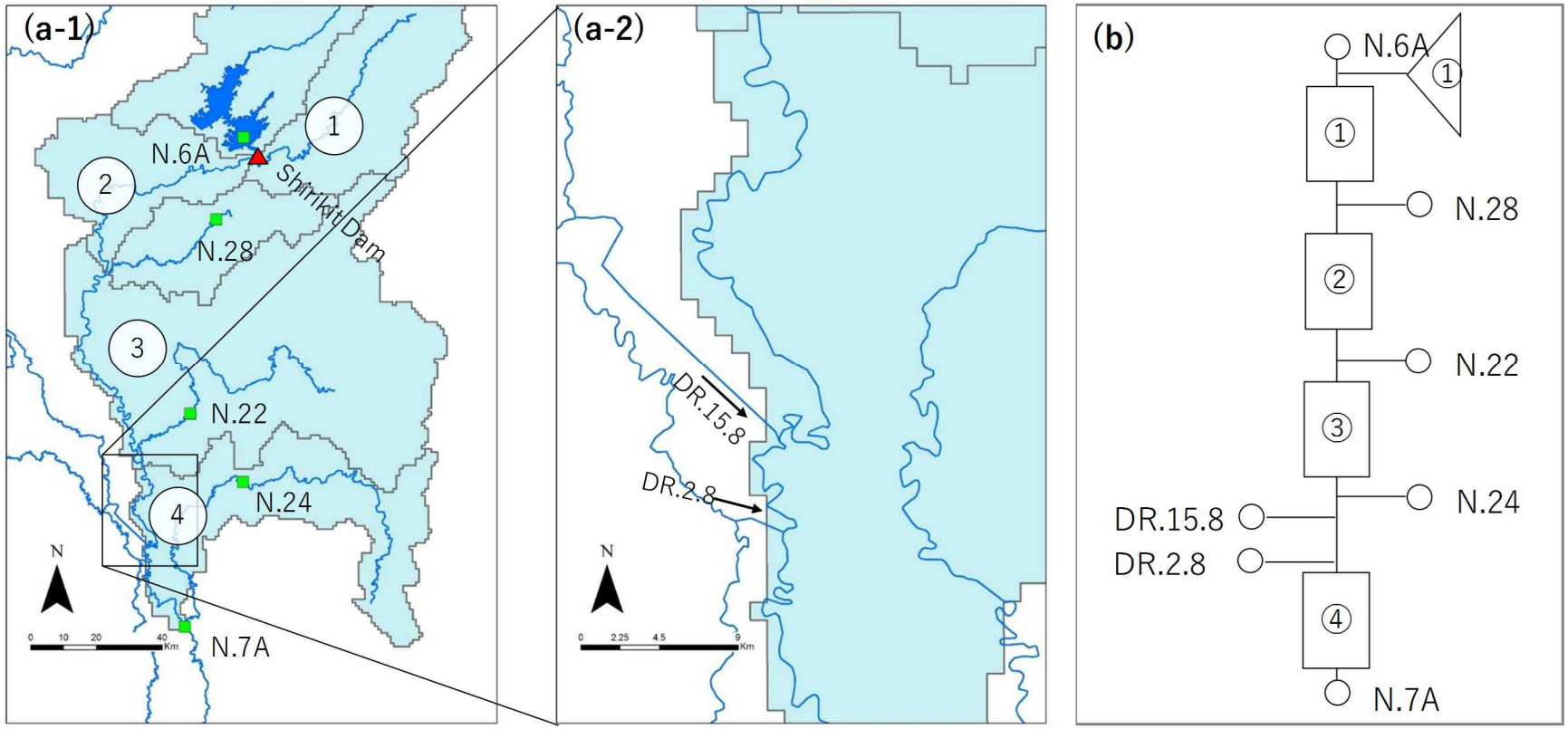

Fig. 4.3 The divided watersheds for SFM in the upper Nan River basin. (a-1) location map. Green rectangles indicate runoff stations. (a-2) enlarged view around DR.15.8 and DR 2.8, (b) pattern diagram. Rectangles indicate river channel sections, triangles indicate watershed sections.

[river channel model]

For each river channel section, S-Q_o relationship was investigated by using the "area and velocity curve" created at the cross-section of some runoff stations (Fig. 4.4). The area and velocity curve is the graphic representation of the relation among water depth, cross-section areas, and discharges. And it allows to determine the cross-section areas corresponding to each discharge value. S corresponding to a given amount of Q_o was calculated by the equation as following (also see. Fig. 4.5):

$$S(Q) = \sum_i A_i(Q_o) \times L_i$$

Here

$A_i(Q_o)$: the cross-section area of cross-section i

L_i: the distance between half way points or river channel section boundaries from cross-section i

Based on the least-square regression line from the logarithm of S and Q_o pairs, K and P were calculated as the intercept and the slope (Fig. 4.6, Fig. 4.7).

According to JICE (1999), the initial time delay T_l for each river channel section was calculated as follows:

$$T_l = 7.36 \times 10^{-4} L I^{-0.5} \qquad (7)$$

Here,

L: length of river channel

I: average river channel slope

[watershed model]

K and P were calculated by reserve coefficient method (JICE 1999) as follows:

$$K = 43.4 C I^{1/3} L^{1/3} \qquad (8)$$

$$p = 1/3 \qquad (9)$$

Here,

C: watershed roughness coefficient (in present study, 0.038 for crop land was used)

I: watershed slope. The slope from runoff point to the most distal point of watershed streams.

L: stream length. The length from runoff point to the most distal point of watershed streams.

the initial time delay T_l for each river channel section was calculated as follows (JICE 1999):

$$T_l = 0.0470 \times L - 0.56 \qquad (10)$$

Here,

L: stream length. The length from runoff point to the most distal point of watershed streams.

Q_b for each watershed section was defined as the allocation of discharge of the downmost-stream runoff station (P. 7A or N. 7A) on July 1, depending on the ratio of each watershed section area to the entire watershed area. Because July 1, 2014 was before the flooding season in the region and without big rainfall in the previous week, the discharge on July 1 can be assumed as baseflow. Q_b for each watershed section was

calculated by the equation as following:

$$Q_{bi} = Q_d \times \frac{A_i}{\sum_i A_i} \qquad (11)$$

Here,

Q_{bi}: base flow discharge for watershed section i

Q_d: discharge of the downmost-stream runoff station

A_i: area of watershed section i

According to JICE (1999), f and r_{sa} were defined as 0.5 and 100 mm/hr. T_l was calculated by equation (7) and calibrated by the same methods as previously described.

The all parameters for SFM calculated by the above equations were shown in Table 4.1.

Table 4.1 parameters used for SFM of the upper basin of the Ping and the Nan River.

(a) The Ping River

		river channel			watershed
	Unit	①	②	③	②
K		66.34	199.53	210.18	73.7
P		0.5753	0.5996	0.5676	0.333
T_l		0.65	26.94	20.53	2.08
f		-	-	-	0.5
r_{sa}	mm/hr	-	-	-	100
Q_b	m^3/s	-	-	-	12.1
A	km^2	-	-	-	2263

(b) The Nan River

		river channel				watershed
	Unit	①	②	③	④	①
K		821.49	598.73	274.03	141.19	164.593
P		0.5016	0.5338	0.6611	0.7436	0.333
T_l		90	6.38	2.49	6.41	6.31
f		-	-	-	-	0.5
r_{sa}	mm/hr	-	-	-	-	100
Q_b	m^3/s	-	-	-	-	10.6
A	km^2	-	-	-	-	1685

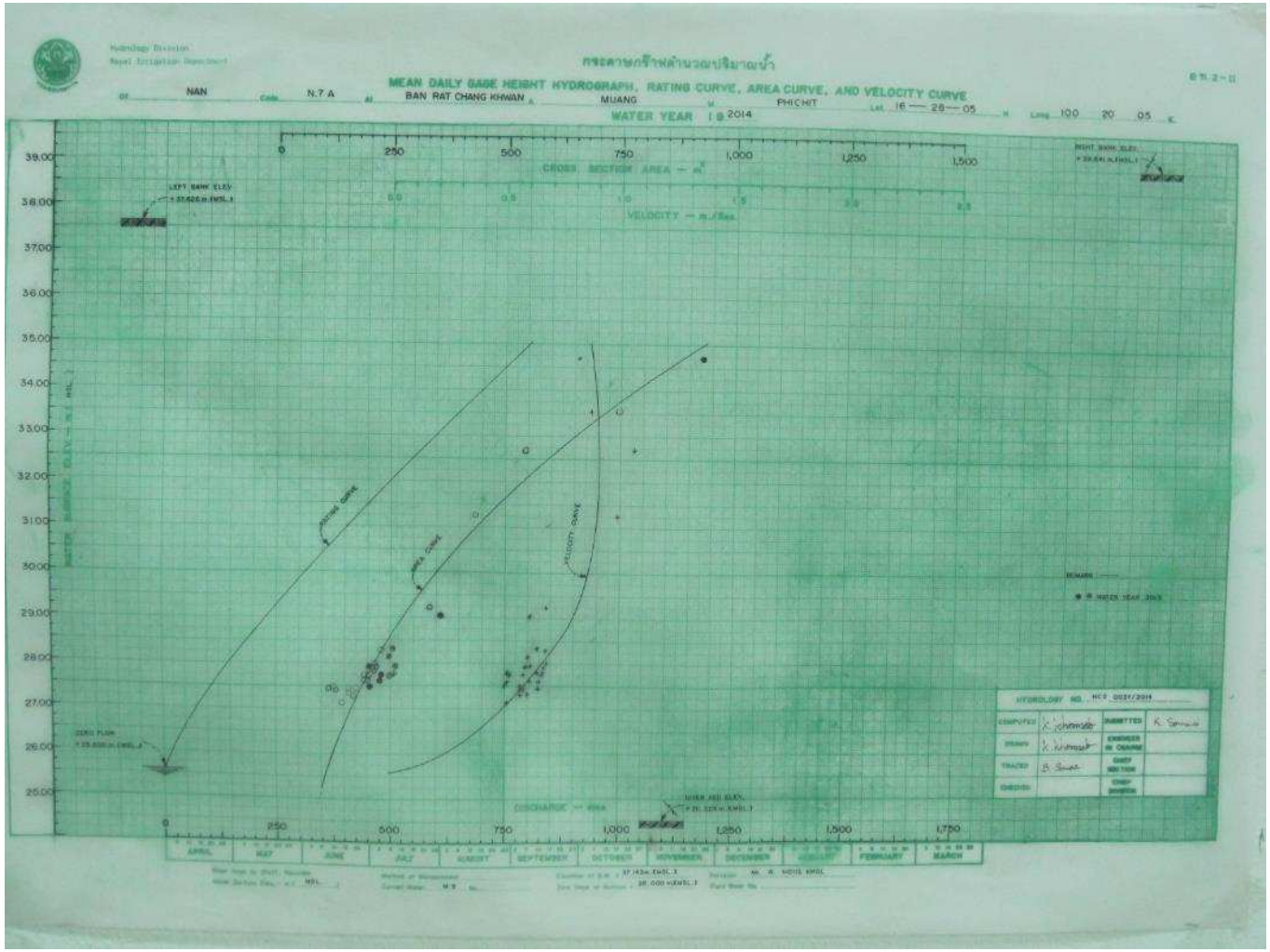

Fig. 4.4 The example of area and velocity curve. The figure was is adapted from http://hydro-2.com/

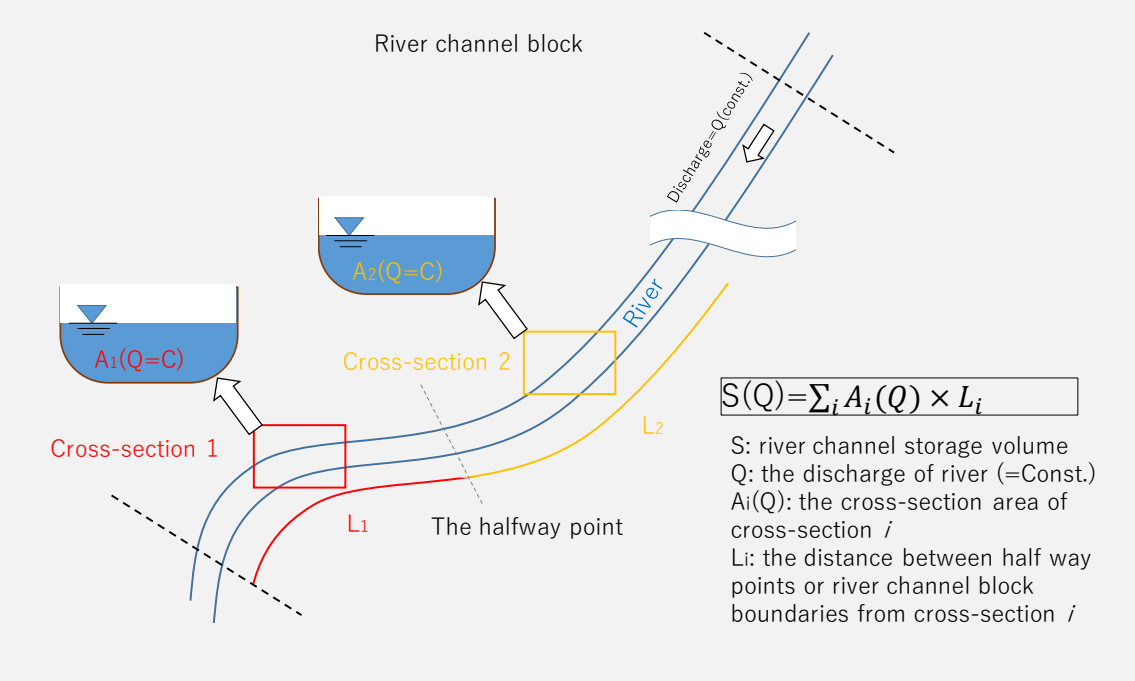

Fig. 4.5 The calculation procedure of a river channel storage volume

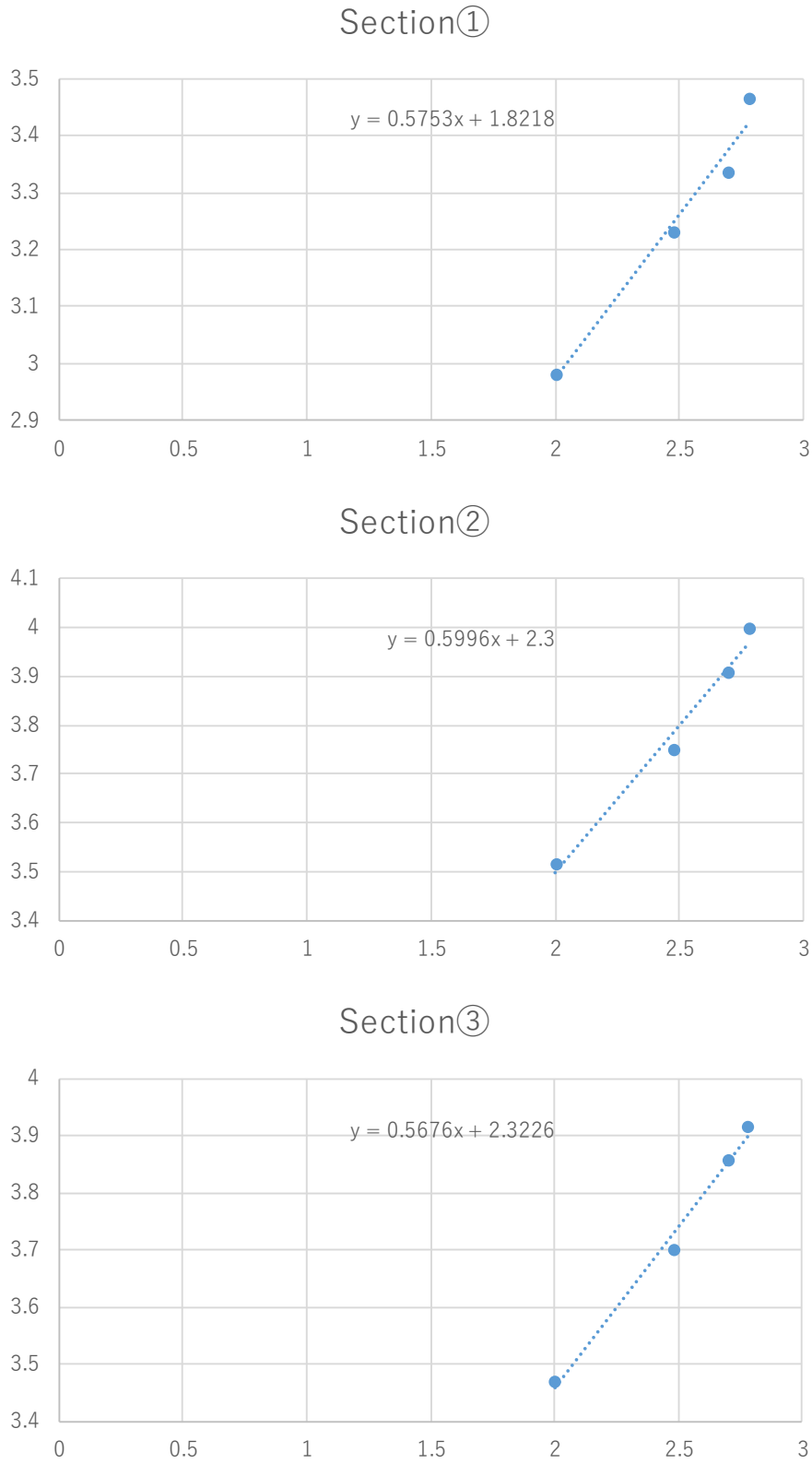

Fig. 4.6 The logarithmic plots of S and Q_o at each river channel section of the Ping River. K and P were calculated as the intercept and the slope of the least-square regression line.

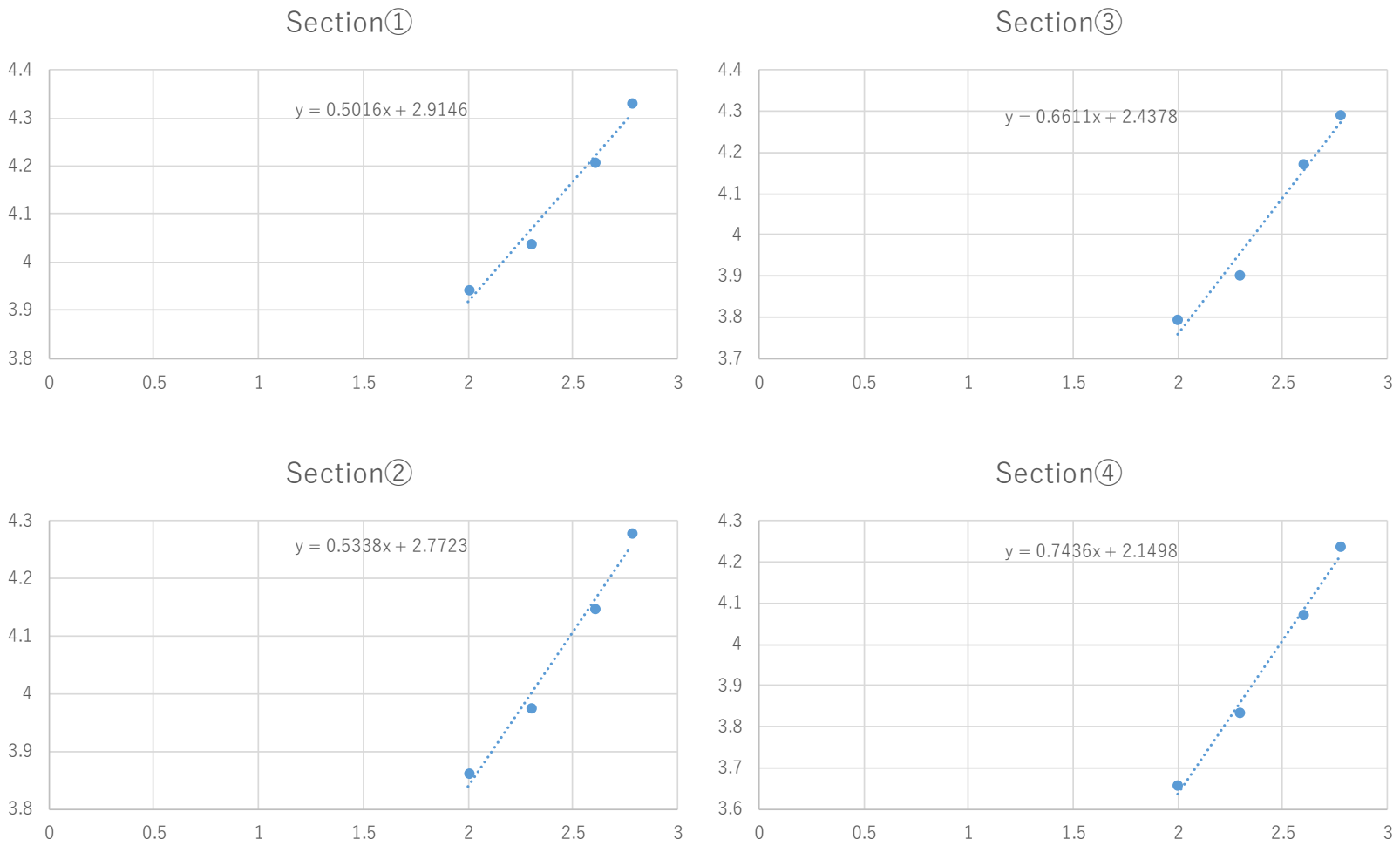

Fig. 4.7 The logarithmic plots of S and Q_o at each river channel section of the Nan River. K and P were calculated as the intercept and the slope of the least-square regression line.

As a preprocess for scenario A, the original 2014 flood was simulated to validate the accuracy of the SFM model. Fig. 4.8 shows the discharges result at P. 7A runoff station. R^2 was 0.661 between the daily SFM discharge and the observed discharge. Fig. 4.10 shows the discharges result at N. 7A runoff station. R^2 was 0.914 between the daily SFM discharge and the observed discharge.

Subsequently, the discharges of P. 12 and N. 6A were respectively replaced with the inflows into the Bhumibol Dam and the Shirikit Dam, then SFM was computed as the scenario A. The results were shown in Fig. 4.9 and Fig. 4.11. The discharges for scenario A at P. 7A and N. 7A were predicted more than twice the discharge observed.

Stream discharges for each runoff station (Fig. 4.2) was obtained from RID (http://hydro-2.com/). The SFM analysis was conducted using CommonMP (CommonMP Committee, ver.1.4.0.1). The landscape parameters were calculated using ArcGIS ver. 10.2 (ESRI Japan, Tokyo, Japan).

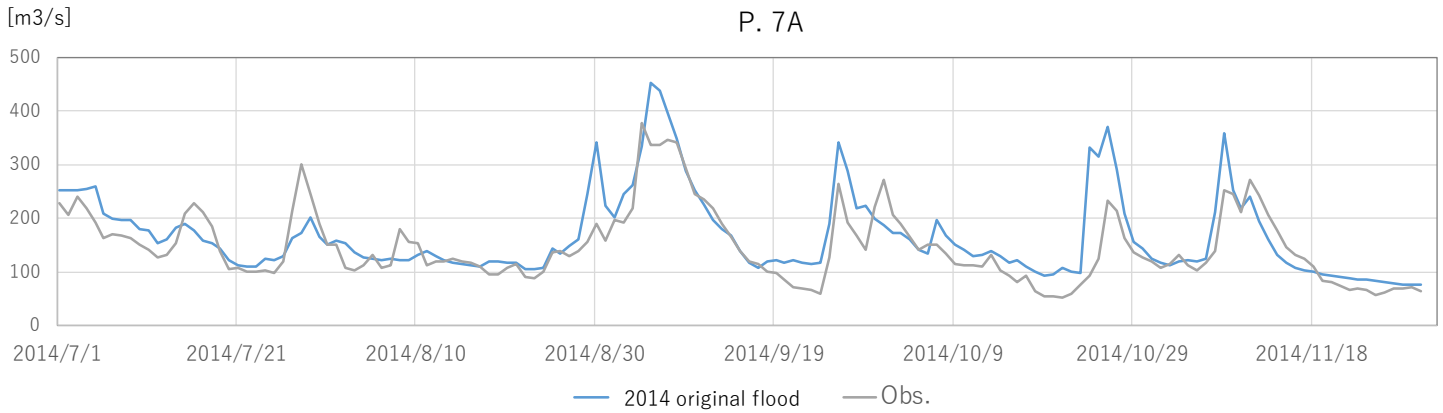

Fig. 4.8 The discharges at P. 7A runoff station. Blue line indicates the result of the SFM for original 2014 flood, gray line indicates the observed discharge at P. 7A.

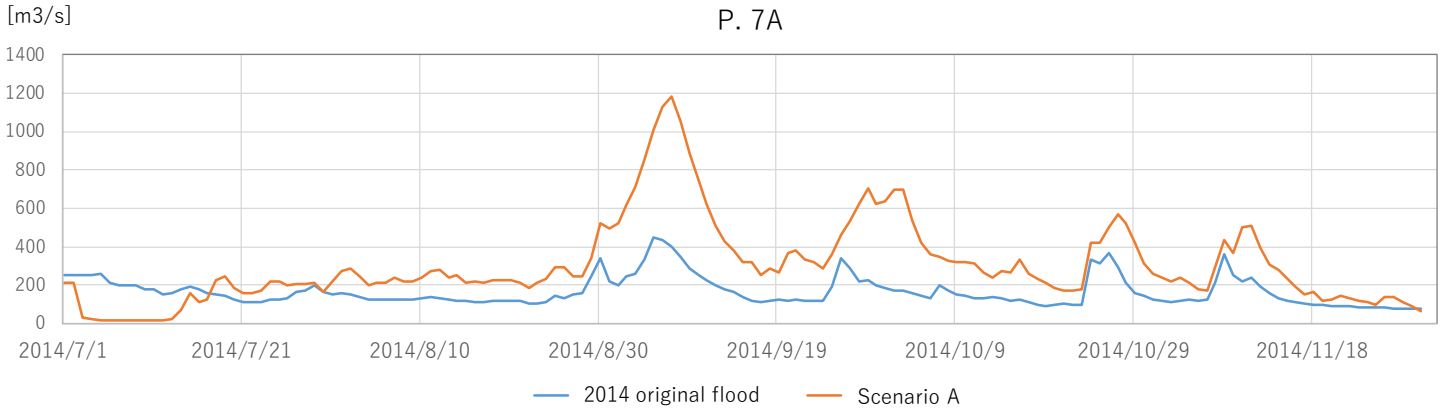

Fig. 4.9 The discharges at P. 7A runoff station. Blue line indicates the result of the SFM for original 2014 flood, orange line indicates the result of the SFM for scenario A.

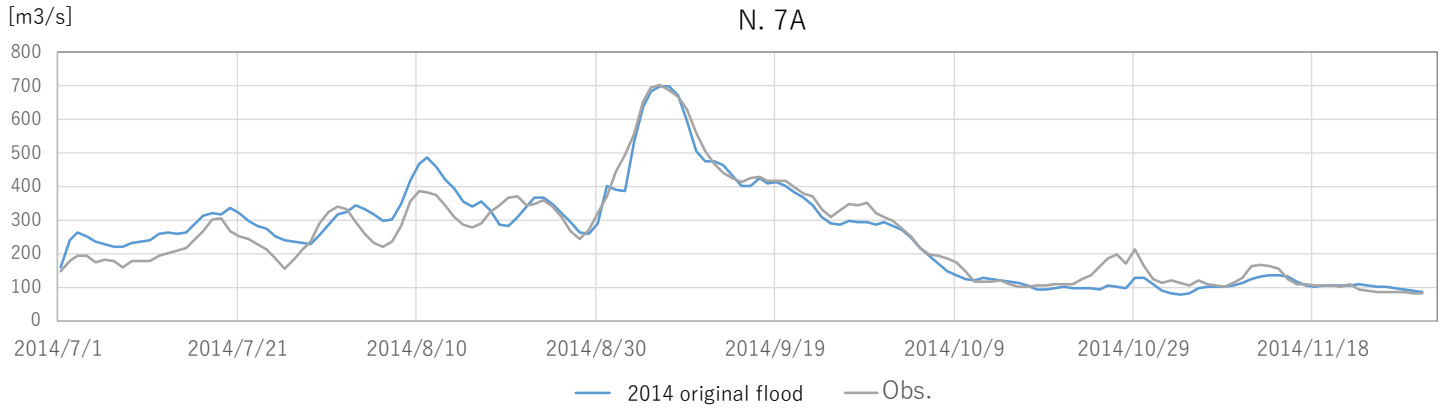

Fig. 4.10 The discharges at N. 7A runoff station. Blue line indicates the result of the SFM for original 2014 flood, gray line indicates the observed discharge at N. 7A.

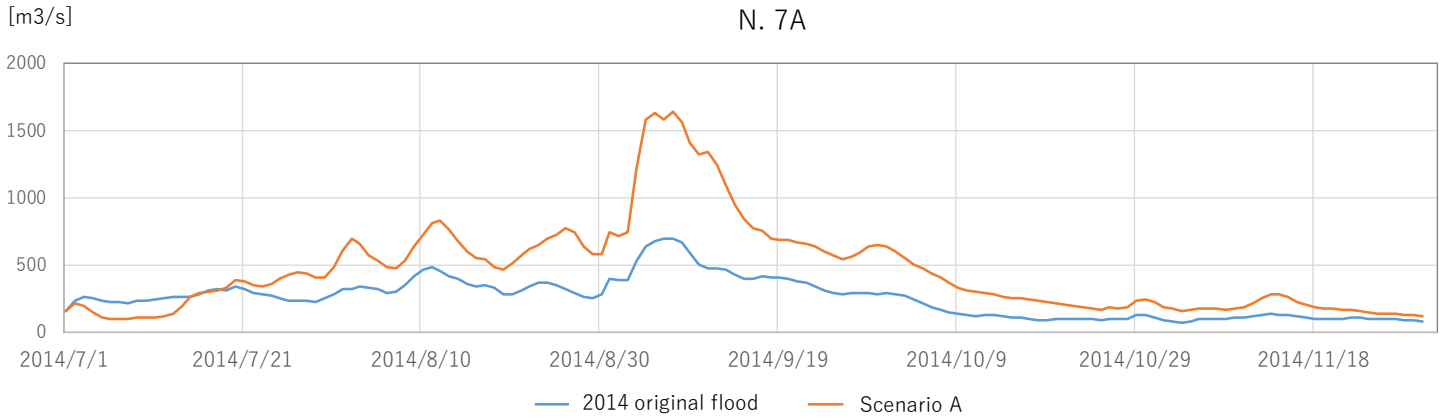

Fig. 4.11 The discharges at N. 7A runoff station. Blue line indicates the result of the SFM for original 2014 flood, orange line indicates the result of the SFM for scenario A.

4.2.3 Input data and Scenario setup for Scenario B

In scenario B, the discharges at Y. 17 runoff stations with Kaeng Sua Ten Dam was sumilated, in order to use it in iRIC model (Fig. 4.12). Kaeng Sua Ten Dam is the new dam planned in the Yom River which is the only major tributary that have no large scale dam on the mainstream.

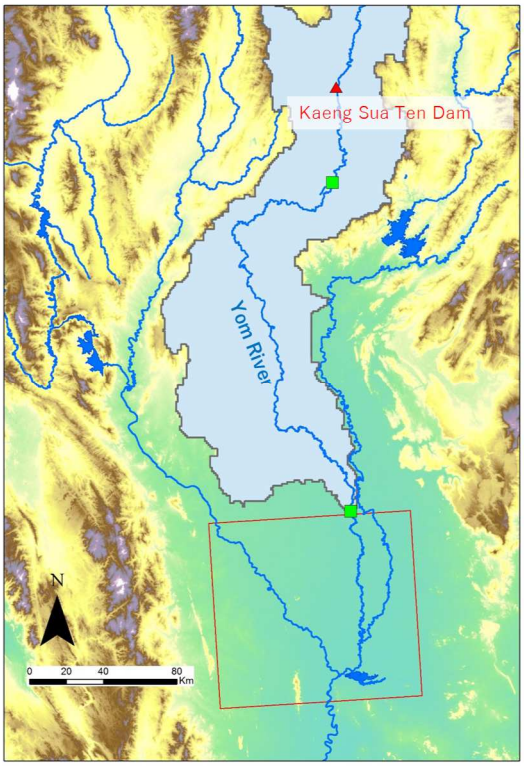

Fig. 4.12 Objected area of scenario B. A red rectangle represents the objected area of iRIC model. A red triangle indicates the location of the Kaeng Sua Ten Dam.

The Kaeng Sua Ten Dam

The Kaeng Sua Ten Dam is the new dam project planned on the upper stream of the Yom River . The dam has the largest volume among 107 new dam projects which RID conducted feasibility studies, and was estimated to be effective to ease flooding in the lower northern part of Thailand by JICA (2013). The dam was planned in 1991, however the plan was abandoned due to the protest of civil groups and NGOs (Bangkok Post 2011). In 2011, under Yingluck cabinet, the debate about the dam was held among stakeholders (Bangkok Post 2012). However, up to the present time, the dam plan is not carried forward. Although the political decision about the dam should be based on accurate and thorough information and studies, the knowledge about the dam impact, in particular on environmental aspects is insufficient.

Table 4.2 The specifications of the Kaeng Sua Ten Dam

Features	Unit	
Dam Type		Rockfill
Dam height	m	69
Catchment Area	km^2	3538
Reservoir Area	km^2	66.78
Effective Storage Volume	MCM	1175
Maximum Discharge of Spillway	m^3/s	5355 (Radial Gate ×4)
Maximum Discharge of Discharge Conduit	m^3/s	100
Storage volume at Crest of Spillway	MCM	560

Fig. 4.13 shows the divided watersheds for SFM in the upper Yom River basin. the upper Yom River basin was divided into 2 partitions. The discharge data from Y. 1C runoff station was used as inflows, and from D. 15.8 and D 2.8 runoff stations were used as outflows (Fig. 4.13b).

For each river channel section (Fig. 4.13b), S-Q_o relationship was investigated by using the area and velocity curve in the same way in scenario A. Based on the least-square regression line from the logarithm of S and Q_o pairs, K and P were calculated as the intercept and the slope (Fig. 4.14). The initial time delay T_l for each river channel section was calculated by equation (7).

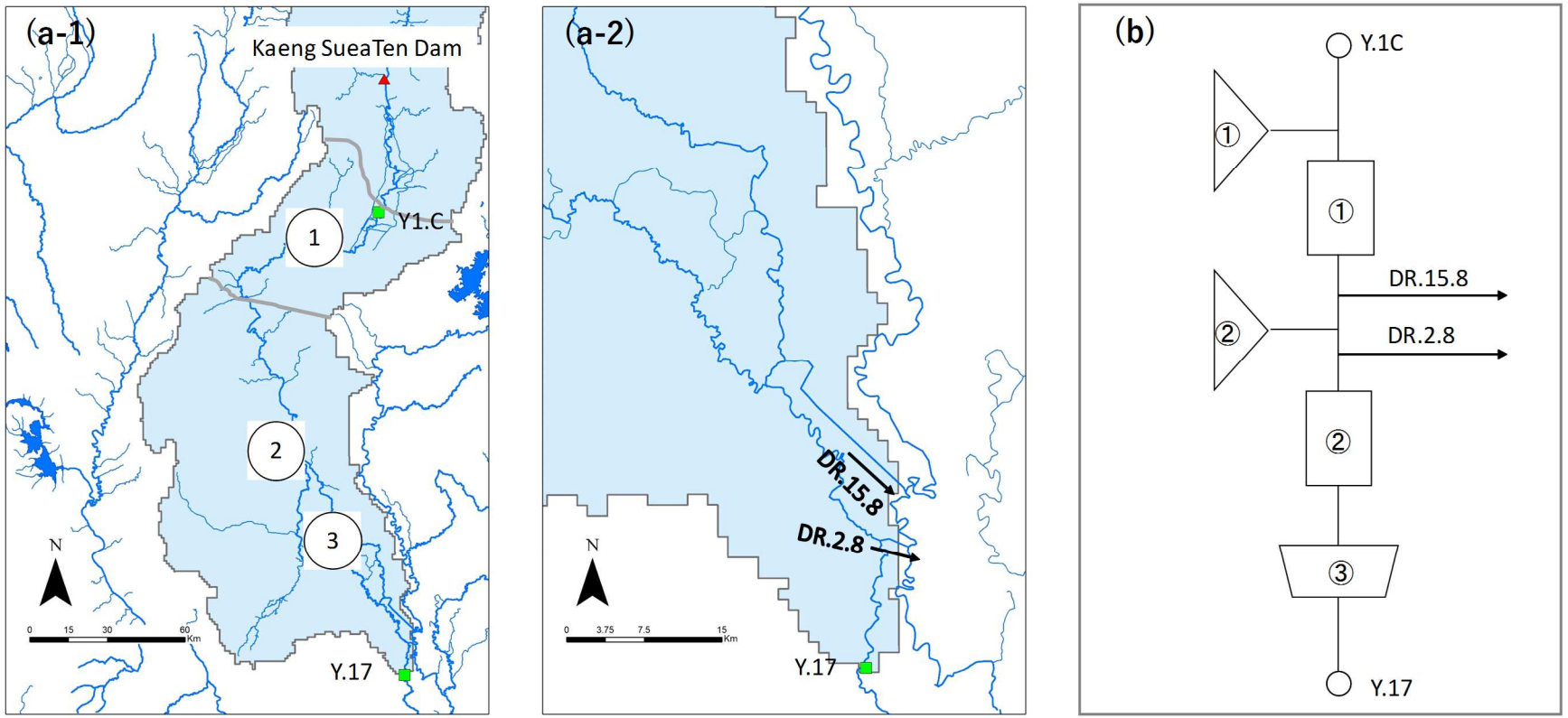

Fig. 4.13 The divided watersheds for SFM in the upper Yom River basin. (a-1) Location map. Green rectangles indicate runoff stations. (a-2) Enlarged view around DR.15.8 and DR 2.8, (b) Pattern diagram. Rectangles indicate river channel sections, triangles indicate watershed sections, and a trapezoid indicates a virtual slit dam.

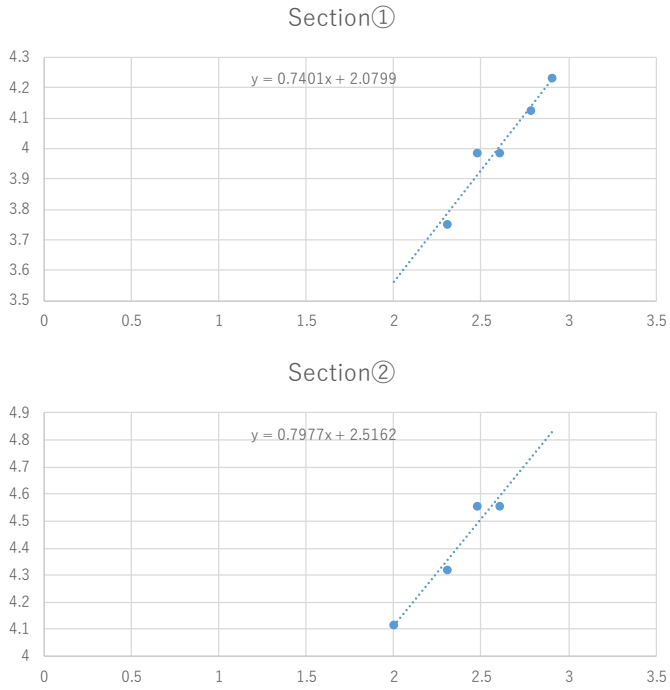

Fig. 4.14 The logarithmic plots of S and Q_o at each river channel section of the Yom River. K and P were calculated as the intercept and the slope of the least-square regression line.

For each watershed block (Fig. 4.9b), K and P were calculated by reserve coefficient method using equation (8) and (9). T_l and Q_b were respectively calculated by equation (10) and (11). According to JICE (1999), f and r_{sa} were defined as 0.5 and 100 mm/hr.

The all parameters for SFM calculated by the above computing were shown in Table 4.3.

Table 4.3 parameters used for SFM of the upper basin of the Yom River.

		river channel		watershed	
	Unit	①	②	①	②
K		120.2	328.25	91.72	139.15
P		0.7401	0.7977	0.333	0.333
T_l		88	86.06	0.63	6.93
f		-	-	0.5	0.5
r_{sa}	mm/hr	-	-	100	100
Q_b	m^3/s	-	-	4.5	3.5
A	km^2	-	-	2475	1932.5

Fig. 4.15 shows the observed discharges at Y. 1C runoff station and Y. 17 runoff station in 2014. Y. 1C is located at the upstream of Y.17 (Fig. 4.11). The floods from Y. 1C underwent the peak cut before Y. 17 runoff

station, due to the inundation around the red areas shown in Fig. 4.16.

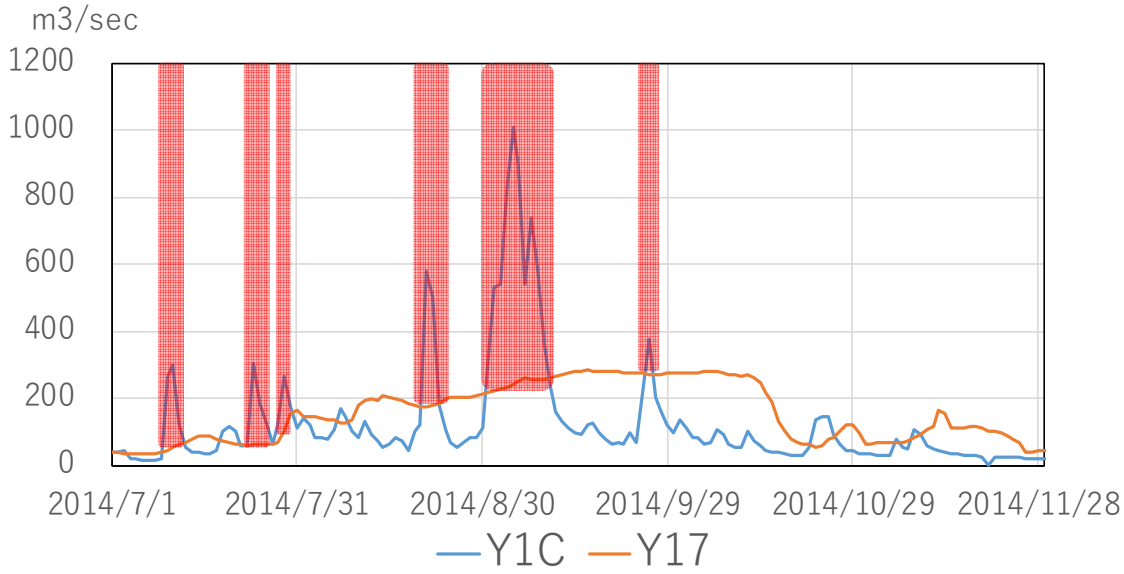

Fig. 4.15 Discharges at Y. 1C runoff station and Y.17 runoff station.

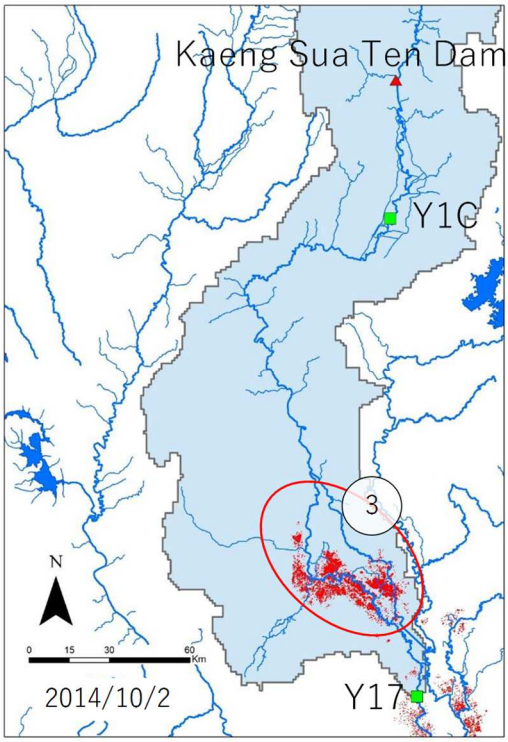

Fig. 4.16 Inundated area map on October 2, 2014 Red areas indicate inundated areas.

In order to consider the peak cut impact into SFM, a virtual slit dam was added at the upstream of Y. 17 (Fig. 4.13b, Fig. 4.17). *H-V* and *H-*Q_{out} relationships were examined at Y. 17 to establish the vertical dam.

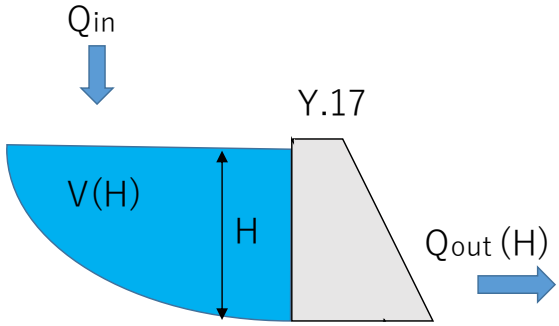

Fig. 4.17 Conceptual diagram of the virtual slit dam at Y. 17. Q_{out} is determined by Q_{in}, *H-V* relationship, and *H*-Q_{out} relationship.

In order to elucidate the *H-V* relationship at Y. 17, the volumes of past inundations at the upper basin of Y. 17 and corresponding water depth ware investigated. The inundated volumes *V* were calculated basing on the observed inundated area (GISTDA 2015) and DEM (digital elevation model) using GIS. The processes to calculate the *V* values were as follows (Fig. 4.18):

(1) Convert inundated area to polyline, in order to calculate inundated area boundaries.

(2) Convert the boundary polylines into raster format with the same resolution of DEM, then extract elevation value for each boundary cell.

(3) Convert the boundary raster into points, the create TIN (Triangle Irregular Network) in order to create water surface.

(4) Convert the TIN into raster format, the minus the DEM in order to calculate the inundated water depth.

(5) Eliminate error water depth cells which negative value due to the limitation of DEM accuracy, then interpolate the eliminated cells based on adjacent water depth values.

(6) sum up the inundated volumes of cells within the Yom River basin

SRTM with 1 arc-second solution was used as DEM. The processes were computed for the inundated data observed on August 16, September 4, 12, November 8, 15, 23 in 2011, and September 7 and 24 in 2014. The water depth at Y. 17 runoff station corresponding with the dates obtained from RID (http://hydro-2.com/). Fig. 4.19 showed the *V-H* plots. The least-square regression line was used as the *H-V* relationship for the virtual dam. Fig. 4.20 showed the *H*-Q_o plots at Y. 17, the quadratic polynomial shown in the figure was used as the *H-V* relationship for the virtual dam.

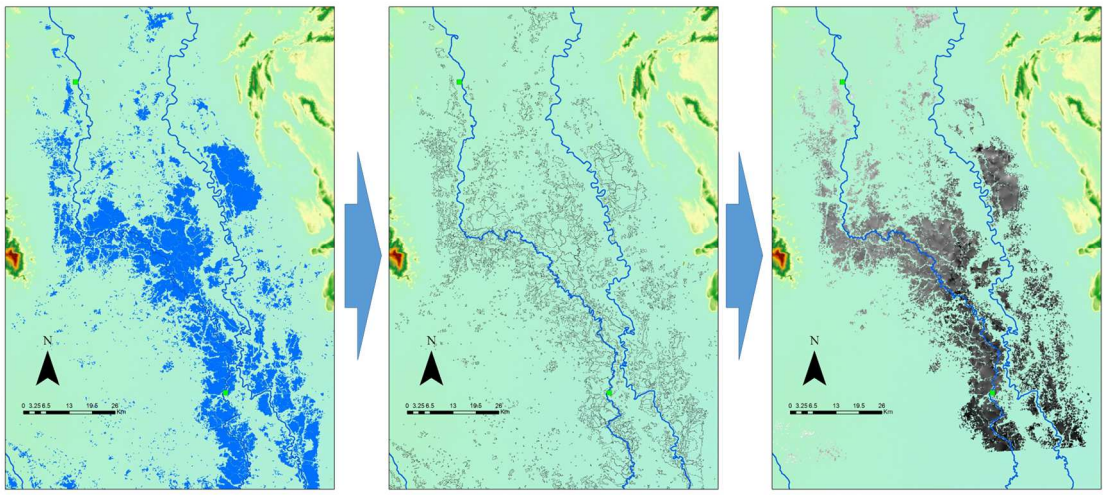

Fig. 4.18 Overview of the calculation processes of inundated volume

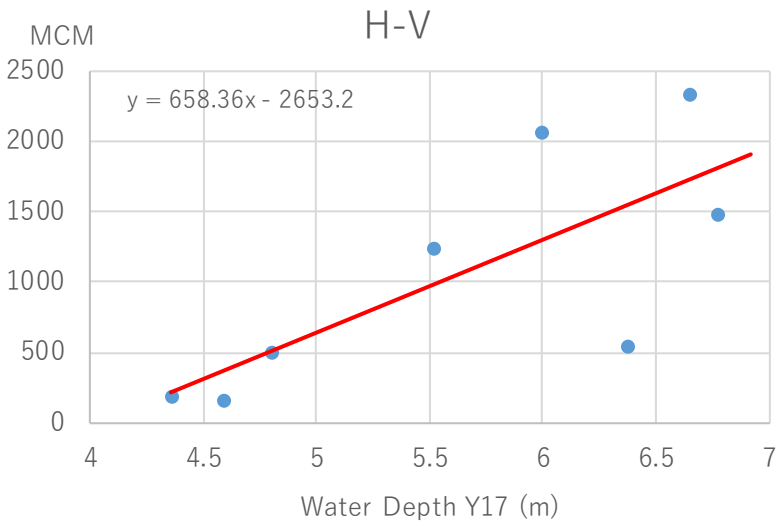

Fig. 4.19 the relationship between inundated volume and water depth at Y. 17.

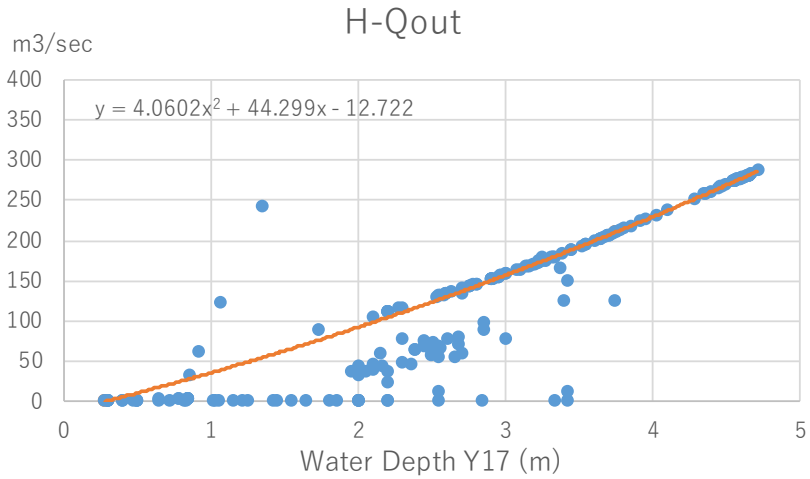

Fig. 4.20 the relationship between dischaerge and water depth at Y. 17.

The operation rule setup for the Kaeng Sua Ten Dam

Table 4.4 shows the operation rule of the Kaeng Sua Ten Dam. In July and November, the dam discharges in the same quantity of inflow, except for when inflow exceeds the maximum discharge of the discharge conduit (=100 m3/s). The excess discharges over 100 m3/s are impounded. From August to October, the dam discharges in the same rule in July until the storage volume exceeds 560 MCM (storage volume at crest of spillway), and it discharges 160 m3/s until the storage volume exceeds 1175 MCM, and it discharges in the same quantity of inflows after the storage volume exceeds 1175 MCM. The discharges 160 m3/s was defined as the most effective discharge which can storage the 2011 flood in full storage capacity.

The inflow discharge of the dam was defined as the allocation of Y. 1C discharge depending on the ratio of the upper watershed area of the dam to the upper watershed area of Y. 1C (7426km^2 for Y. 1C, 3571km^2 for the dam). The initial storage volume of the dam on July 1 was defined as 329MCM (35%), considering the storage ratio of the Bhumibol Dam and the Shirikit Dam on July 1 (35.7%, 38.0%).

Table 4.4 Dam operation rule for Scenario B

	Discharge	
July	August to October	November
Inflow=Discharge	V<560 : max 100m3/sec 560<V<1175: max 160m3/sec 1175<V :Inflow=Discharge	Inflow=Discharge

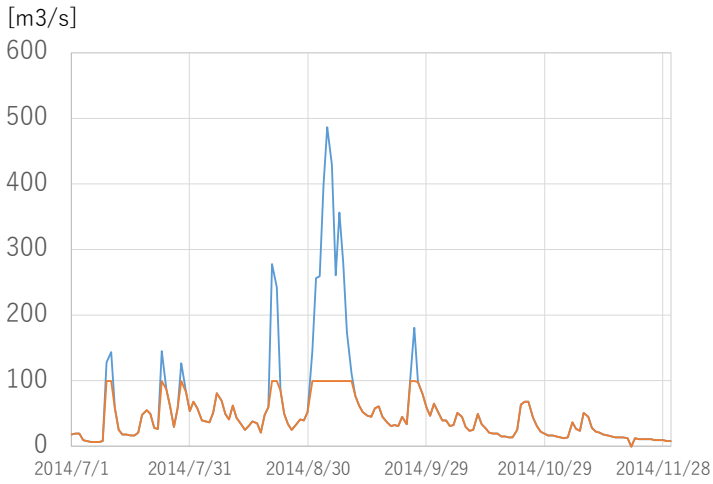

Fig. 4.21 Discharge from Kaeng Sua Ten Dam in 2014. An orange line indicates the discharges from the dam, a blue line indicates inflow to the dam.

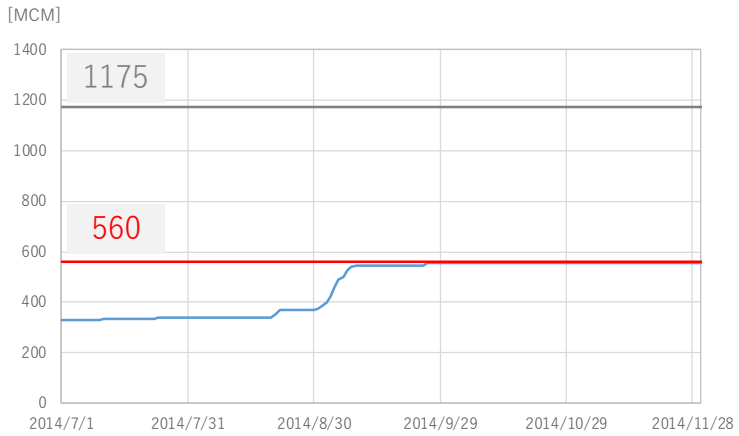

Fig. 4.22 Storage volume of the Kaeng Sua Ten Dam in 2014. A blue line indicates storage volume, a red line indicates storage volume at the elevation of spillway crest.

Fig. 4.21 shows the discharge from the dam. Because the storage volume didn't exceed the volume at the elevation of spillway crest, the maximum discharge of floods was suppressed up to 100 m^3/s through the dam.

As a preprocess for scenario B, the original 2014 flood was simulated to validate the accuracy of the SFM model. Fig. 4.24 shows the discharges result at Y. 17 runoff station. R^2 was 0.869 between the daily SFM discharge and the observed discharge. Subsequently, Y. 1C discharge added the discharge reduction for the dam (Fig. 4.23) was used as boundary inflow in order to computing SFM for the scenario B. The results were shown in Fig. 4.25. The peak discharge at Y. 17 predicted in scenario B decrease from 290.7 m^3/s to 271.5 m^3/s (down 6.6%). The significant decrease of discharge by the dam was found in October, ranged approximately from 45 m^3/s to 90 m^3/s.

Stream discharges for each runoff station (Fig. 4.2) was obtained from RID (http://hydro-2.com/). The SFM analysis was conducted using CommonMP (CommonMP Committee, ver.1.4.0.1). The landscape parameters were calculated using ArcGIS ver. 10.2 (ESRI Japan, Tokyo, Japan).

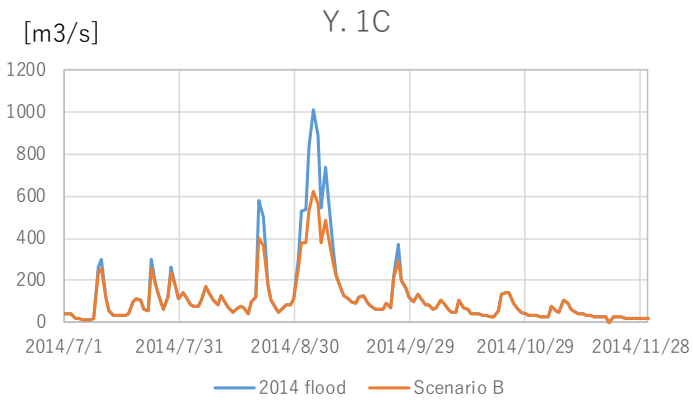

Fig. 4.23 Discharges of Y 1.C. A blue line indicates the discharge in 2014 flood, an orange line indicates the discharge in scenario B.

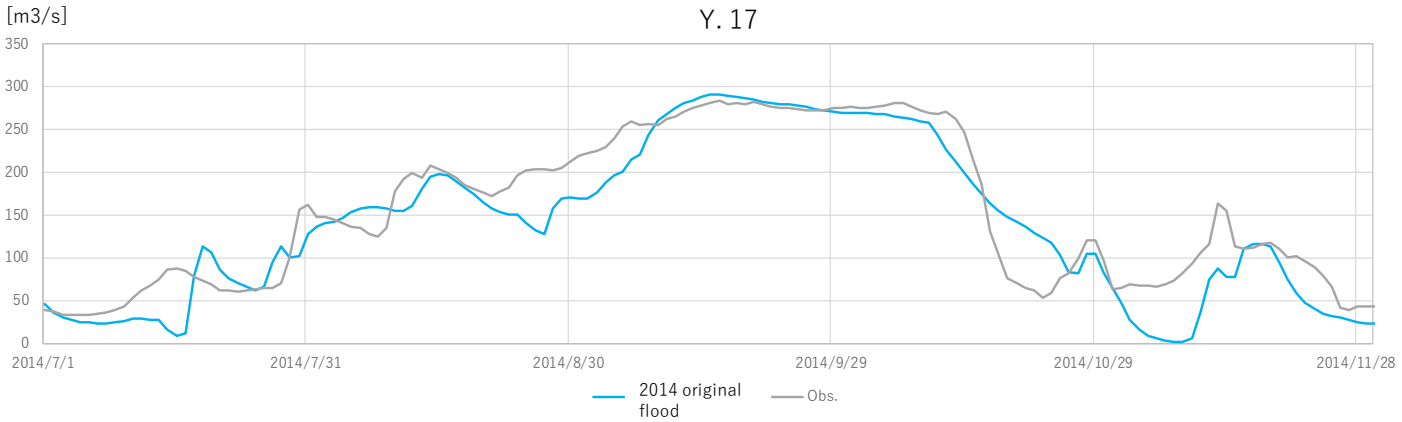

Fig. 4.24 The discharges at Y. 17 runoff station. Blue line indicates the result of the SFM for original 2014 flood, gray line indicates the observed discharge at Y. 17.

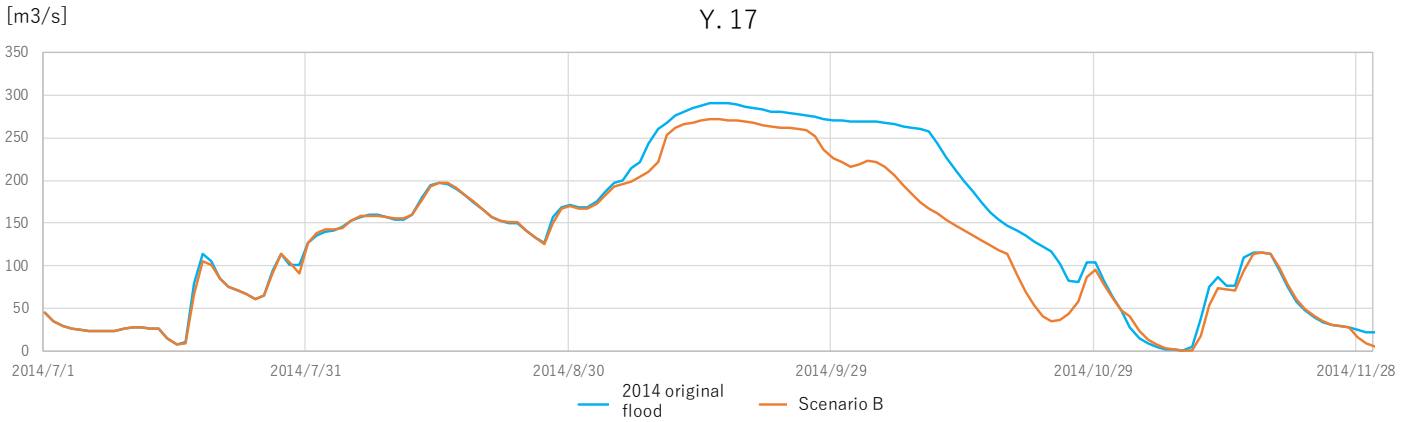

Fig. 4.25 The discharges at Y. 17 runoff station. Blue line indicates the result of the SFM for original 2014 flood, orange line indicates the result of the SFM for scenario B.

4.3 iRIC simulation

4.3.1 iRIC model application for Scenario A

Scenario A was simulated using the iRIC model developed in chapter 3. Stream discharges for runoff station N.7A and P.7A are replaced by the no dam discharges (Fig. 4.9 Fig. 4.11) for Scenario A.

Fig. 4.26 shows the inundated areas simulated in 2014 flood and scenario A by the iRIC model. The grid cells with the maximum depth in the simulation period more than 20 cm were defined as inundated area. The inundated area was 256 km2 for 2014 flood, and was 1209 km^2 for scenario A. In the scenario A, inundated areas appeared in the Ping River basin. This indicate that the Ping River basin has the potential floodplain system which works by a usual year flooding in terms of magnitude. Inundated areas also appeared around the Nan River ranged from the downstream end up to the junction with the Yom River in the scenario A.

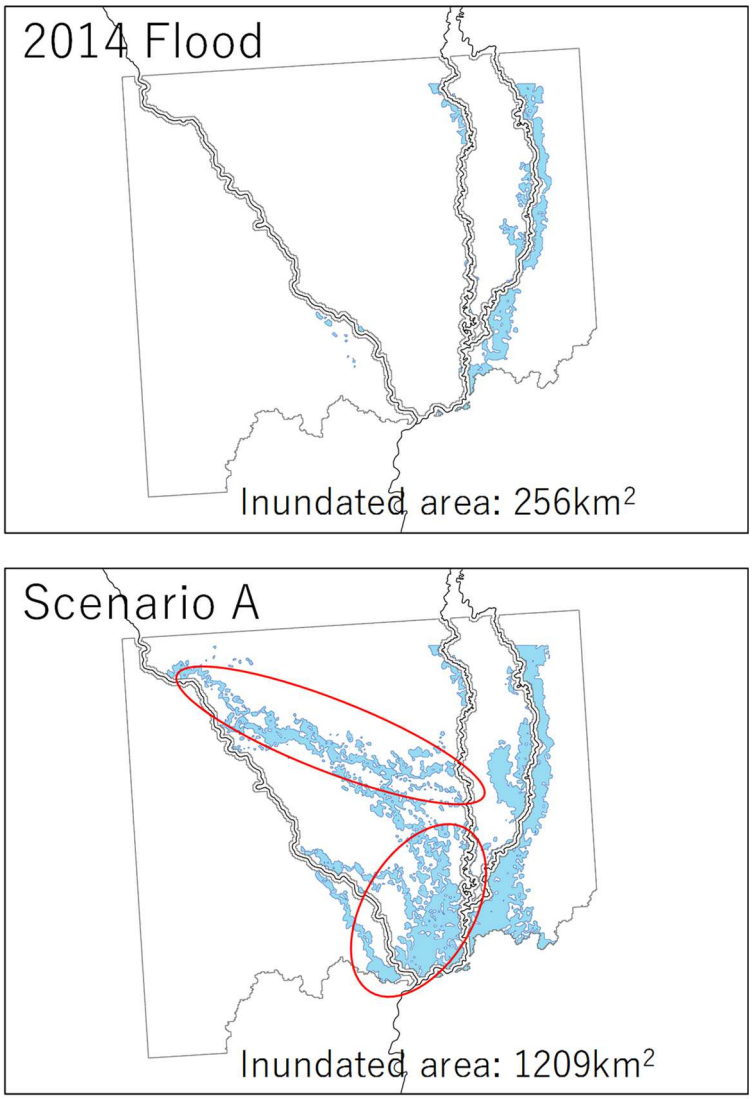

Fig. 4.26 The inundated areas simulated in 2014 flood and scenario A. The grid cells with the calculated maximum depth in the simulation period more than 20 cm were defined as inundated area.

4.3.2 iRIC model application for Scenario B

Fig. 4.27 shows the inundated areas simulated in 2014 flood and scenario B by the iRIC model. The grid cells with the maximum depth in the simulation period more than 20 cm were defined as inundated area. The inundated area was 256 km^2 for 2014 flood, and was 249 km^2 for scenario B. There was no large deference between the inundated areas in 2014 flood and the scenario B. This probably because the discharge from the Yom River was the relatively less than that from the Ping River and the Nan River (Fig. 4.28). This might suggest that the maintenance and improvement of retention areas are required even if the dam was constructed in the Yom River.

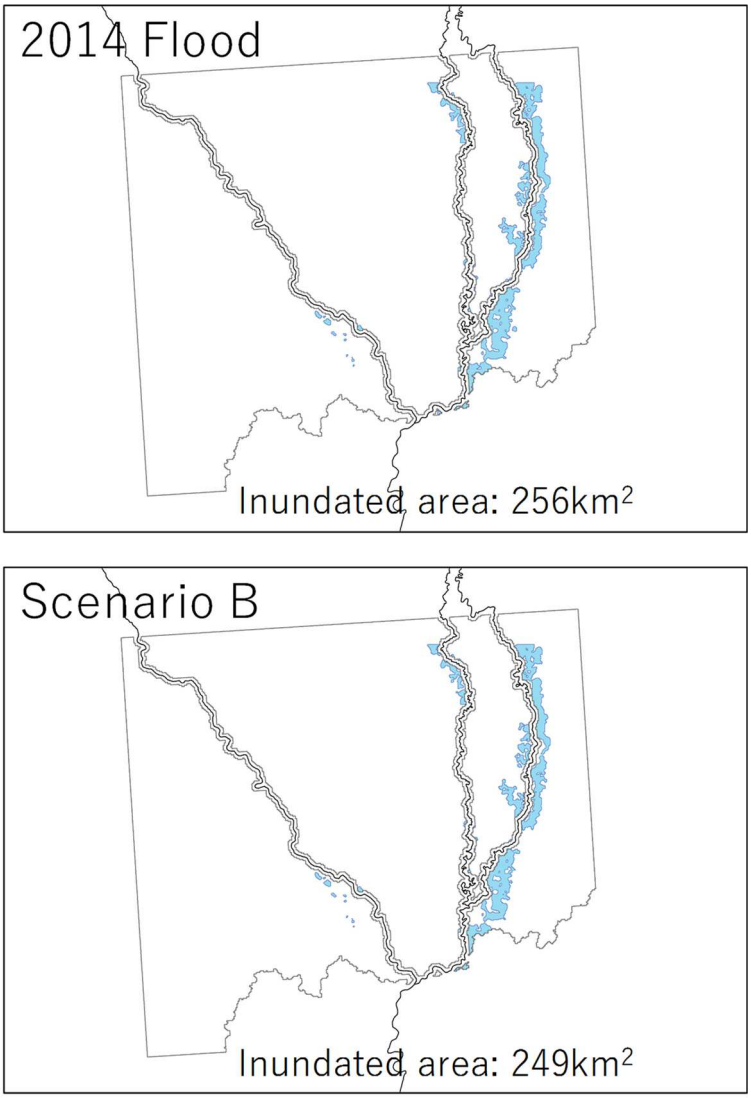

Fig. 4.27 The inundated areas simulated in 2014 flood and scenario B. The grid cells with the calculated maximum depth in the simulation period more than 20 cm were defined as inundated area.

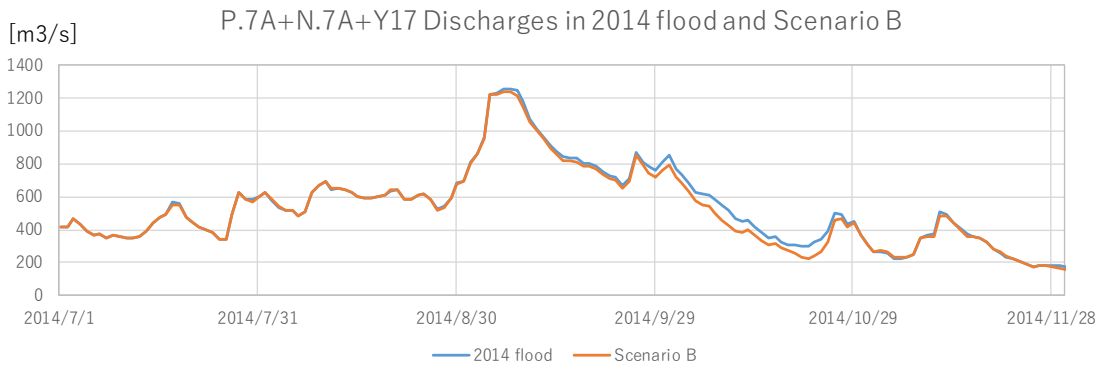

Fig. 4.28 A total of discharges of P. 7A, N. 7A and Y. 17 runoff station in 2014 flood and scenario B.

4.4 Conclusion

The impact of the flood control measures was investigated in two scenarios, using a storage function model and an iRIC model. Scenario A described potential and original floodplain condition in which the two largest dams in the upper Chao Phraya basin don't exist. Scenario B described the future condition with a new dam construction in the Yom River.

In scenario A, inundated area increased more than four times the area in actual 2014 flood. And it was suggested that the Ping River basin of the objected area has the floodplain system in the primal condition (Fig. 4.26). The areas around confluence of the Ping River and the Nan River, where many oxbow lakes exist, were also predicted as the potential floodplains in the primal condition.

In scenario B, there was no large deference between 2014 flood and scenario B in terms of the inundated area. This is probably because the discharge from the Yom River was the relatively less than that from the Ping River and the Nan River and the peak cut effect of the dam in the region is limited (Fig. 4.28). As the limitation of the present study, the dam operation pattern to optimize .

Chapter 5

The relationship between fish species richness and future flood control scenarios

5.1 Introduction

Chao Phraya River is one of major rivers in South-East Asia, and the basin of the river have vast floodplain system. The floodplains are maintained by a regular and long period flood, and many fish species of the basin utilize the predictable and prolonged flood in their life cycle (Rainboth 1996). In the basin, flood control measures have been carried out in accelerating progress, due to the damages of 2011 Thailand flood.

Present study showed the significance of floodplain and flood event on fishes in the basin. Present study also demonstrated the change of the floodplains caused by the future possible dam construction in the middle stream of the Chao Phraya River.

To quantitate the impact of environmental changes on species, Spatial Distribution Model (SDM) was utilized as a powerful tool (Scott et al. 1993, Kiester et al. 1996, Myerset al. 2000). A SDM was established basing on the relationship between species presence/absence distribution and landscape environment, and enable to predict the species loss and sensitivity due to environmental degradations by comparing the SDM predicted results between original environment and deteriorated environment.

In this chapter, I simulated SDM using Maximum Entropy Modeling (Maxent, Phillips et al. 2006) in the middle stream of Chao Phraya River. I also predicted the potential species distributions on maps based on the scenarios which developed in the previous chapter. The gap analysis among 2014 flood and the scenarios was conducted.

5.2 Material and method

There are many SDM methods proposed, for example GLM (Mccullagh, P., Neldeb, J. A. 1983), GAM (Hastie and Tibshirani, 1990), Bioclim (Nix 1986), Domain (Carpenter et al. 1993), GARP (Stockwell and Peters 1999), and Maxent. Several studies compared these methods in terms of predictive performance. Elith et al. (2006) compared 16 modeling method including the methods above using the geographic distributions of different groups of species all over the world and concluded Maxent performed best.

Maxent is a maximum entropy-based machine-learning method and estimates the probability of distribution for a species occurrence and display the probability on a map. Maxent is widely used for creating SDM because of its high predictive accuracy (Merow et al. 2013). MaxEnt uses a list of species occurrence locations as input, and uses a set of environmental landscape predictors (e.g. precipitation, elevation) within a user-defined landscape range.

The Maxents conducted for the 50 species occurred more than 5 sites surveyed (Table 5.1). In the chapter 4, I established the simulation model of the flood regime of the middle stream of the Chao Phraya River, thereby, it is possible to quantitate and use the flood regime characteristics (: magnitude, frequency, timing, duration, Poff et al. (1997) and Richter (1996)) for the SDM. The environmental landscape predictors were Elev, and Mvel, Mdep (as the indices for *magnitude* of flood, see chapter 2), Start (as the index for *timing* of flood), Duration

(as the index for *duration* of flood), and Freq (as the index for *frequency* of flood) (Table 5.2). Mvel, Mdep, Start, Duration, and Freq were the results of the iRIC model in 2014 flood. The predicted SDM was summed in order to elucidate the potential species richness (Fig. 5.1). In addition, the Maxent models in 2014 flood were extrapolated into the floodplain conditions of scenario A and scenario B, in order to predict the responses of the species. The Maxent analysis was computed using MaxEnt software (ver. 3.3.3k).

In order to quantify the changes of fish species richness among scenarios, weighted usable area (WUA) for each the scenario was calculated by following equation.

$$\mathrm{WUA} = \sum_{i} p_i \times A$$

Here,

p_i: probability of distribution for species *i* for each grid cell

A: area of grid cell

Table 5.1 Fish species used in Maxent

Species	Sites	*N*
Acantopsis spp.	16	42
Amblypharyngodon chulabhornae	22	75
Anabas testudineus	24	78
Barbichthys laevis	1	1
Barbonymus altus	15	98
Barbonymus gonionotus	22	109
Barbonymus schwanenfeldii	10	78
Brachirus harmandi	8	14
Channa striata	13	110
Chitala ornata	1	1
Clupeichthys aesarnensis	6	15
Cyclocheilichthys apogon	13	211
Cyclocheilichthys armatus	13	82
Cyclocheilichthys enoplos	9	11
Cyclocheilichthys lagleri	7	15
Dermogenys siamensis	27	103
Esomus metallicus	72	1572
Gobiopterus chuno	9	23
Hemibagrus filamentus	4	6
Hemibagrus spilopterus	2	8
Henicorhynchus siamensis	19	54
Hypsibarbus malcolmi	6	73
Hypsibarbus vernayi	5	14
Labiobarbus leptocheila	8	24
Labiobarbus siamensis	22	73
Lepidocephalichthys hasselti	7	18
Mastacembelus armatus	6	8
Mystacoleucus marginatus	26	298
Mystus albolineatus	11	22
Mystus multiradiatus	11	40
Mystus mysticetus	9	43
Notopterus notopterus	6	8
Oreochromis niloticus	13	66
Oryzias sp.	22	108
Osteochilus sp.	6	11
Osteochilus vittatus	13	19
Oxyeleotris marmorata	5	8
Parachela oxygastroides	6	43
Paralaubuca typus	13	83
Parambassis siamensis	41	419
Pristolepis fasciata	14	38
Puntioplites proctozysron	18	45
Puntius brevis	17	125
Rasbora aurotaenia	5	15
Rasbora borapetensis	10	20
Rasbora dusonensis	10	52
Rasbora paviana	11	51
Trichopodus microlepis	39	409
Trichopodus pectoralis	8	23
Trichopodus trichopterus	67	682
Trichopsis pumila	24	99
Trichopsis vittata	70	576
Xenentodon cancila	6	10

Table 5.2 Variables used in Maxent

	Unit	Description
Elev	m	Elevation of survey site above sea
MVel	m/s	Maximum current velocity of survey site predicted by the iRIC model
MDep	m	Maximum water depth of survey site predicted by the iRIC model
Start	days	Start date of inundation for survey site predicted by the iRIC model
Duration	days	Number of days during survey site inundated predicted by the iRIC model
Freq		Number of times survey site was inundated predicted by the iRIC model

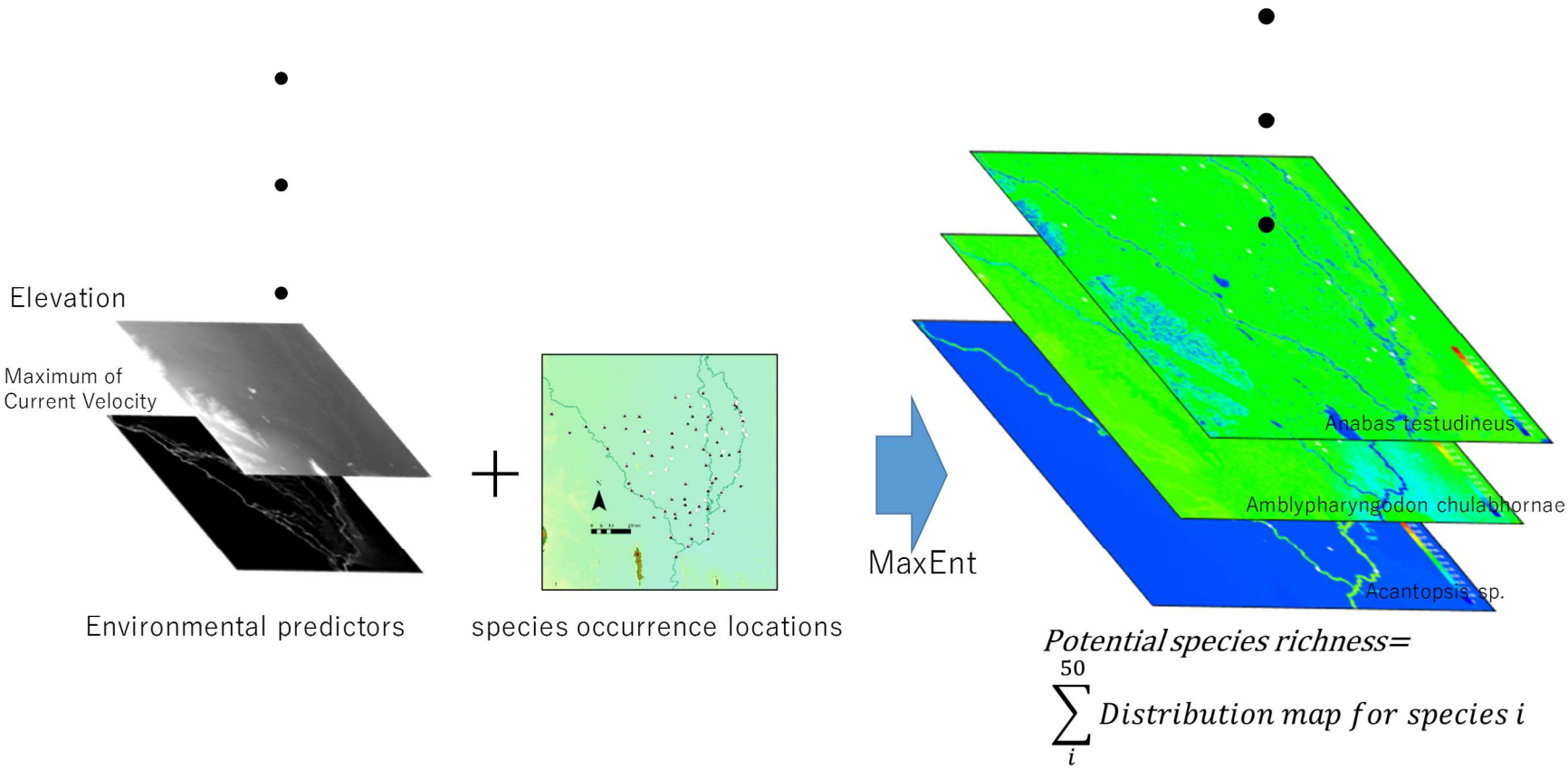

Fig. 5.1 Conceptual diagram of the Maxent analysis.

5.3 Result and discussion

Fig. 5.2 shows the potential species richness predicted for 2014 flood. The fish species richness ranged from 15.3 to 25.8. Most high biodiversity areas were found in the main river stream in which distribution of many fluvial fishes predicted. While many limnophilic species and floodplain migratory species intensively occurred in the floodplains along the Nan River and the Bueng Boraphet Lake. The result indicates the existence of floodplain generally increase fish species richness in the region, as well as the result of chapter 2. In present status, the adjacent floodplains of the Nan River and the Bueng Boraphet Lake satisfy many species' environmental requirements and are regarded as the prior areas for conservation. The Bung Boraphet Lake is known as the habitat for 54 fish species (Thai Fisheries Department 2005), and the fishery resources play a positive and significant role for the provincial economy.

Fig. 5.3 shows the potential species richness predicted for scenario A (no dam scenario). The fish species richness ranged from 15.3 to 26.0. The high limnophilic and floodplain migratory species richness areas appeared in the Ping River basin are local scale "Hotspots" which means the region with a significant high biodiversity under threat from human impacts defines by Myers et al. (2000). These areas are considered as the prior areas for restoration of floodplain. Because the areas are not suitable for intensive land-use for the reason that the areas are inundated by the flooding with larger magnitude than usual year (2014). Additionally, because it is generally cost saving to restore flood dynamics in potential floodplains.

Fig. 5.4 shows the potential species richness predicted for scenario B (dam construction scenario). The fish species richness ranged from 15.5 to 25.4. There was no big difference between scenario B and 2014 flood. However, as the limitation of the present study, the prevention of longitudinal migration and recruitment by the dam for fishes is not considered. For example, *Henicorhynchus lobatus* is suggested to longitudinally migrate more than 200 km in the Mekong River, and its migration behavior is substantially restricted in some fragment sub-basin by damming (Fukushima et al. 2014). Moreover, inland fisheries might be impacted particularly in mountainous area where it is an important source of protein for populations. Although the ecologies of most of fish species in Southeast Asia remain unclear, future studies should thoroughly investigate the potential impact of the dam.

The WUA for 2014 flood and the scenarios were shown in Fig. 5.5. Approximately WUA of 120000 [Sp. No. $\times m^2$] have been lost by present flood control conditions. Most of the losses caused by the reduction of floodplain in the Ping River basin. As shown in chapter 2, the richness of floodplain migratory species in the mainstream of the Ping River is lower than that in the mainstreams of other rivers, the restoration of floodplains in the basin is urgent issue. In the other hand, the loss of WUA caused by constructing the new dam in Yom river was limited.

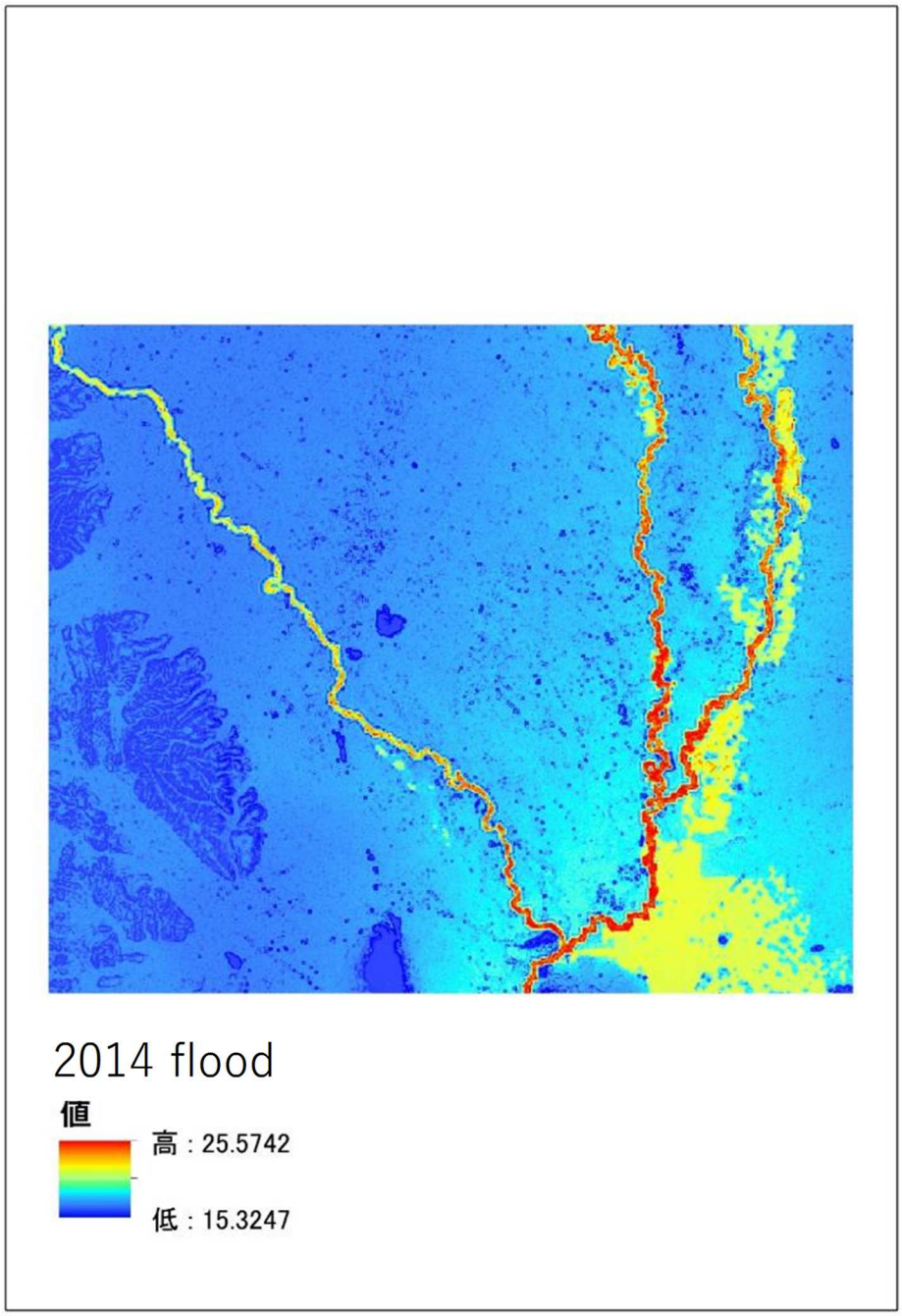

Fig. 5.2 The potential species richness predicted for 2014 flood (original condition).

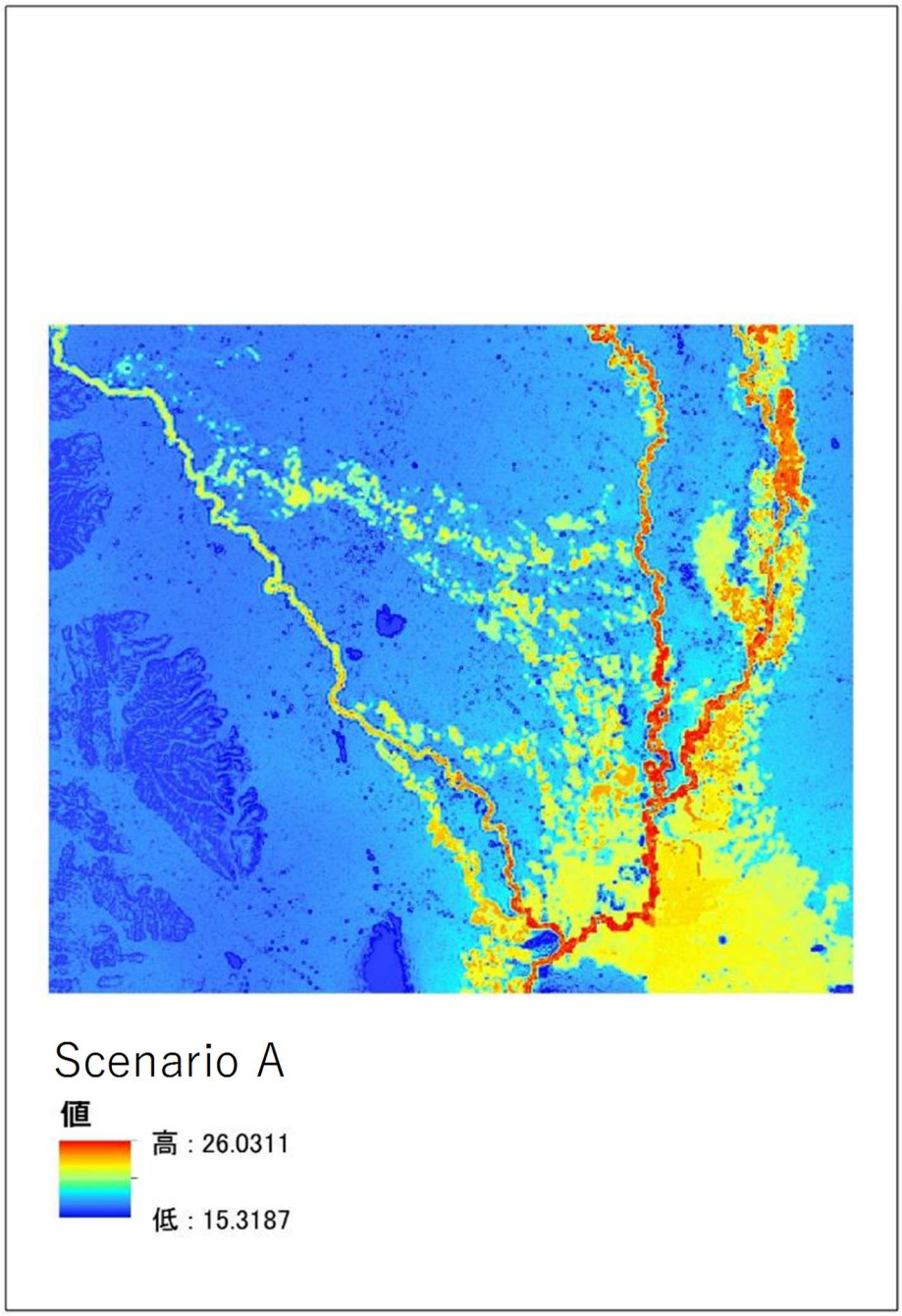

Fig. 5.3 The potential species richness predicted for scenario A.

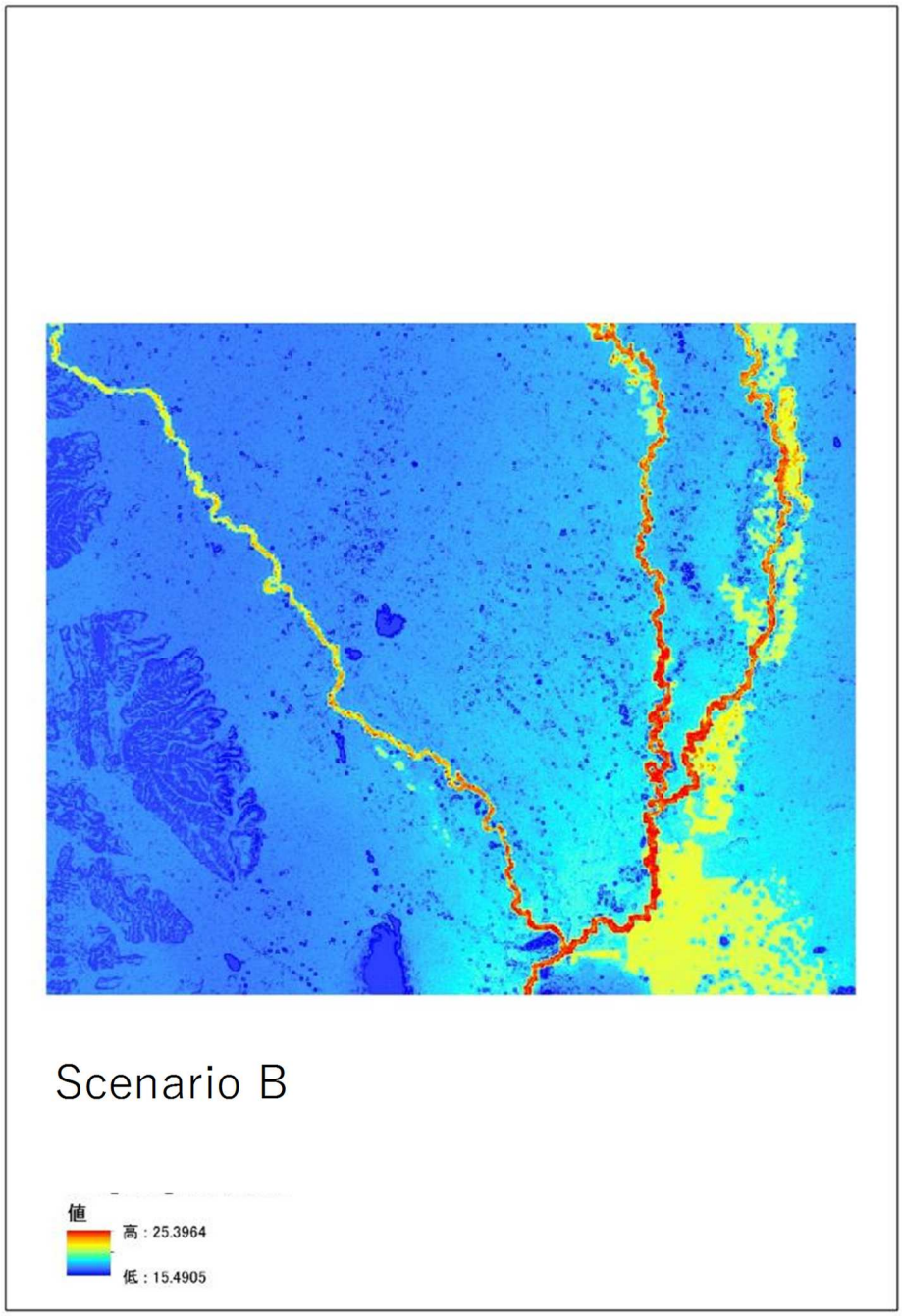

Fig. 5.4 The potential species richness predicted for scenario B.

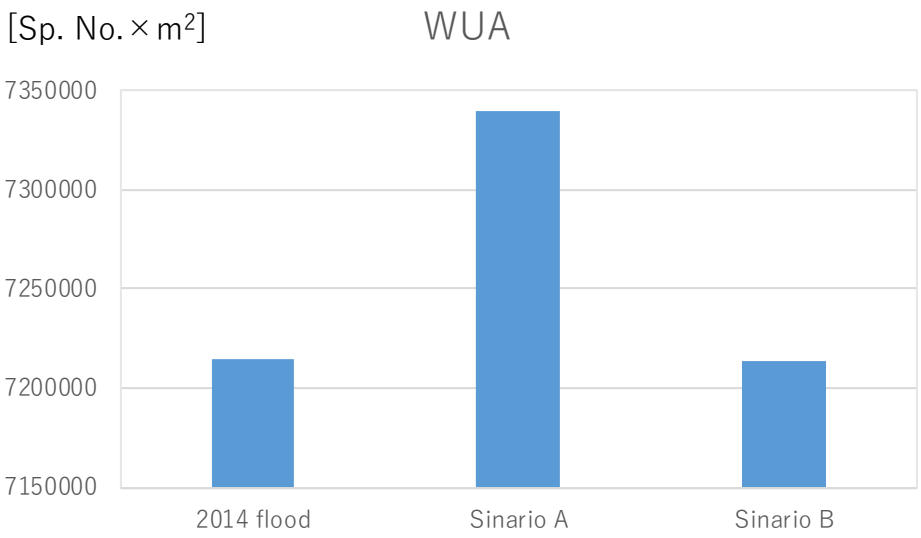

Fig. 5.5 Weighted Usable Area for each scenario.

Chapter 6

Suggestions for fish richness conservation in the middle stream of the Chao Phraya basin

6.1 Introduction

The previous chapters showed that the floodplains play important ecological roles for fish biodiversity in the middle stream of the Chao Phraya River. The key question asked in this chapter is these: what kinds of floodplains are an important environment for fish species? what kinds of floodplain environments are lacking in the basin? These are essential knowledge for suggesting effective conservation plan.

In this chapter, I simulated fish richness response to each floodplain quality predictors and visualized the lacking floodplain environments for each sub-basin of three tributaries in the region using MaxEnt software.

6.2 Materials and methods

The response of each species to the certain two floodplain environmental predictors was figured by extrapolating the Maxent model developed in chapter 5 (Fig. 6.1). Fig. 6.1 showed the example of response map of *Amplypharyngodon chulaphornae* to MVel and MDep. In this demonstration, the predictors except for MVel and MDep were assigned these averages, and MVel and MDep distributions were setup to increase their value respectively with x-coordinate and y-coordinate of the predictor map. The predicted map for each species were summed in order to elucidate the response of species richness. The extrapolations were conducted for the 50 species as well as chapter 5 (Table 5.1) in a *MVel-MDep* plane and *Start-Duration* plane.

In addition, Cross-tabulation tables of floodplain area ratio were created from the ten classification of a *MVel-MDep* plan and *Start-Duration* plane at even intervals for each tributary basin (Fig. 6.2). The cross-tabulation tables represent the amount and attribution of the floodplains contained for each tributary basin.

In order to visualize the lacking floodplain environments for each sub-basin of three tributaries, the summed response maps and the cross-tabulation tables was overlapped.

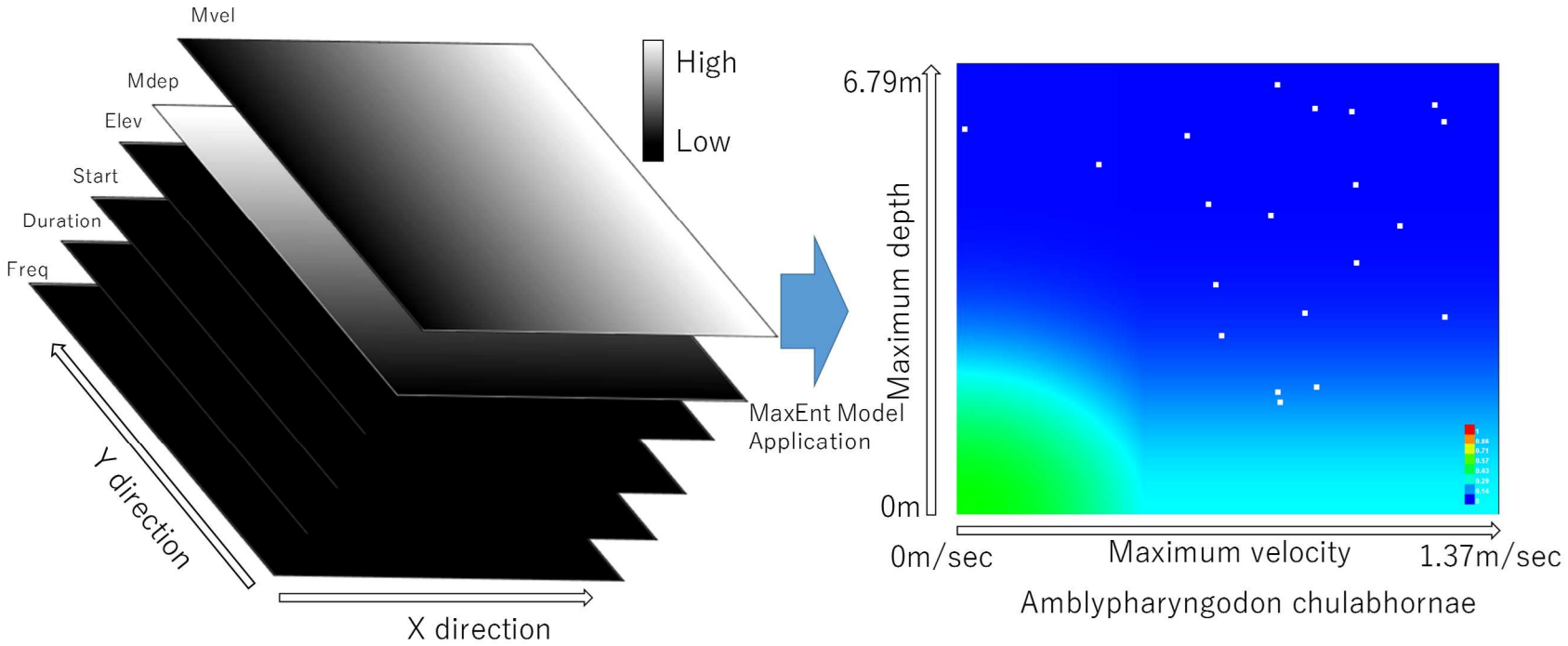

Fig. 6.1 Conceptual diagram of the visualization of suitable floodplain conditions for each species using Maxent model.

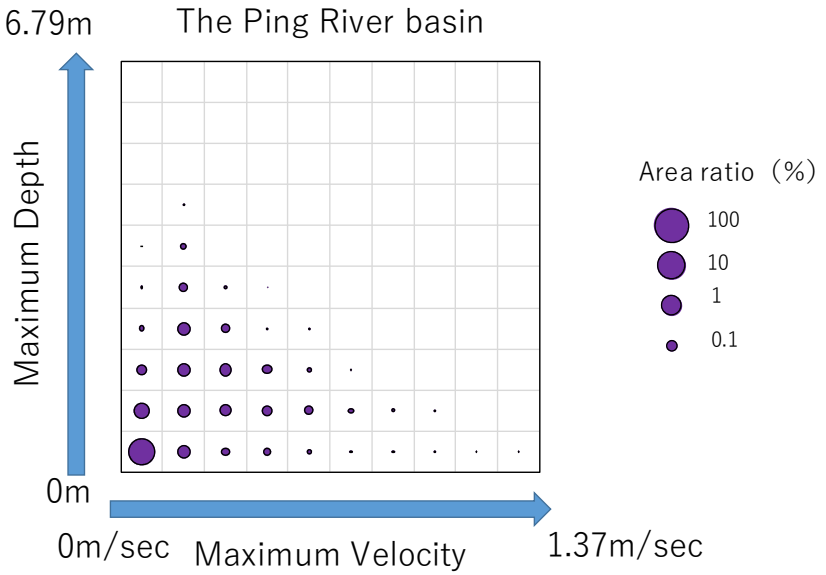

Fig. 6.2 Example of the Cross-tabulation tables of floodplain area ratio in a *MVel-MDep* plane for the Ping River basin.

6.3 Result and discussion

Fig. 6.3 showed the overlap figures of a response map and a cross-tabulation table in a *MVel-MDep* plane for each sub-basin of three tributaries. The areas enclosed by red lines in Fig. 6.3b and Fig.6.3c were lacking in the Ping River basin. These areas indicate the waterbodies limnophilic and large-scale habitat inundated by the floods. The areas showed high potential species richness due to be suitable habitats for both the limnophilic species such as *Trichopodus trichopterus*, and the lacustrine species such as *Labiobarbus leptocheila*, and *Barbonymus gonionotus* (Fig. 6.4). Thereby, it is suggested that the restoration of large-scale floodplain waterbodies adjacent to the Ping River such as oxbow lakes and old river channels are effective conservation plan for the basin. It is also effective to improve the connectivity between the riparian lakes and the mainstream of the river, which ease the migration of fishes.

Fig. 6.5 showed the overlap figures of a response map and a cross-tabulation table in a *Start-Duration* plane for each sub-basin of three tributaries. The areas with high potential species richness enclosed by orange lines in Fig. 6.3b and Fig.6.3c were lacking in the Ping River basin. Especially the enclosed area by the red line in the Nan River basin showed high potential species richness, and considered to have high conservation value. The areas enclosed the orange lines were the areas inundated at the beginning of the flooding. These environment is supposed to be invaluable because the coincidence of a flood timing and a spawning timing is one of the key factors to maintain the populations of floodplain dependent species (Humphries et al. 1999). The areas enclosed the red lines in the Nan River basin were the areas where not only inundate at the beginning of the flooding but also poorly drain the flood waters. The inundated duration is also important because by which the growth of juveniles was determined.

6.4 Conclusion and Suggestion for fish richness conservation

The conservation of floodplains and fishes in the region is important for many reasons. The Chao Phraya River Basin is known for its high fish biodiversity. More than 690 freshwater fish species have been recorded and many utilize the floodplains during their life cycle (Rainboth 1996, Kottelat and Whitten 1996). Moreover, inland fisheries have long been a part of Thai culture and are an important source of protein, especially for rural populations. Based on catch, the Thailand inland fishery ranked 13th in the world in 2012 (Moffitt and Cajas-Cano 2014). Floodplains are maintained by dynamic interactions between flooding and landscape, and floodplains are disappearing at an accelerating rate in Southeast Asia, primarily as a result of changing hydrology caused by large-scale irrigation schemes and dams (Tockner and Stanford 2002). Mateo et al. (2014) investigated the impact of the operation of large-scale dams since the 2011 Thailand flood and found that the inundated area in the Chao Phraya River Basin was reduced by 40%.

The impact of the Kaeng Sua Ten Dam on the fish species richness might be limited at least for the species characterized by lateral migration behavior in the middle stream of the Chao Phraya River basin. However, the results don't support that the impact on the species characterized by longitudinal migration behavior is limited. Because the ecology of fishes in Southeast Asia is still in the first stage and the ecologies of most of fish species remains unclear, the impact of the dam on the fishes should be thoroughly investigated, including the effectiveness of flood control.

In present status, the adjacent floodplains of the Nan River and the Bueng Boraphet Lake satisfy many species' environmental requirements and are regarded as the prior areas for conservation. The Bung Boraphet Lake is known as the habitat for 54 fish species (Thai Fisheries Department 2005) and for 187 bird species, and is considered to be of international conservation importance (BirdLife International 2004, Scott 1989). While the Nan River basin was relatively paid less attention. Only small number of studies reported the species endemism of the river (e.g. Suvarnaraksha 2015, Lothongkham et al. 2014). In this study the fish species richness of the river and its floodplain was the same or more than the that of the Bueng Boraphet Lake in any scenarios. This dissertation recommends giving the further conservation priority for the Nan River and its floodplain.

In the present study, the main stream of the Ping River, which has a smaller floodplain area compared with the other two rivers, showed a relatively low fish species richness. The reduction in floodplain area secondary to flood control measures (e.g., the Bhumibol Dam) may affect species richness, especially of migratory species in the Ping River Basin, such as *Barmonymus altus*, *Barmonymus gonionotus*, *Cyclocheilichthys armatus*, *Cyclocheilichthys enoplos*, *Esomus mettalicus*, *Henicorhynchus siamensis*, *Paralabuca typus*, *Parambasis siamensis*, *Hemibagrus filamentus*. While, the Ping River basin was revealed to have flood plain system which works in usual flood year by the scenario analysis. For the basin, it is suggested that the restoration of large-scale floodplain waterbodies adjacent to the Ping River such as oxbow lakes and old river channels are effective conservation plan.

On the other hand, flooding has the potential to cause serious damage to the economy of Thailand (e.g., the 2011 Thailand flood). Further studies are needed to assess the respective advantages and disadvantages of

flood control measures in the Chao Phraya River Basin and to identify the best approach to protect both the economy and biodiversity.

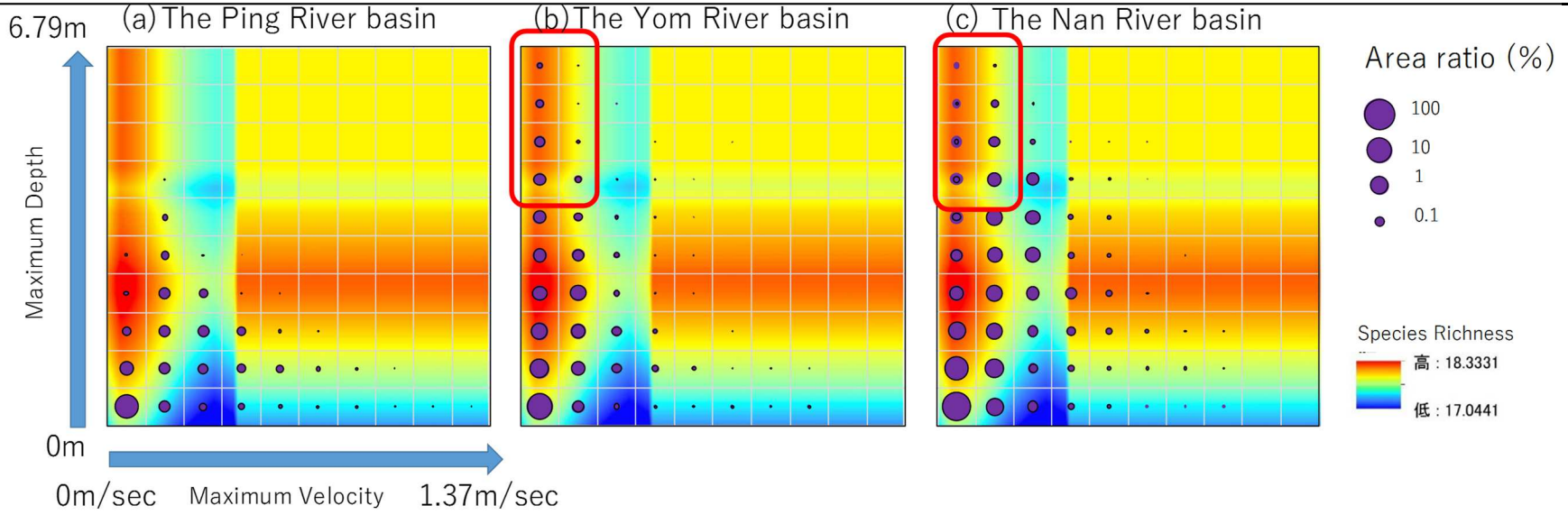

Fig. 6.3 The overlap figures of a response map and a cross-tabulation table in a *MVel-MDep* plane for each sub-basin of three tributaries.

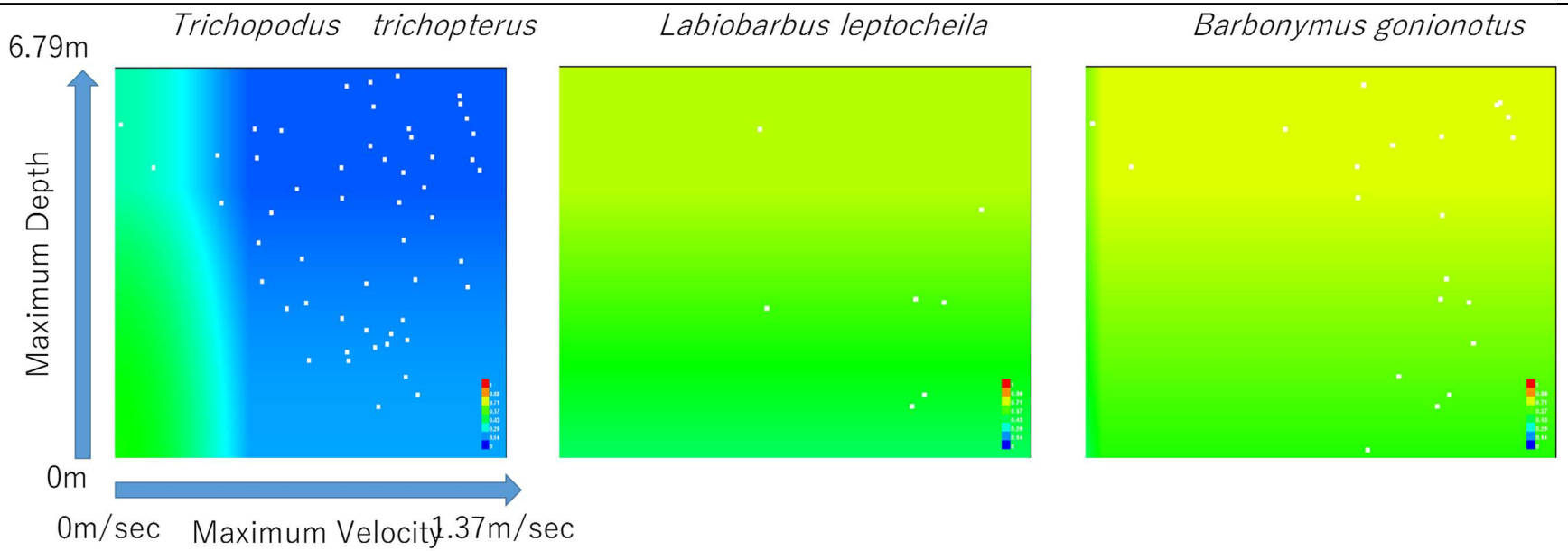

Fig. 6.4 The response map of three species to MVel and MDep.

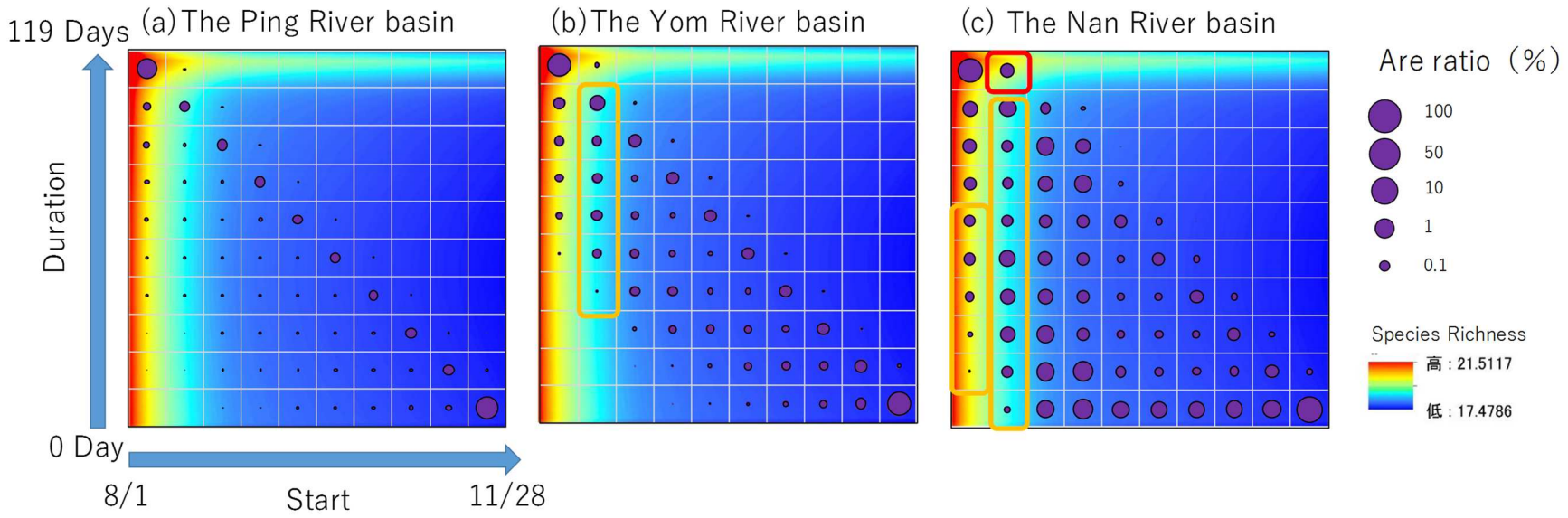

Fig. 6.5 The overlap figures of a response map and a cross-tabulation table in a *Start-Duration* plane for each sub-basin of three tributaries.

Appendix

The fine scale prediction of Urban Density (UD) for inundation analysis using Landsat OLI image: a case study of Nakhon Sawan, Thailand

Abstract

I studied the fine scale prediction method of Urban Density (UD) for inundation analysis using Landsat OLI image, in Nakhon Sawan, Thailand.

A generalized additive model (GAM) and model selection using Akaike's Information Criteria (AIC) in two different seasons (March and November) were conducted. The result showed as follows. 1) The explanation power of the models using the explanation variables calculated by Landsat OLI image in November were relatively higher than that of the models in March. 2) UD in 30m grid squares was strongly positively related to Urban Index, At-satellite Brightness Temperature, and Color Complexity which was defined as the indicator of complexity in color distribution pattern of satellite image in this paper. The coefficient of determination R^2 of the best model was 0.649.

The result suggest that UD can be predicted in the decent accuracy for inundation analysis in Nakhon Sawan without much effort and cost. This prediction method cloud be applied the urban areas threatened with flood risk in the world.

A.1 Introduction

近年の異常気象や都市化の進展は，世界各地の降雨特性や流出形態を大きく変化させており，災害外力の増大によって都市域に深刻な洪水被害が発生すると予想されている（Walther, G.R. et al. 2002；Allen, M.R. et. Al. 2002）．市街地における氾濫流の挙動は，建築物や道路空間などに大きく影響されるため，都市域の洪水氾濫を精度よく予測するためには，これらの効果を考慮した解析を行うことが重要である（Kawaike et al. 2002, Miura et al. 2011；Uchida and Kawahara 2006）.

都市域の氾濫解析において，個々の建築物の形状を境界条件として取り込むことは，多大な労力と演算時間を要することから，実務の場では，解析格子ごとの建物占有率 UD (Urban Density) をメッシュ特性として解析に反映する方法が一般的に用いられている（Kurihara et al. 1996, NILIM 2014）.

建物占有率 UD のデータの取得に関しては，国土地理院が，「基盤地図情報」として，日本の一部地域で 1/2,500，全国で 1/25,000 のスケールで「建築物の外周線」を公開しており、これらのデータからメッシュ毎の UD データを作成し氾濫解析に使用することが可能である．しかし，基礎的な GIS 情報の整備が進んでいない海外の途上国の多くでは，衛星画像や都市計画図などから建築物を抽出し，一から UD データを作成する必要があり，廉価で簡捷な UD の推定手法の確立が求められている.

既往の研究においては，建築物と道路などの人工物を合わせて不浸透域 (Imeprvious Area) として推定したものが多い（例えば，Lee, S. et. Al. 2005；Yuan, F.，2007）．建築物のみを対象とした研究で

は，Kawamura et al.（1995，1996，1998）や Hayasaka et al. (1997)が，Landsat TM の衛星画像解析から，UD と都市化指標 UI (urbanization index) との間に強い相関があることを報告しており，衛星画像から UD を省力的に推定可能であることが示唆されている．しかし，いずれの研究においても，数百 m スケールのメッシュサイズにおいて建物占有率の推定を行っており，氾濫解析が対象とするような数 m から数十 m のメッシュスケールでの推定精度や推定手法を確立する必要がある．
そこで，本稿では，海外でも適用可能で，省力的な建物占有率 UD の推定手法を提案することを目的に，タイ国の洪水頻発地域であるナコンサワン市街地において，Landsat OLI の衛星画像より取得した各種指標と建物占有率 UD との関係を検討した．

A.2 Material and method

A.2.1 Study area

ナコンサワン市は，チャオプラヤ川流域の中流に位置する都市で，人口 225,903 人，行政区の面積は 748.27 km2 である（2010 年 The Population And Housing Census タイ王国統計局）．地形はチャオプラヤ流域の上流域と下流域を分かつ狭窄部であり，ナコンサワン市でピン川，ヨム川，ナン川の 3 川が合流し，チャオプラヤ川となる（Fig. A.1）．年間降水量は 1,149mm で明瞭な雨季と乾季があり，雨季に度々洪水の被害にさらされる．ナコンサワンの市街地の外側には，主にさとうきび畑と水田が広がっている．

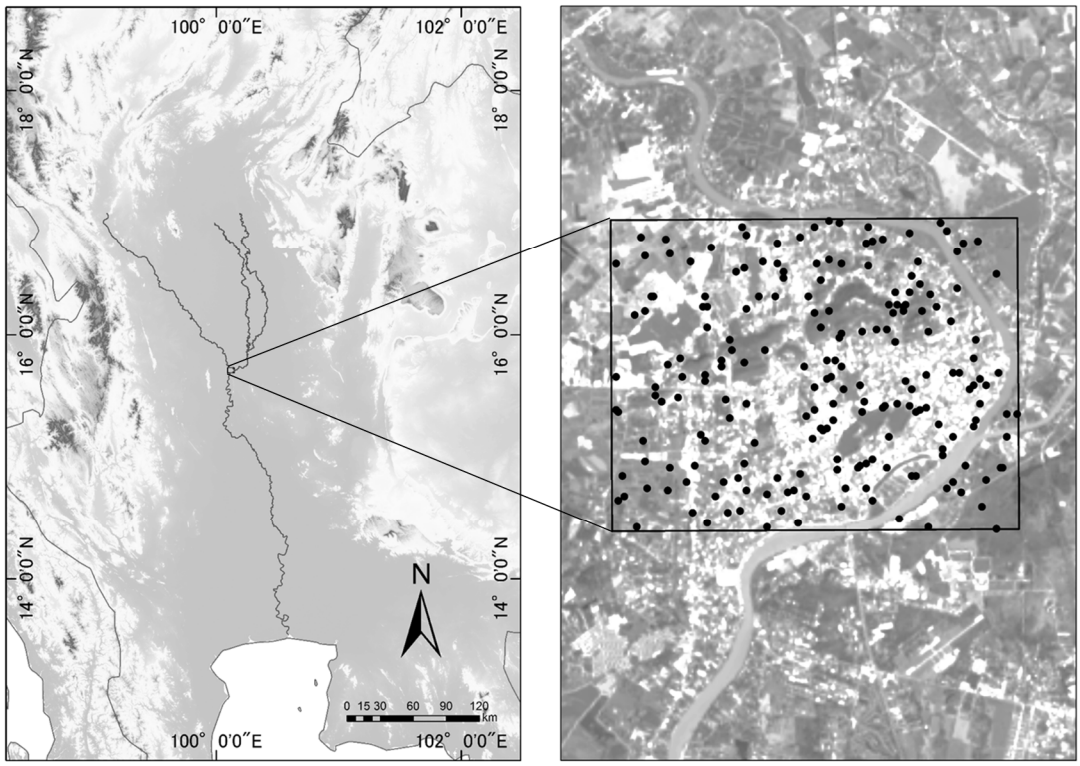

Fig. A.1 Study area location. The reference area is indicated by black rectangle. The sampling mesh sites are indicated by black dots.

A.2.2 Materials

衛星データは，アメリカ地質調査所（USGS）の運用する Landsat8 衛星により観測された OLI（Operational Land Imager）センサ画像を利用した．OLI センサは，およそ 30m の中解像度を有しており，USGS の HP から無料で入手可能である．センサの諸元を Table A.1 に示す．データを解析するにあたって，都市化指標 UI や植生指標 NDVI などの指標は季節的に変化するため，使用する衛星画像の季節によって建物占有率の推定精度に差が出ることが予想された. そのため, 乾季である 2014 年 3 月 29 日，雨季である 2014 年 10 月 16 日の 2 画像を用い，それぞれの画像について，UD の推定と精度の比較を行った.

Table A.1 Specifications of Landsat OLI sensor

Spectral Bands	Wavelength	Band Number
Coastal Aerosol	0.433 - 0.453 µm	Band 1
Blue	0.450 - 0.515 µm	Band 2
Green	0.525 - 0.600 µm	Band 3
Red	0.630 - 0.680 µm	Band 4
Near Infrared (NIR)	0.845 - 0.885 µm	Band 5
SWIR1	1.560 - 1.660 µm	Band 6
SWIR2	2.100 - 2.300 µm	Band 7
Panchromatic	0.500 - 0.680 µm	Band 8
Cirrus	1.360 - 1.390 µm	Band 9
Thermal Infrared (TRIS) 1	10.30 - 11.30 µm	Band 10
Thermal Infrared (TRIS) 2	11.50 - 12.50 µm	Band 11

A.2.3 Calculation of Index and UD

対象とした 2 画像からそれぞれ水域を除外した後，以下の式により，各ピクセルのデジタルナンバーを反射率へと変換した（USGS, 2015）.

$$\rho_i = \frac{M_\rho * DN_i + A_\rho}{\sin(\theta_{SE})} \qquad (1)$$

ここで，ρ_i：バンド i の反射率，DN_i：バンド i の DN 値，M_ρ：バンド i の反射率ゲイン，A_ρ：バンド i の反射率バイアス，θ_{SE}：衛星通過時の太陽高度.

上式による変換後，Table A.2 に示す指標を抽出し解析に用いた．後述する CC を除く指標は， (2) , (3) , (4) , (5) , (6)式より求めた.

$$UI = \frac{\mathrm{Band7} - \mathrm{Band5}}{\mathrm{Band7} + \mathrm{Band5}} \quad (2)$$

$$NDBI = \frac{\mathrm{Band6} - \mathrm{Band5}}{\mathrm{Band6} + \mathrm{Band5}} \quad (3)$$

$$NDVI = \frac{\mathrm{Band5} - \mathrm{Band4}}{\mathrm{Band5} + \mathrm{Band4}} \quad (4)$$

$$BA = \mathrm{NDBI} - \mathrm{NDVI} \quad (5)$$

$$T = \frac{\mathrm{K2}}{\ln\left(\frac{\mathrm{K1}}{\mathrm{ML} * \mathrm{DN}_{10} + \mathrm{AL}} + 1\right)} - 273.15 \quad (6)$$

ここで，*Band i*：バンド i の反射率，*K1*: Band10 の温度変換定数 1，*K2*: Band10 の温度変換定数 2，*ML*：バンド 10 の放射輝度ゲイン，*AL*：バンド 10 の放射輝度バイアス．UI, NDBI, NDVI は，無単位の比演算の値であるため、地形効果や大気散 7 乱効果などが各バンドで全て同じであれば、理論的にはそれらの値を除去・軽減することが期待できる（Akiyama et al. 2006）．正確な地表面温度の算出には大気補正や物質の反射率補正などが必要になってくるが本稿では行っておらず, 輝度温度 T は，相対値である．指数の算出には，ESRI 社の ArcGIS (ver.10.2) を用いた．

Table A.2 Explanatory variables in the models to predict UD (Band *i*: Landsat's band order, K1: Band-specific thermal conversion constant 1, K2: Band-specific thermal conversion constant 2, ML: Band-specific multiplicative rescaling factor, AL: Band-specific additive rescaling factor)

Vriables	Index	Formula	Reference
UI	Urban Index 都市化指数	$UI = \frac{\mathrm{Band7} - \mathrm{Band5}}{\mathrm{Band7} + \mathrm{Band5}}$	Kawamura et. al., 1998
NDBI	Normalized Differences Built-up Index 正規化都市化指標	$NDBI = \frac{\mathrm{Band6} - \mathrm{Band5}}{\mathrm{Band6} + \mathrm{Band5}}$	Zha et. al., 2003
NDVI	Normalized Differences Vegetation Index 正規化植生指標	$NDVI = \frac{\mathrm{Band5} - \mathrm{Band4}}{\mathrm{Band5} + \mathrm{Band4}}$	Tucker, C.J., 1979
BA	Built-up Area 開発指標値	$BA = \mathrm{NDBI} - \mathrm{NDVI}$	Zha et. al., 2003
T	At-satellite Brightness Temperature 輝度温度（℃）	$T = \frac{\mathrm{K2}}{\ln\left(\frac{\mathrm{K1}}{\mathrm{ML} * \mathrm{DN}_{10} + \mathrm{AL}} + 1\right)} - 273.15$	USGS, 2015
CC	Color Complexity 色複雑度	$CC^2 = \frac{1}{5}\sum_{i=1}^{5}(Ri - \bar{R})^2 + \frac{1}{5}\sum_{i=1}^{5}(Gi - \bar{G})^2 + \frac{1}{5}\sum_{i=1}^{5}(Bi - \bar{B})^2$	

後述するように，本稿では衛星画像から得られる指数の回帰モデルで UD の推定を行ったが，この回帰アプローチでは，道路や裸地を多く含むメッシュにおいて，過大な予測値が算出される傾向が見られた．11 月の衛星画像より取得した UI による単回帰の予測値と実測値において，乖離の大きかったメッシュの Google earth 画像を Fig. A.2 に例示する．

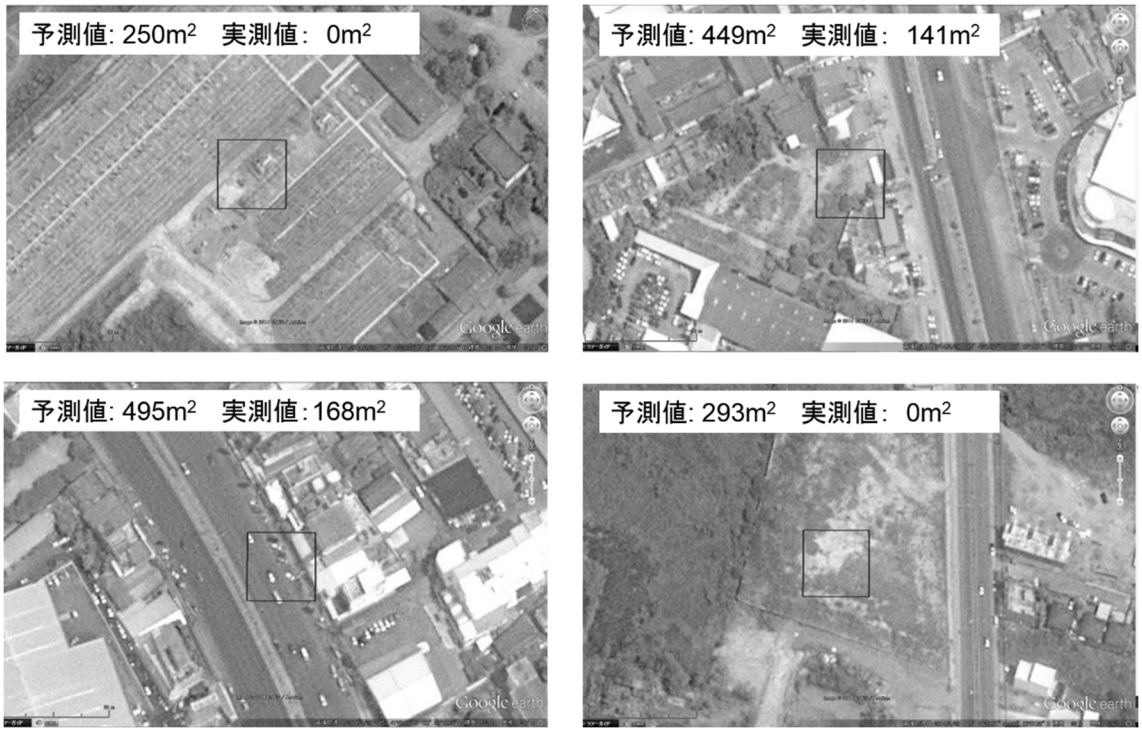

Fig. A.2 The sample meshes which had big gap between predicted UD and observed UD by the GAM single regression model using UI. The black rectangle indicates sampling mesh.

そのため，本稿では，建築物と道路や裸地を分離する指標，色複雑度 CC (Color Complexity) を開発した．CC は，対象とするメッシュとそれに隣接するメッシュ（Fig. A.3）の RGB ベクトルの標準偏差であり式 (7) により求めた．この演算操作により類似の色要素をもつ広い空間に属するメッシュでは小さな値が算出され, 対して地物の輪郭などでは高い値が算出される. CC の算出結果を Fig. A.4 に例示する.

$$CC^2 = \frac{1}{5}\sum_{i=1}^{5}(Ri-\bar{R})^2 + \frac{1}{5}\sum_{i=1}^{5}(Gi-\bar{G})^2 + \frac{1}{5}\sum_{i=1}^{5}(Bi-\bar{B})^2 \qquad (7)$$

ここで，R_i:メッシュ i の Band4 反射率，$\bar{R}$：対象メッシュおよびそれに隣接するメッシュの R 値の平均，G_i：メッシュ i の Band3 反射率, $\bar{G}$：対象メッシュおよびそれに隣接するメッシュの G 値の平均B_i：メッシュ i の Band2 反射率，B_i：対象メッシュおよびそれに隣接するメッシュの B 値の平均.

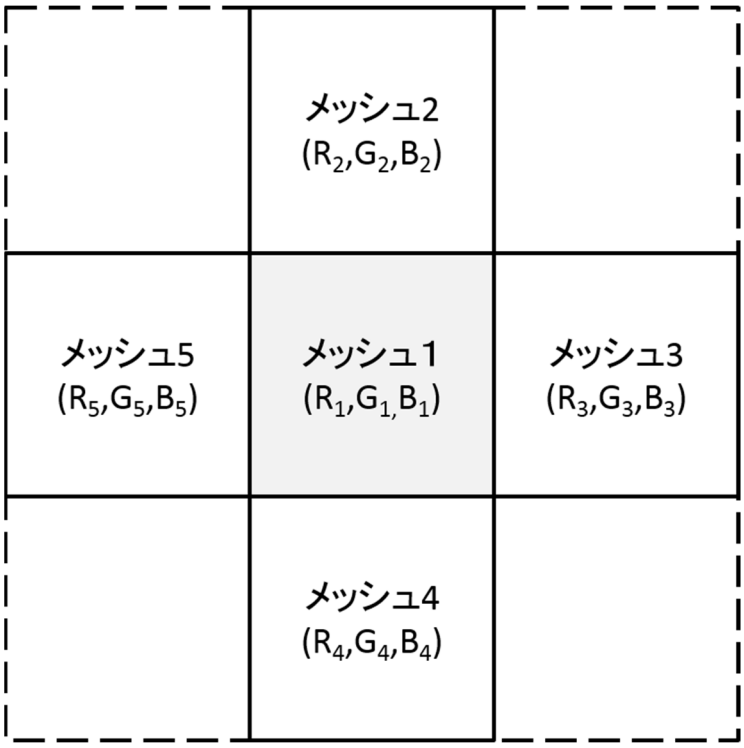

Fig. A.3 CC (Color Complexity) calculate area. Gray mesh indicates target mesh. CC was calculated as the standard deviation among target mesh and neighboring 4 meshes.

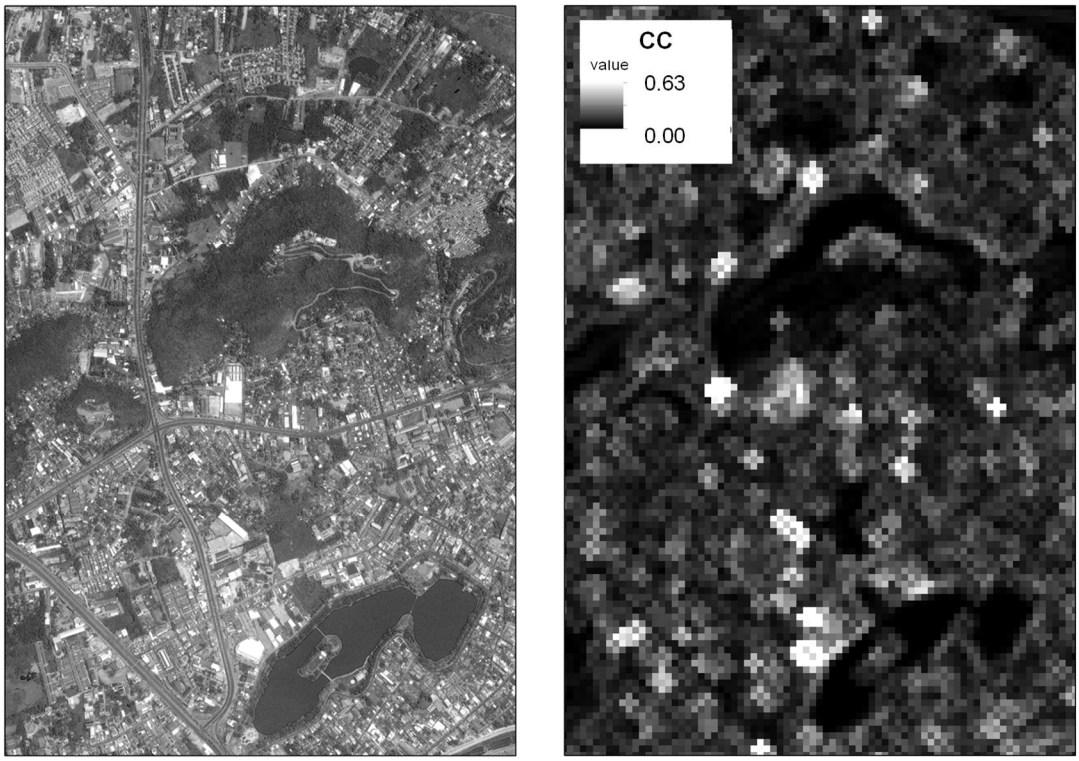

Fig. A.4 Left: The satellite image of reference area. Right: The result of calculation of CC.

建物占有率 UD の算出は以下のように行った．まず，ArcGIS (ver.10.2)を用いて，Fig. A.1 の対象地域

の範囲（26.86km^2）で，ランドサットのピクセルと同一形状のメッシュ（30m×30m）を作成し，そこから水域と重なるメッシュを除外した．その後，作成したメッシュの中からランダムに 200 個のメッシュをサンプルし，サンプルメッシュのデータセットを kmz ファイル形式に変換した．出力した kmz ファイルを，Google earth (ver. 7.1.2.2041) に読み込み，目視により各サンプルメッシュに含まれる建築物の外周線を作成した．Google earth の航空写真の撮影日は 2014 年 3 月 29 日であった．再度その外周線データを ArcGIS に読み込み，各メッシュの建築物面積を計算して，メッシュの面積で除して UD を求めた．

A.2.4 Statistic analysis

UD とランドサット衛星写真から得られた各指標との関係性を明らかにするために，3 月 29 日と 11 月 24 日のそれぞれの季節で一般化加法モデル（以下 GAM）による多重回帰モデル選択を行った．GAM は，一般化線形モデルをノンパラメトリック回帰に拡張したもので，目的変数と説明変数の非線形関係をうまく表現することができる (Hastie and Tibshirani, 1990).

説明変数として，Table A.2 のすべての指数を使用し，目的変数は 30m メッシュ当たりの建物占有率 UD を使用した．ただし，多重共線性の問題を避けるため，各指数間で高い相関（ピアソンの積率相関係数 r>0.7）を示す変数は同一モデルに組み込んで解析に使用しなかった. モデルの選択基準は AIC (Akaike 1973) を用い，AIC の優秀な（小さな値の）モデルについて UD との関係について検討を行った．

GAM は R パッケージ (version 3.1.1) の mgcv パッケージを用いて計算した．モデル選択には，R の dredge 関数（MuMIn パッケージ）を使用した．

A.3 Result

モデル選択の結果，11 月の UI，T，CC を使用したモデルが最も優れたモデルであると判断された（Table A.3）．ベストモデルにおける UI，T，CC それぞれの変数の部分的な推定値を Fig. A.5 に示す．Fig. A.5 は，モデル内で他の説明変数による効果を一定としてその説明変数だけ反動させた場合の UD 推定値とその推定誤差を示している．

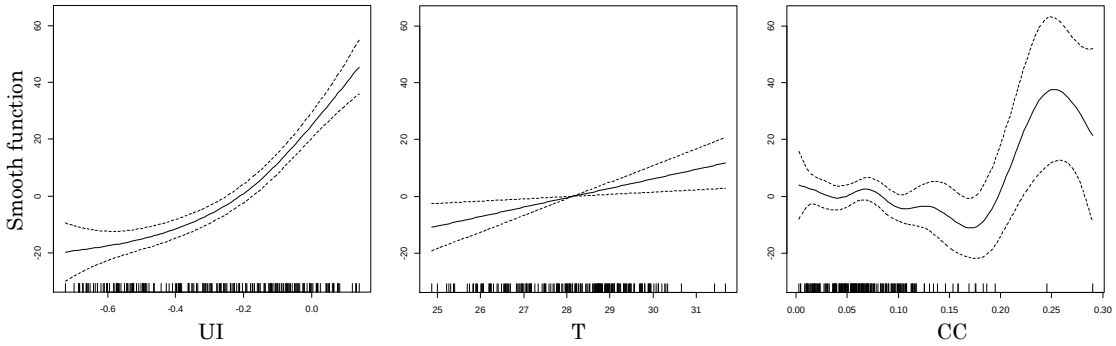

Fig. A.5 Partial Additive effect on urban density of variables (UI, T, CC). The solid lines show fits derived from the generalized additive mixed model. Dashed lines are 95 % confidence interval of the effect.

UI，T，CC を使用したベストモデルの当てはまりを Fig. A.6，ナコンサワン市街地にモデルを外挿し

た結果を Fig. A.7 に示す．R^2 値は 0.649 であった．ここで，R^2 値の算出は，モデルの推定 UD が 0%を下回るものは 0%に，100%を超えるものは 100%に変換して行った． 3 月，11 月共にベストモデルの AIC は null モデルの AIC を下回り，いずれの変数も有意 (P<0.05) であった．

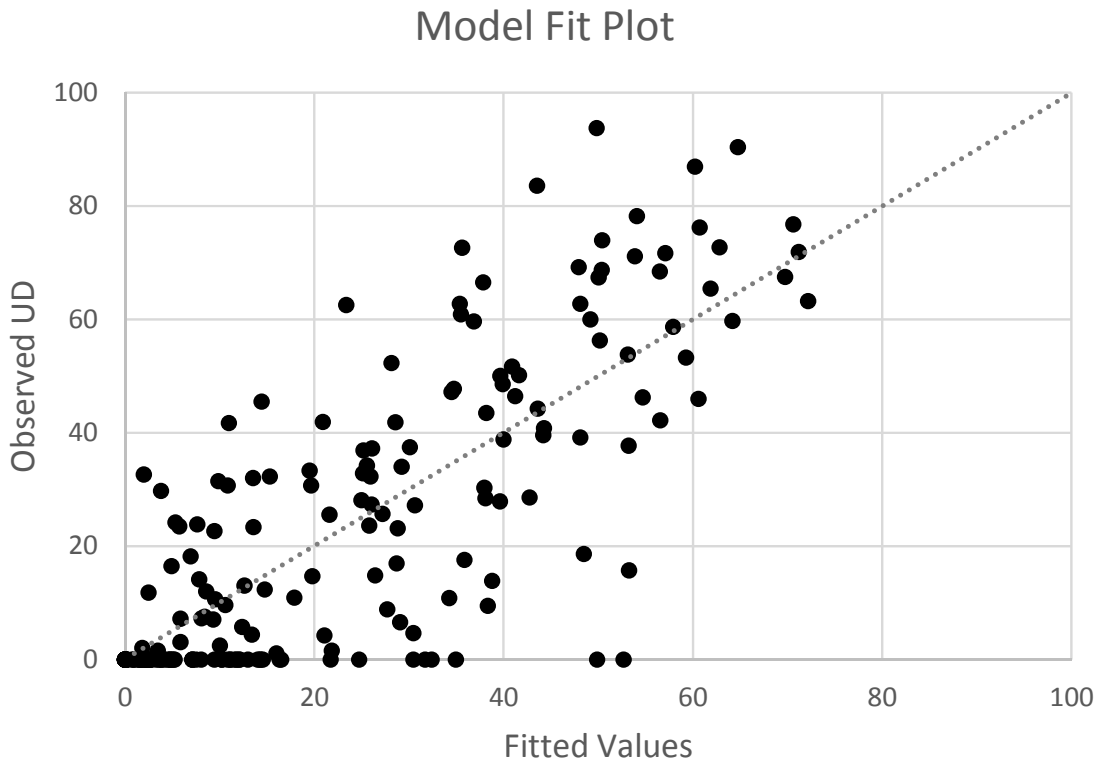

Fig. A.6 The relationship between predicted UD and observed UD.

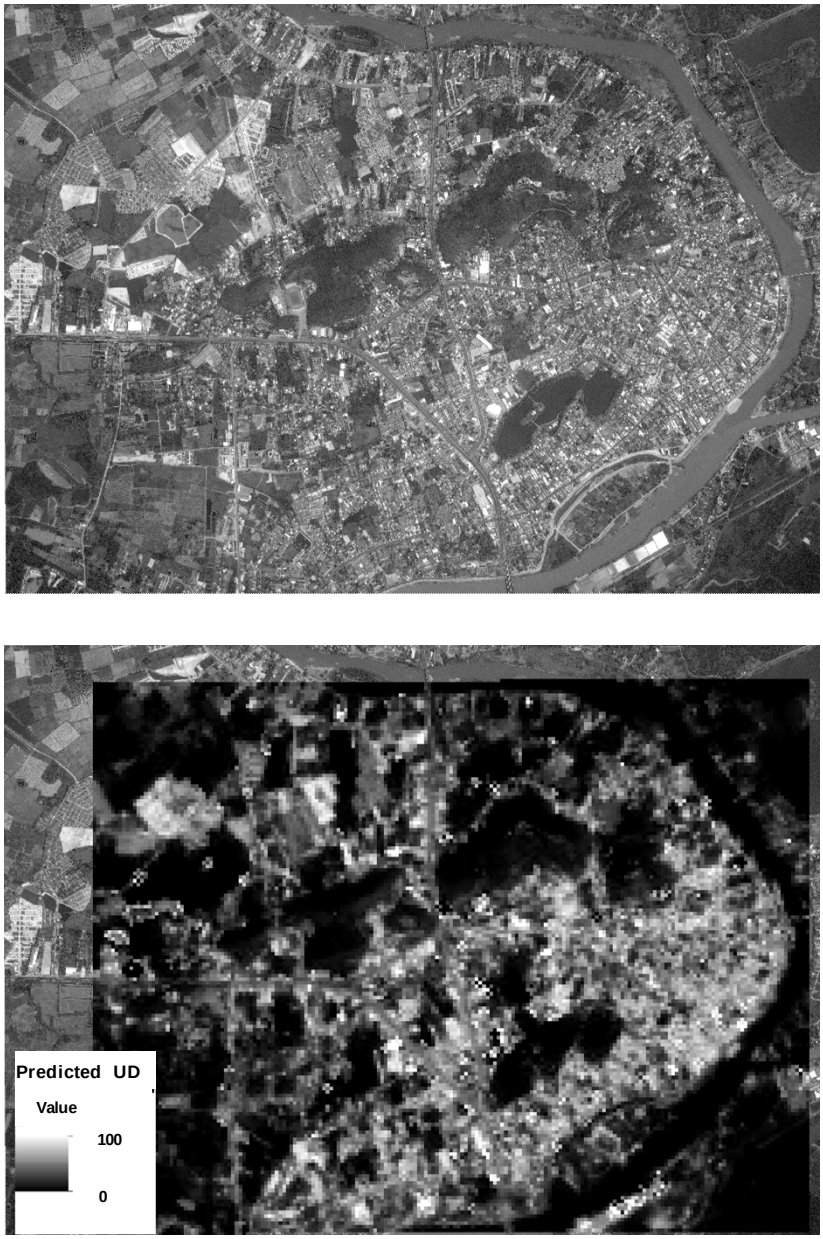

Fig. A.7 The result of predicted UD by the best model in reference area.

A.4 Discussion

全体の傾向として，3 月よりも，11 月の指数を使用したモデルのほうが，説明力が高かった（Table A.3）．これは，乾季よりも雨季の方が，植生の活性が高いため，各メッシュの植生状況が RED 帯や NIR 帯のバンドの反射率に正確に反映されやすいためと考えられる（Yang, F. et. al. 2012）．世界の他地域において，本稿の手法で UD の推定を行う場合には，季節性に十分配慮する必要があることが明らかとなった.

Table A.3 Summary of GAM analysis and AIC model selection. (a) March, (b) November.

(a) March

						Variables					
Model	AIC	ΔAIC	Wi	R^2	Intercept	UI	NDBI	NDVI	BA	T	CC
Top	1719	0	0.207	0.554	22.2***	+***	NA	NA	NA	+***	NA
2	1721	34	0.204	0.555	22.2***	+***	NA	NA	NA	+***	+
3	1729	42	0.183	0.533	22.2***	NA	NA	NA	+***	+***	NA
4	1730	44	0.179	0.544	22.2***	+***	NA	NA	NA	NA	+
NULL	1873	187	0.000		22.2***	NA	NA	NA	NA	NA	NA

Level of significance: *** P < 0.001, ** P < 0.01, * P < 0.05

(b) November

						Variables					
Model	AIC	ΔAIC	Wi	R^2	Intercept	UI	NDBI	NDVI	BA	T	CC
Top	1686	0	0.306	0.649	22.2***	+***	NA	NA	NA	+**	+*
2	1692	5	0.289	0.614	22.2***	+***	NA	NA	NA	+*	NA
3	1692	6	0.287	0.636	22.2***	+***	NA	NA	NA	NA	+*
4	1697	10	0.272	0.597	22.2***	+***	NA	NA	NA	NA	NA
NULL	1873	187	0.000		22.2***	NA	NA	NA	NA	NA	NA

Level of significance: *** P < 0.001, ** P < 0.01, * P < 0.05

単独で UD を説明するために最も優れていた変数は，11 月の UI であった．一方で，本稿における UD と UI との単独での GAM モデルの R^2 値は 0.522（3 月），0.597（11 月）であった．既往の研究により報告されている UD と UI との R^2 値はおおよそ 0.6 から 0.8 であり（e.g. Kawamura 1998），本稿の結果はややあてはまりが悪かった．これは，既往の研究で，UD を求めたメッシュサイズが 500m 程度と本研究の 30m スケールより大きく，各メッシュに含まれる道路や駐車場などの UI では建築物と区別が困難な要素の面積が，大スケールのメッシュで平準化されやすいことが要因であると考えられる．

AIC モデル選択による UI，T，CC を使用したベストモデルの R2 値は 0.649 であった．工学的用途で氾濫解析に組み込むために，一定程度の予測精度を持ったモデルを構築できたと考える．本稿の提案した UD 推定手法では，ArcGIS 以外のソフトウェア，使用データは無償のものであった．廉価であることに加えて，本稿の手法は，ランドサット衛星画像が整備されている場所なら世界各地のどこでも適応可能であり，解析範囲が広範な場合でも，省力的に UD の推定が可能であるという利点を有しており，洪水の頻発する途上国での活用が期待される．

References

References

Agostinho, A.A., Gomes, L.C., Veríssimo, S., Okada, E.K. (2004) Flood regime, dam regulation and fish in the Upper Paraná River: Effects on assemblage attributes, reproduction and recruitment. Reviews in Fish Biology and Fisheries, 14 (1): 11-19.

Agostinho, A.A., Gomes, L.C., Zalewski, M. (2001) The importance of floodplains for the dynamics of fish communities of the upper river Paraná. Ecohydrology and Hydrobiology, 1 (1-2): 209-217.

Amoros, C., Bornette, G. (2002) Connectivity and biocomplexity in waterbodies of riverine floodplains. Freshwater Biology, 47 (4): 761-776.

Anjos, M.B., De Oliveira, R.R., Zuanon, J. (2008) Hypoxic environments as refuge against predatory fish in the Amazonian floodplains. Brazilian Journal of Biology, 68 (1) :45-50.

Asahi, K., Yoshida, Y., Tsunematsu, H., Shimizu, Y., Nelson, J. (2012) Development of the iRIC software for river analysis. River Flow 2012 - Proceedings of the International Conference on Fluvial Hydraulics. 2: 1133-1138.

Aselman, I., Crutzen, P.J. (1989) Global distribution of natural wetlands and rice paddies, their net primary productivity, season- ality and possible methane emissions. Journal of Atmospheric Chemistry 8: 307–358.

Bangkok Post (2011) Floodgates reopen in dam debate, Thailand. Bangkok

Bangkok Post (2015) Govt seeks B900bn for water plan. http://www.bangkokpost.com/lite/topstories/455087/govt-seeks-b900bn-for-water-plan (accessed 10 November. 2015)

BirdLife International (2004) Important Bird Areas of Asia: Key Sites for Conservation BirdLife International, Cambridge.

Boedeltje, G., Bakker, J.P., Brinke, A.T., Van Groenendael, J.M., Soesbergen, M. (2004) Dispersal phenology of hydrochorous plants in relation to discharge, seed release time and buoyancy of seeds: The flood pulse concept supported. Journal of Ecology, 92 (5): 786-796.

Bonvechio, T.F., Allen, M.S. (2005) Relations between hydrological variables and year-class strength of sportfish in eight Florida waterbodies. Hydrobiologia, 532 (1): 193-207.

Bozelli, R.L., Thomaz, S.M., Padial, A.A., Lopes, P.M., Bini, L.M. (2015) Floods decrease zooplankton beta diversity and environmental heterogeneity in an Amazonian floodplain system

Brinson, M.M. (1993) Changes in the functioning of wetlands along environmental gradients

Broxton, P.D., Zeng, X., Sulla-Menashe, D., Troch, P.A., (2014) A Global Land Cover Climatology Using MODIS Data. J. Appl. Meteor. Climatol., 53: 1593–1605.

Burnham, K.P., Anderson, D.R.(2002) Model Selection and Multimodel Inference: A Practical Information-theoretic Approach. 2nd edn. Springer New York.

CRED (2012) Annual Disaster Statistical Review 2011 The numbers and trends. http://cred.be/sites/default/files/2012.07.05.ADSR_2011.pdf (accessed 10 November. 2015)

Carpenter G., Gillison A.N., Winter J. (1993) DOMAIN: a flexible modelling procedure for mapping potential distributions of plants and animals. Biodiversity and Conservation, 2 (6): 667-680

Carsten F. Dormann, Jane Elith, Sven Bacher, Carsten Buchmann, Gudrun Carl, Gabriel Carré,

References

Jaime R. García Marquéz, Bernd Gruber, Bruno Lafourcade, Pedro J. Leitão, Tamara Münkemüller, Colin McClean, Patrick E. Osborne, Björn Reineking, Boris Schröder, Andrew K. Skidmore, Damaris Zurell andSven Lautenbach (2013) Collinearity: a review of methods to deal with it and a simulation study evaluating their performance. Ecography, 36(1): 27-46.

Center for International Earth Science Information Network - CIESIN - Columbia University, and Centro Internacional de Agricultura Tropical - CIAT. (2005). Gridded Population of the World, Version 3 (GPWv3): Population Density Grid, Future Estimates. Palisades, NY: NASA Socioeconomic Data and Applications Center (SEDAC). http://dx.doi.org/10.7927/H4ST7MRB. (accessed 10 November. 2015)

Cham, T. C., Mitani Y., Ikemi, H. (2015) Simulation of Modeling Approach for Flood Condition and Proposed Flood Protection at Midstream of Chao Phraya River Basin, Thailand. American Journal of Environmental Protection. 3(3): 84-94.

Chefaoui RM, Lobo JM (2007) Assessing the conservation status of an Iberian moth using pseudo absences. J Wildl Manage 71: 2507–2516.

Constanza, R., d'Arge, R., de Groot, R., Farber, S., Grasso, M., Hannon, B., Limburg, K., Naeem, S., Neill, R.V., Paruelo, J., Raskin, R.G., Sutton P., Van der Belt, M. (1997) The value of the world's ecosystem services and natural capital. Nature 387: 253–260.

Dufrene, M., and P. Legendre. 1997. Species assemblages and indicator species: The need for a flexible asymmetrical approach. Ecological Monographs 67: 345-366.

Elith, J., H. Graham, C., P. Anderson, R., Dudík, M., Ferrier, S., Guisan, A., J. Hijmans, R., Huettmann, F., R. Leathwick, J., Lehmann, A., Li, J., G. Lohmann, L., A. Loiselle, B., Manion, G., Moritz, C., Nakamura, M., Nakazawa, Y., McC. M. Overton, J., Townsend Peterson, A., J. Phillips, S., Richardson, K., Scachetti-Pereira, R., E. Schapire, R., Soberón, J., Williams, S., S. Wisz, M. (2006) Novel methods improve prediction of species' distributions from occurrence data. Ecography. 29(2): 129-151

Erwin K.L. (2009) Wetlands and global climate change: the role of wetland restoration in a changing world. Wetlands Ecol Manage (2009) 17: 71–84

Ferrer-Castán, D., Vetaas, O.R. (2005). Pteridophyte richness, climate and topography in the Iberian Peninsula: Comparing spatial and nonspatial models of richness patterns. Global Ecology and Biogeography, 14 (2): 155-165.

Finlayson, C.M., Davidson, N.C. (1999) Global review of wetland resources and priorities for wetland inventory: summary report. In CM Finlayson & Spiers AG (eds), Global Review of Wetland Resources and Priorities for Wetland Inventory. Supervising Scientist Report 144, Supervising Scientist Group, Canberra: 1-13.

Fisheries Department (FD) (2005) Annual Report 2005 Survey of Fish Species in Bung Boraphet. Nakhon Sawan. Inland Fisheries Research and Development Center.

Fleiss, J.L. (1981). Statistical methods for rates and proportions (2nd ed.). New York. John Wiley.

Frutos. A., Olea. P.P., Vera. R. (2007) Analyzing and modelling spatial distribution of summering lesser kestrel: The role of spatial autocorrelation. Ecological Modelling 200 (1-2): 33-44.

Fukushima, M., Jutagate, T., Grudpan, C., Phomikong, P., Nohara, S., (2014) Potential Effects of Hydroelectric Dam Development in the Mekong River Basin on the Migration of Siamese Mud Carp (Henicorhynchus

siamensis and H. lobatus) Elucidated by Otolith Microchemistry. PLoS ONE 9(8): e103722

GISTDA. (2015) http://flood.gistda.or.th/ (accessed 14 May. 2015)

Gallo-Sánchez, L.J., Aguirre-Ramírez, N.J., Palacio-Baena, J.A., Ramírez-Restrepo, J.J. (2009) Zooplankton (Rotifera and Microcrustacea) and its relationship with the level water changes in Ayapel floodplain lake (córdoba) Colombia. Caldasia, 31 (2): 339-353.

Gehrke, P.C. (1992) Diel abundance, migration and feeding of fish larvae (Eleotridae) in a floodplain billabong. Journal of Fish Biology, 40 (5): 695-707.

Gordon H. C. (1989) The habitat diversity and fish reproductive function of floodplain ecosystems. Environmental Biology of Fishes: 1-27.

Humphries P., King A.J., Koehn J.D. (1999) Fish, flows and flood plains: Links between freshwater fishes and their environment in the Murray-Darling River system, Australia. Environmental Biology of Fishes, 56 (1-2): 129-151

Hydro and Agro Informatics Institute. (2015) http://www.thaiwater.net/web/ (accessed 14 May. 2015)

Imanishi, A. (2010) Special Issue"Development of the City Biodiversity Index. Journal of the Japanese Society of Revegetation Technology, 36(3): 383–384.

Ishioka, T. (2000) Extended K-means with an Efficient Estimation of the Number of Clusters. Ouyou toukeigaku Vol. 29No. 3: 141-149.

Izaguirre, I., O'Farrell, I., Tell, G. (2001) Variation in phytoplankton composition and limnological features in a water-water ecotone of the Lower Paraná Basin (Argentina). Freshwater Biology, 46 (1): 63-74.

JICA (2013) Project on a Comprehensive Flood Management Plan for the Chao Phraya River Basin in Thailand: Final Report Vol. 2. Japan International Cooperation Agency, Tokyo (in Japanese)

JICE (1999) The Guide to planning small-and-medium-sized river management. Tokyo. Japan Institute of Country-ology and Engineering (in Japanese)

Jarvis, A., Reuter, H.I., Nelson, A., Guevara, E. (2008) Hole-filled SRTM for the globe Version 4, available from the CGIAR-CSI SRTM 90m Database. http://srtm.csi.cgiar.org (accessed 10 November. 2015)

Jin, X., Chi, Y., Ji, R., Chen, Y., Liu, C. (2014) Analysis the environment influence of spatial and temporal variation of strategy of land-based pollution for river cross section. Journal of Chemical and Pharmaceutical Research, 6 (5): 1636-1640.

Kano Y, Adnan MSB, Grudpan C, Grudpan J, Magtoon W, Musikasinthorn P, Natori Y, Ottomanski S, Praxaysonbath B, Phongsa K, Rangsiruji A, Shibukawa K, Shimatani Y, So N, Suvarnaraksha A, Thach P, Thanh PN, Tran DD, Utsugi K, Yamashita T. (2013) An online database on freshwater fish diversity and distribution in Mainland Southeast Asia. Ichthyological Research 60: 293-295

Kano, Y., Kawaguchi, Y., Yamashita, T., Shimatani, Y. (2010) Distribution of the oriental weatherloach, Misgurnus anguillicaudatus, in paddy fields and its implications for conservation in Sado Island, Japan. Ichthyological Research, 57 (2): 180-188.

Keitt T.H., Bjørnstad O.N., Dixon P.M., Citron-Pousty S. (2002) Accounting for spatial pattern when modeling organism-environment interactions. Ecography, 25 (5): 616-625.

Keruzoré, A.A., Willby, N.J., Gilvear, D.J. (2013) The role of lateral connectivity in the maintenance

of macrophyte diversity and production in large rivers. Aquatic Conservation: Marine and Freshwater Ecosystems, 23 (2): 301-315.

Kiester, A.R., Scott, J.M., Csuti, B., Noss, R.F., Butterfield, B., Sahr, K., White, D. (1996) Conservation prioritization using GAP data. Conservation Biology, 10: 1332-1342

Kimura, T. (1967) Storage function method. Public Works Research Institute (in Japanese)

Kolding J., van Zwieten P.A.M. (2012) Relative lake level fluctuations and their influence on productivity and resilience in tropical lakes and reservoirs. Fisheries Research, 115-116: 99-109.

Kottelat, M. (2013) The fishes of the inland waters of Southeast Asia: A catalogue and core bibliography of the fishes known to occur in freshwaters, mangroves and estuaries. Raffles Bulletin of Zoology, (SUPPL.27): 1-663.

Kottelat, M., Whitten, T. (1996) Freshwater biodiversity in Asia: with special reference to fish. World Bank Technical Paper, 343.

Kruskal, J. B. (1964) Multidimensional scaling by optimizing goodness of fit to a nonmetric hypothesis. Psychometrika 29: 1-27.

Legendre P, Legendre L (1998) Numerical ecology. Elsevier, Amsterdam.

Lehner, B., Döll, P. (2004) Development and validation of a global database of lakes, reservoirs and wetlands. Journal of Hydrology, 296 (1-4): 1-22. DOI: 10.1016/j.jhydrol.2004.03.028

Liang, C., Song, J., Yue, F., Zhang, J., (2014) Water environmental protection strategy of Dagu River Basin in Qingdao, China. WIT Transactions on Engineering Sciences, 84: 753- 759.

Lichstein, J.W., Simons, T.R., Shriner, S.A., Franzreb, K.E. (2002) Spatial autocorrelation and autoregressive models in ecology. Ecological Monographs 72 (3): 445-463.

Lothongkham, A., Arbsuwan, S., Musikasinthorn, P. (2014) Garra waensis, a new cyprinid fish (Actinopterygii: Cypriniformes) from the Nan River basin of the Chao Phraya River system, northern Thailand. Zootaxa. 3790(4): 543-554

Loiselle B.A., Howell C.A., Graham C.H., Goerck J.M., Brooks T., Smith K.G., Williams P.H. (2003) Avoiding Pitfalls of Using Species Distribution Models in Conservation Planning. Conservation Biology, 17 (6): 1591-1600

Machida, S., Iguchi, M., Kaiduka, S., Satoh, T., Hine, Y., Ono, Y. (1981) Geomorphology Dictionary. Ninomiya Books, Tokyo

Mateo, C.M., Hanasaki, N., Komori, D., Tanaka, K., Kiguchi, M., Champathong, A., Sukhapunnaphan, T., Yamazaki, D., Oki, T. (2014) Assessing the impacts of reservoir operation to floodplain inundation by combining hydrological, reservoir management, and hydrodynamic models. Water Resources Research, 50 (9): 7245-7266.

Matthews, W. J. (1998) Patterns in Freshwater Fish Ecology. Chapman and Hall, London

McCullash P., Nelder J. (1989) Generalized linear models, 2nd edn. Chapman & Hall, London.

Mccullagh, P., Neldeb, J. A. (1983) Generalized linear models. London. Chapman and Hall

Merow C., Smith M.J., Silander J.A. (2013) A practical guide to MaxEnt for modeling species' distributions: What it does, and why inputs and settings matter. Ecography. 36(10): 1058-1069

References

Merron, G.S., Mann, B.Q. (1995) The reproductive and feeding biology of Schilbe intermedius Rüppell in the Okavango Delta, Botswana. Hydrobiologia, 308 (2): 121-129.

Mihaljević, M., Stević, F., Špoljarić, D., Pfeiffer, T.Z. (2015) Spatial pattern of phytoplankton based on the morphology-based functional approach along a river-floodplain gradient. River Research and Applications, 31 (2): 228-238.

Minchin, P. R. (1987) An evaluation of the relative robustness of techniques for ecological ordination. Vegetatio 96: 89-108.

Miyazaki, Y., Terui, A., Yoshioka, A., Kaifu, K., Washitani, I. (2013) Fish species composition of temporary small lentic habitats in the floodplains of the Shubuto River System: Factors affecting species richness and suggestions for conservation and restoration. Japanese Journal of Conservation Ecology 05/2013; 18(1): 55–68. (in Japanese)

Moffitt, C.M., Cajas-Cano, L. (2014) Blue Growth: The 2014 FAO State of World Fisheries and Aquaculture. Fisheries, 39 (11): 552-553.

Moran, P. A. P. (1950). "Notes on Continuous Stochastic Phenomena". Biometrika 37 (1): 17-23.

Moser, M., Prentice, C. and Frazier, S. (1996) A Global Overview of Wetland Loss and Degradation. www.ramsar.org/about/about_wetland_loss.htm

Myers, N., Mittermeier, R., Mittermeier, G. C., Dafonsega, G. A. B., Kent, J. (2000). Biodiversity hotspots for conservation priorities. Nature 403: 853–858.

Myers, N., Mittermeler, R.A., Mittermeler, C.G., Da Fonseca, G.A.B., Kent, J. (2000) Biodiversity hotspots for conservation priorities. Nature, 403 (6772): 853-858.

Myers, N., Mittermeler, R.A., Mittermeler, C.G., Da Fonseca, G.A.B., Kent, J. (2000) Biodiversity hotspots for conservation priorities. Nature, 403: 853-858

Nix, H. (1986) A biogeographic analysis of Australian elapid snakes. Atlas of elapid snakes of Australia. Bureau of Flora and Fauna. Canberra: 4–15.

Oki, T. (2012) The Chaophraya flood 2011 and flood disaster of Thailand. The University of Tokyo. (In Japanese).

Olson, D.M. & Dinerstein, E. (1998) The global 200: a represen- tation approach to conserving the earth‘s most biologically valuable ecosystems. Conservation Biology 12: 502–515.

Overmars K.P., De Koning G.H.J., Veldkamp A. (2003) Spatial autocorrelation in multi-scale land use models. Ecological Modelling, 164 (2-3): 257-270.

Pander J., Mueller M., Geist J., (2015) Succession of fish diversity after reconnecting a large floodplain to the upper Danube River. Ecological Engineering (75): 41-50.

Pease, A.A., Justine Davis, J., Edwards, M.S., Turner, T.F. (2006) Habitat and resource use by larval and juvenile fishes in an arid-land river (Rio Grande, New Mexico). Freshwater Biology, 51 (3): 475-486.

Permanent Mission of Thailand to the United Nations (2015) Top Stories : Statement of the Prime Minister of Thailand at the Third United Nations World Conference on Disaster Risk Reduction. http://www.thaiembassy.org/permanentmission.geneva/en/news/4749/54484-Statement-of-the-Prime-Minister-of-Thailand-at-the.html(accessed 10 November. 2015)

References

Petry, P., Bayley, P.B., Markle, D.F. (2003) Relationships between fish assemblages, macrophytes and environmental gradients in the Amazon River floodplain. Journal of Fish Biology, 63 (3): 547-579.

Phillips, S., J., Anderson, R., P., Schapire, R., E. (2006) Maximum entropy modeling of species geographic distributions. Ecological Modelling, 190/3-4: 231-259

Pinheiro, J.C., Bates, D.M. (2000) Mixed-effects Models in S and S-plus. Springer, New York.

Poff, N. L., Allan, J. D., Bain, M. B., Karr, J. R., Prestegaard, K. L., Richter, B. D., Stromberg, J. C. (1997). The natural flow regime: A paradigm for river conservation and restoration. BioScience, 47(11): 769–784.

Prajamwong S, Suppataratarn P. (2009) Integrated: Flood Mitigation Management in the Lower Chao Phraya River Basin. Expert Group Meeting on Innovative Strategies Towards Flood Resilient Cities in Asia-Pacific 2009 Meeting Documents.

Rainboth, W.J. (1996) Fishes of the Cambodian Mekong. FAO Species Identification Field Guide for Fishery Purposes. FAO, Rome.

Ramsar & IUCN (1999) Wetlands and global change [www docu- ment]. URL http://www.ramsar.org/key_unfccc_bkgd.htm

Ravenga, C., Brunner, J., Henninger, N., Kassem, K. & Payne, R. (2000) Pilot Analysis of Global Ecosystems. Freshwater Systems. Washington DC, USA: World Resources Institute.

Richter, B. D., Baumgartner, J. V., Powell, J., & Braun, D. P. (1996). A Method for Assessing Hydrologic Alteration within Ecosystems. Conservation Biology, 10(4): 1163–1174.

Ross S. T., Baker J. A. (1983) The response of fishes to periodic spring floods in a southeastern stream. The American Midland Naturalist Journal, 109: 1-14.

Sayama T., Tatebe Y., Iwami Y., Tanaka S. (2015) Hydrologic sensitivity of flood runoff and inundation: 2011 Thailand floods in the Chao Phraya River basin. Natural Hazards and Earth System Sciences, 15 (7): 1617-1630.

Scott, J.M., Davis, F., Csuti, R., Noss, B., Butterfield, B., Groves, C., Anderson, H., Caicco, S., D'Erchia, F., Edwards, T.C., Jr., Ulliman, J., Wright, R.G. (1993) Gap Analysis: a geographic approach to protection of biological diversity. Wildlife Monographs, 123:1-41

Scott DA (1989) A Directory of Asian Wetlands. IUCN, Gland, Switzerland

Simões, N.R., Dias, J.D., Leal, C.M., de Souza Magalhães Braghin, L., Lansac-Tôha, F.A., Bonecker, C.C. (2013) Floods control the influence of environmental gradients on the diversity of zooplankton communities in a neotropical floodplain. Aquatic Sciences, 75 (4): 607-617.

Sommer, T.R., Harrell, W.C., Feyrer, F. (2014) Large-bodied fish migration and residency in a flood basin of the Sacramento River, California, USA. Ecology of Freshwater Fish, 23 (3): 414-423.

Sommer, T.R., Nobriga, M.L., Harrell, W.C., Batham, W., Kimmerer, W.J. (2001) Floodplain rearing of juvenile chinook salmon: Evidence of enhanced growth and survival. Canadian Journal of Fisheries and Aquatic Sciences, 58 (2): 325-333.

Sriwongsitanon, N., Surakit, K., Hawhins, P. R., Chandrasena, N. (2007). Decision support tools for water resource management: a case study of Bung Boraphet wetland, Thailand. Journal of Development and Sustainability Agriculture. 2: 17-26

References

Stockwell D., Peters D. (1999) The GARP modelling system: Problems and solutions to automated spatial prediction. International Journal of Geographical Information Science, 13 (2): 143-158

Su, F., Zhou, C., Shi, W., Du, Y. (2004) Spatial heterogeneity of demersal fish in East China Sea. Chinese Journal of Applied Ecology 15 (4): 683-686.

Suvarnaraksha, A. (2012) Schistura maejotigrina, a new stream loach (Pisces: Nemacheilidae) from northern Thailand. Zootaxa, (3586): 131-137.

Suvarnaraksha, A. (2015) A new species of highland loach, Schistura sirindhornae, from the upper Chao Phraya River basin, Thailand (Pisces: Ostariophysi: Nemacheilidae). Zootaxa, 3962 (1): 158-170.

Suvarnaraksha, A. (2015) A new species of highland loach, Schistura sirindhornae, from the upper Chao Phraya River basin, Thailand (Pisces: Ostariophysi: Nemacheilidae). Zootaxa, 3962 (1): 158-170.

Takasao, T., Takamura, K., Shimizu, A. (1986) A basic study on frequency of hydrologic data in the Lake Biwa Basin. Disaster Prevention Research Institute Annuals. B (in Japanese)

Tamada, Y., Hoshikawa H., Funadu, T., (2013) Thailand 2011 flood: the records and lessons, IDE-JETRO, Chiba. (in Japanese)

Tanaka, W., Kano, Y., Yamasita, T., Saitou, K., Kawaguchi, Y., Shimatani, Y. (2011) Determinants of the Misgurnus anguillicaudatus population and its application to conservation planning in Sado Island, Japan. Ecology and Civil Engineering, 14 (1): 1-9. (in Japanese with English abstract)

Tebakari, T., Fukami, K., Suvanpimol, C., Miyamoto, M., Yamada T. (2005) Foundational Study on Water Use and Flood Control Effect by the Large Scale Reservoir －A Case Study in Upper Chao Phraya River Basin, Kingdom of Thailand－The Journal of Japan Society of Civil Engineers, Ser. B1 Vol.49 (in Japanese)

Thai Meteorological Department. (2015) http://www.tmd.go.th/en/archive/thailand_climate.pdf (accessed 14 May. 2015)

The IUCN Red List of Threatened Species (2015) http://www.iucnredlist.org/ (accessed 14 November. 2015)

Tockner, K., Stanford, J. A. (2002). Riverine flood plains: present state and future trends. Environmental Conservation, 29(03): 308–330.

UN Population Division (2015) World Population Prospects: The 2015 Revision. United Nations, New York

Vidthayanon, C. (2002) Peat swamp fishes of Thailand. Office of Environmental Policy and Planning, Bangkok, Thailand (In Thai)

Vidthayanon, C. (2005) Thailand red data: fishes Bangkok, Thailand. Office of Natural Resources and Environmental Policy and Planning.

Vitousek, P.M., Mooney, H.A., Lubchenco, J. & Melillo, J.M. (1997) Human domination of earth's ecosystems. Science 277: 494–499.

Ward, J.V., Tockner, K., Schiemer, F. (1999) Biodiversity of floodplain river ecosystems: Ecotones and connectivity. River Research and Applications, 15 (1-3): 125-139.

Wetlands, 13 (2 Supplement): 65-74.

World Bank (2012) Thai flood 2011: rapid assessment for resilient recovery and reconstruction planning : Overview. http://documents.worldbank.org/curated/en/2012 (accessed 10 November. 2015)

Yamamoto, K.C., Freitas, C.E.D.C., Zuanon, J., Hurd, L.E. (2014) Fish diversity and species composition in

small-scale artificial reefs in Amazonian floodplain lakes: Refugia for rare species? Ecological Engineering, 67: 165-170.

Yuji Masutomi, Yusuke Inui, Kiyoshi Takahashi and Yuzuru Matsuoka, Development of highly accurate global polygonal drainage basin data, Hydrological Processes, 23: 572-584, DOI 10.1002hyp.7186, 2009

Zakaria-Ismail, M. (1994) Zoogeography and biodiversity of the freshwater fishes of Southeast Asia. Hydrobiologia, 285 (1-3): 41-48.

http://www.ramsar.org/key_unfccc_bkgd.htm (accessed 14 November. 2015)